NEURAL RESPONSES TO INJURY: PREVENTION, PROTECTION, AND REPAIR
Annual Technical Report
1996-1997

Submitted by

Nicolas G. Bazan, M.D., Ph.D.
Project Director

Period Covered: 20 September, 1996 through 19 September, 1997

Cooperative Agreement DAMD17-93-V-3013

between

United States Army Medical Research and Development Command
(Walter Reed Army Institute of Research)

and

Louisiana State University Medical Center
Neuroscience Center of Excellence

Volume 1 of 9

Neuroscience Core Research Facilities

Project Directors:
R. Ranney Mize, Ph.D.
Nicolas G. Bazan, M.D., Ph.D.

AD_____

COOPERATIVE AGREEMENT NUMBER DAMD17-93-V-3013

TITLE: Neural Responses to Injury: Prevention, Protection, and Repair

PRINCIPAL INVESTIGATOR: Nicolas G. Bazan, M.D., Ph.D.

CONTRACTING ORGANIZATION: Louisiana State University
School of Medicine
New Orleans, Louisiana 70112-2234

REPORT DATE: October 1997

TYPE OF REPORT: Annual

PREPARED FOR: U.S. Army Medical Research and Materiel Command
Fort Detrick, Maryland 21702-5012

REPORT DOCUMENTATION PAGE

Form Approved
OMB No. 0704-0188

1. AGENCY USE ONLY *(Leave blank)*	2. REPORT DATE	3. REPORT TYPE AND DATES COVERED
	October 1997	Annual (20 Sep 96 - 19 Sep 97)

4. TITLE AND SUBTITLE
Neural Responses to Injury: Prevention, Protection, and Repair

5. FUNDING NUMBERS
DAMD17-93-V-3013

6. AUTHOR(S)
Bazan, Nicolas G., M.D., Ph.D.

7. PERFORMING ORGANIZATION NAME(S) AND ADDRESS(ES)
Louisiana State University School of Medicine
New Orleans, Louisiana 70112-2234

8. PERFORMING ORGANIZATION REPORT NUMBER

9. SPONSORING / MONITORING AGENCY NAME(S) AND ADDRESS(ES)
U.S. Army Medical Research and Materiel Command
Fort Detrick, Maryland 21702-5012

10. SPONSORING / MONITORING AGENCY REPORT NUMBER

11. SUPPLEMENTARY NOTES

12a. DISTRIBUTION / AVAILABILITY STATEMENT
Approved for public release; distribution unlimited

12b. DISTRIBUTION CODE

13. ABSTRACT *(Maximum 200 words)*

In Year 4 of the DOD Agreement, the Calcium Imaging Facility has continued to support DOD-Funded projects and to serve as a core facility for Neuroscientists throughout the LSUMC campus. Usage of the Facility has been divided up at approximately 20 percent hardware and software maintenance and development, 40 percent DOD-funded investigations, and 40 percent other neuroscience projects.

14. SUBJECT TERMS
Prevention, Injury, Neural Response

15. NUMBER OF PAGES
1466

16. PRICE CODE

17. SECURITY CLASSIFICATION OF REPORT	18. SECURITY CLASSIFICATION OF THIS PAGE	19. SECURITY CLASSIFICATION OF ABSTRACT	20. LIMITATION OF ABSTRACT
Unclassified	Unclassified	Unclassified	Unlimited

FOREWORD

Opinions, interpretations, conclusions and recommendations are those of the author and are not necessarily endorsed by the U.S. Army.

____ Where copyrighted material is quoted, permission has been obtained to use such material.

____ Where material from documents designated for limited distribution is quoted, permission has been obtained to use the material.

____ Citations of commercial organizations and trade names in this report do not constitute an official Department of Army endorsement or approval of the products or services of these organizations.

__✓__ In conducting research using animals, the investigator(s) adhered to the "Guide for the Care and Use of Laboratory Animals," prepared by the Committee on Care and Use of Laboratory Animals of the Institute of Laboratory Resources, National Research Council (NIH Publication No. 86-23, Revised 1985).

✓
____ For the protection of human subjects, the investigator(s) adhered to policies of applicable Federal Law 45 CFR 46.

____ In conducting research utilizing recombinant DNA technology, the investigator(s) adhered to current guidelines promulgated by the National Institutes of Health.

____ In the conduct of research utilizing recombinant DNA, the investigator(s) adhered to the NIH Guidelines for Research Involving Recombinant DNA Molecules.

____ In the conduct of research involving hazardous organisms, the investigator(s) adhered to the CDC-NIH Guide for Biosafety in Microbiological and Biomedical Laboratories.

Nicolas G. Bazan, MD, PhD Nov 1, 1997

PI - Signature Date

TABLE OF CONTENTS

This Technical Report covers the progress made in the fourth year of this Cooperative Agreement in one project of the original proposal. We hope that this format of the report will facilitate its handling. The table of contents for all the projects has been included in each volume.

Nicolas G. Bazan, M.D., Ph.D.
Director, LSU Neuroscience Center
Program Director, USAMRDC Cooperative Agreement
New Orleans, LA
October 16, 1997

Table of Content

Cooperative Agreement Between the US Army Medical Research and Development Command and The LSU Neuroscience Center of Excellence

DAMD17-93-V-3013 20 September, 1993 - 19 October, 1997 $13,860,000

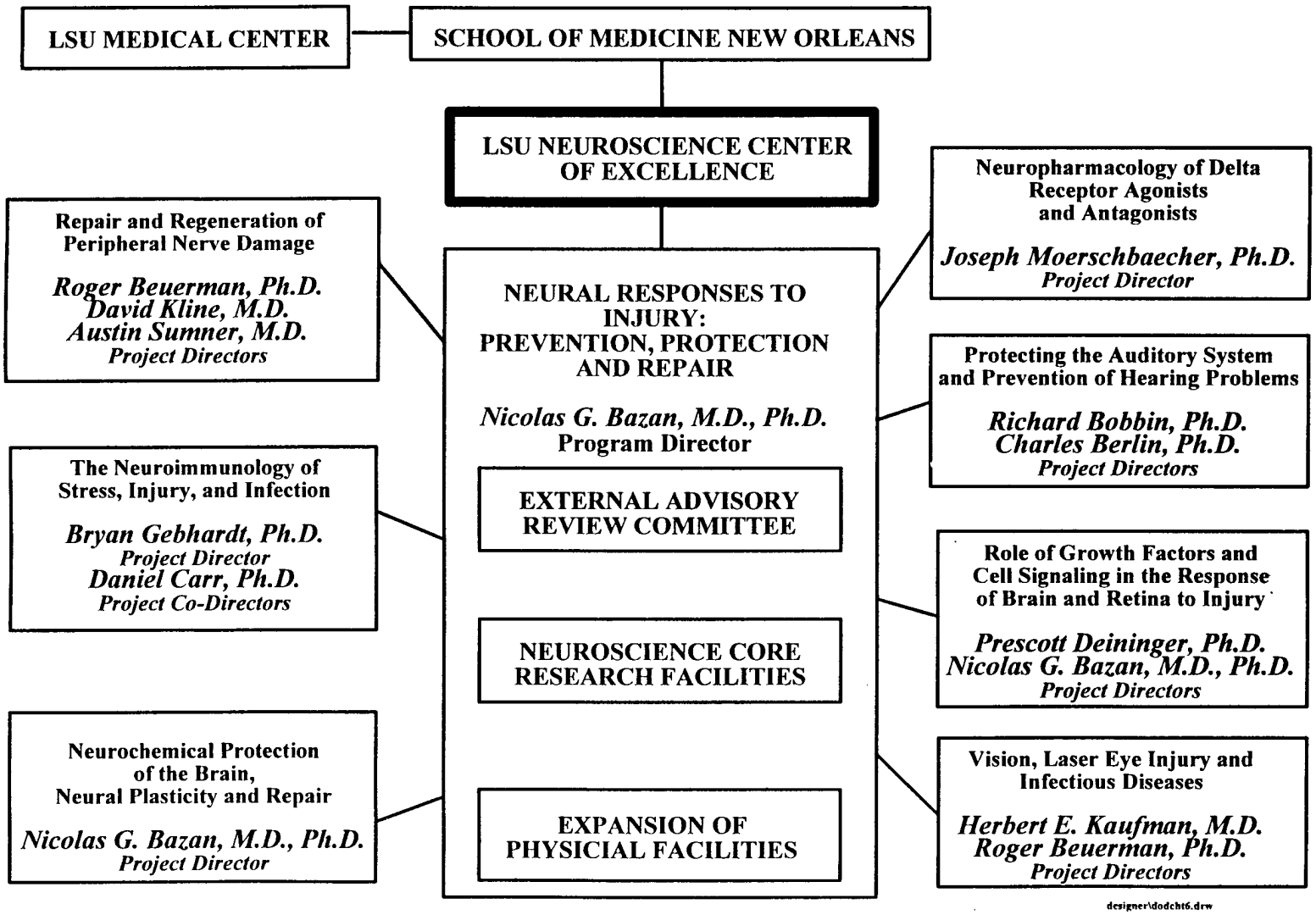

SCHOOL OF
MEDICINE IN NEW ORLEANS
Louisiana State University
Medical Center
2020 Gravier Street, Suite "B"
New Orleans, LA 70112-2234
Telephone: (504) 568-6700
Telefax: (504) 568-5801

Neuroscience Center
Office of the Director

October 18, 1997

Commander
U.S. Army Medical Research and Material Command (USAMRMC)
ATTN: MCMR-RMI-S
Building 504
Fort Detrick
Frederick, MD 21702-5012

RE: Fourth Annual report, Cooperative Agreement No. DAMD17-93-V-3013
Neural Responses to Injury: Prevention, Protection, and Repair

Dear Sir,

Please find enclosed the original and two copies of the fourth annual report for the Cooperative Agreement, reference above, between the USAMRMC and the Louisiana State University Medical Center School of Medicine, Neuroscience Center of Excellence. This report represents the research carried out during the fourth year of this agreement (20 September, 1996, to date). It is organized per project, each corresponding to a chapter of the original application. The critiques of the projects, as reported to us after the second annual report was reviewed by your office, have been taken into consideration in the preparation of these technical reports, and we believe that your comments concerning the last report have enabled us to more concisely report our progress.

We are very pleased with the progress that has been made in the fourth year of this agreement. As you will observe from the enclosed technical reports, our investigators have enjoyed a great deal of success on the projects, judging by their publications as well as by the technical reports themselves.

I am very pleased to inform you that the construction for the two additional floors of research space which are complete and at 90% working capacity. These two new floors provide additional laboratory space for the LSU Neuroscience Center as well as for the housing of the shared Core

Research Facilities equipment. Office space is also be available for the faculty and staff of the LSU Neuroscience Center of Excellence.

Please let me know if there is any further information that I can provide you.

Sincerely,

Nicolas G. Bazan, MD, PhD
Boyd and Villere Professor of
Ophthalmology, Biochemistry
and Molecular Biology, and Neurology
Director, LSU Neuroscience Center

NEUROSCIENCE CORE RESEARCH FACILITY

Core Research Facility Equipment at the Medical Education Building

In Year 4 of the DOD Agreement, the Calcium Imaging Facility (CIF) has continued to support DOD-Funded projects and to serve as a core facility for Neuroscientists throughout the LSUMC campus. Usage of the Facility has been divided up at approximately 20% hardware and software maintenance and development, 40% DOD-funded investigations, and 40% other neuroscience projects. Further descriptions of the specific projects are given in subsequent sections regarding the Medical Education Building.

Core Research Facility Equipment at the Eye Center

A second color dye sublimation printer has been added to the imaging facility lab at the Lions Eye building to facilitate production of high quality color and black and white printouts.

A Pentium-based PC workstation has been added to the imaging facility lab. This PC is used for two dimensional analyses of data obtained from video cameras attached to the confocal microscope as well as other compatible microscopes at the Neuroscience Center. This workstation has helped solve some problems that Noran could not solve with their 2D software. In addition, images obtained with video cameras are in color, and this information is often important in image analysis; the confocal microscope obtains data via PMTs which are on a grey scale, so no color information is included. A low light level, cooled charged-couple device (CCD) 3-color camera (Hamamatsu) resides with this PC imaging workstation. This camera has the ability to integrate low level light or fluorescent signal and can also store up to two images in memory, allowing for three

levels of color overlay from the same field. The image can then be sent to a color monitor and/or to the PC imaging workstation (by use of a frame grabber) for analysis. The PC imaging workstation also serves as an image archive for the Neuroscience Center with the purchase of a rewritable gigabyte jukebox tower that allows multiple swapable gigabyte disks to be loaded and analyzed.

A heated perfusion system has been purchased for the confocal microscope. This system will address the importance of temperature and on/off signals for analysis of cellular responses. The system is compatible with one used at the MEB.

Maintenance and Instrument Development at the Medical Education Building

The Facility has continued to add equipment useful to investigators that utilize the Noran Laser Scanning Confocal Microscope (LSCM). The main addition this year was a dual-technology, Dye-sublimation/Thermal wax color printer. This printer allows rapid access to a hard-copy of imaging results and enables us to produce publication quality images. Also, a perfusion chamber is now available so that bathing solutions can be changed rapidly while imaging cells. This has proved most useful in the studies where drugs need to be added to cells while measuring $[Ca^{2+}]_i$. Other equipment now available, includes a tissue slicer equipped for the production of living brain slices and a 1.3 Gb optical disk drive for off-line archiving of images. Software development in the Facility has also progressed. The electrophysiology data acquisition software, pClamp 6.0, has been installed and used in some preliminary trials. Noran has released a new version of their InterVision software for both image acquisition and image analysis. This software incorporates several new features requested by LSUMC users, including time-lapse capabilities, better pseudo-color capabilities, and image integration. It also has expanded image storage capacity so that more images

can be stored during a single experiment. All of these added capabilities have been installed, and their use is being fully explored as experiments proceed.

The Service contract on the LCSM, funded by the DOD, has played a vital role in maintaining the CIF this year. In December, several investigators noted a deterioration in the quality of the images collected in the facility. Consultation with Noran's technical support determined that this was due to a combination of factors, including a broken primary dichroic mirror holder and reduced efficiency of the laser. Although it required two visits from the technical support personnel and about six weeks of down-time for the CIF, both of these problems were fixed, and we ended up with a new laser that has better performance than the original one. More recently, there was an increase in the number of system errors and crashes involving the on-line optical disk used for image storage. Again, the problem was quickly resolved with the help of Noran's technical support, and the facility was operational with minimal down-time.

Maintenance and Instrument Development at the Eye Center

Dr. DeCoster has spent the necessary time to link the confocal and other imaging workstations and PCS via the local area network so that large images may be sent by using FTPs or other network utilities for printing or image analysis. This saves time that would otherwise be used shuffling disks between PCS and workstations so that files could be printed or analyzed. In addition, Dr. DeCoster has maintained the Indy workstation so that compatible software (such as Adobe Photoshop) can be used on both Silicon Graphics and Windows/DOS platforms. Dr. DeCoster also serves as the administrator for the imaging workstations in the imaging facility lab at the Neuroscience Center, dealing with such issues as data storage and file management, printing, slide

making, and microscope/camera use, as well as the necessary training needed for other scientists and technicians to make use of the instrumentation.

DOD-Funded Investigations

Current research projects at the Medical Education Building

Drs. Mize and Bobbin continue to be the principal DOD-funded users of the MEB Facility. They each have either finished, or are still working on, several projects utilizing the CIF equipment.

a) Distribution and Function of Calcium Binding Proteins in the Rat Superior Colliculus. (R.J. Cork, F-S. Lo and R.R. Mize)

This is an ongoing project with Dr. Mize as P.I.. Major progress was made this year, in that this project successfully competed for NIH funding from the National Eye Institute, in large part based on preliminary data collected in the CIF using DOD support. So far, the distributions of the calcium binding proteins (CaBP), Calbindin (CB) and Parvalbumin (PV), in neurons of the rat superior colliculus (SC) have been mapped using fluorescently labeled antibodies; and electrophysiology experiments, done by Dr. Lo, have characterized some of the membrane properties of cells in the optic layer, some of which contain CB. The two CaBP appear to be expressed in complementary sublaminar tiers that represent functional layers of neurons distinct from the morphological laminae of the colliculus. There is a dense band of CB-cells, centered in the optic layer. Electrophysiological recordings made from the optic layer reveal that these cells have characteristic membrane properties, including low threshold calcium spikes and a unique high frequency burst firing mode.

These experiments use the mutilabel protocols in the InterVision system, and customized look-up tables have been developed to display double-labeled images in pseudocolor. Two abstracts, detailing the results of these experiments, were presented at the Society for Neuroscience meeting in November '95 (San Diego, CA), and a manuscript describing the distributions of the CaBP in the SC is about to be submitted.

b) Involvement of NOS in synaptic plasticity.

(R.J. Cork, F-S. Lo, and R.R. Mize)

This new project is shortly to be awarded NIH funding from the National Institute of Neurological Diseases and Stroke, as a joint grant to the three co-investigators. Much of the preliminary data for the grant application was obtained with CIF support. This data included preliminary $[Ca^{2+}]_i$ measurements, electrophysiology, and immunocytochemistry. The project, which will start early in 1997, seeks to explore the role of nitric oxide synthase in directing axons to their targets in the developing rodent SC. This will be approached in three ways; electrophysiology, calcium imaging, and immunohistochemistry. The studies will principally focus on any interactions between NO, NOS, and the NMDA receptor during the early postnatal development of the colliculus. The results of early experiments suggest that NO is not involved in the formation of the patch/cluster system in the intermediate gray layer of the SC (Mize et al., 1996). This may be because the patches are composed of cholinergic afferents rather than glutamatergic ones. Drs. Lo, Cork and Mize have also begun to examine the development of synaptic currents, particularly NMDA, and the onset of long term depression (LTD) and potentiation (LTP) in the neonatal rat. This data will be compared to the development of NOS expression in the rodent SC.

c) Production of an acutely dissociated cell preparation suitable for calcium imaging.

(C. Leblanc, R.J. Cork and R.R. Mize)

This was a short project done by a Neuroscience graduate student who did a lab rotation in the CIF. The aim was to work out conditions for producing dissociated SC neurons that could be loaded with calcium indicators and imaged to measure either resting $[Ca^{2+}]_i$ levels or transient calcium responses to neurotransmitters. Such a preparation is an important part of the above two projects. Most of this project concentrated on determining the best methods for cell dissociation and the best ways to obtain maximum numbers of viable neurons in the preparations. Several successful experiments were done making dissociated cells and recording calcium transients induced in them with neurotransmitters. Some of these results were included in the preliminary data for the NIH grant application described in (b) above.

d) Calcium Transients in Response to Extracellular ATP in Isolated Cochlear Hair Cells.

(C. Chen, R.J. Cork, and R.P. Bobbin)

To extend their patch-clamp studies, Drs. Chen and Bobbin recorded calcium transients in the cells of their in vitro cochlear preparation. Preliminary experiments have shown that these cells can be loaded with indo-1-AM, and transient elevations of cytoplasmic calcium have been recorded in response to extracellularly applied ATP. These measurements will be extended to different cochlear cell types to determine if ATP functions as an extracellular signaling molecule. The patch-clamp equipment in the CIF has been installed and tested successfully with the cochlear preparation. In future it is expected that patch-clamp experiments will be combined with simultaneous calcium measurements. The preliminary data collected in the CIF has been included in a grant proposal submitted to NIH by Drs. Chen and Bobbin. Dr. Cork is included on that grant as a collaborator, and

a significant portion of the experiments will be done in the CIF.

Current research projects at the Eye Center

a) Role of lipid mediators in neuronal signaling processes.

(M. A. DeCoster and N. G. Bazan).

PAF continues to be tested in a complex set of experiments to address the immediate, long term, independent, and modulatory roles of this potent lipid mediator. While our research results are supported by recently published results (from other laboratories) that PAF rarely exerts a direct calcium increase on neurons, we have for the first time shown the neuroprotective effects of PAF receptor antagonist against excitatory amino acid toxicity to primary cultured hippocampal neurons. PAF alone may provide neuroprotective effects to neurons in culture. This is consistent with our observed results that long-term treatment with PAF may desensitize neurons as far as calcium response, to subsequent glutamate stimulation.

b) Phospholipases A_2 as factors in neuronal toxicity.

(M. A. DeCoster, M. Kolko, E. Rodriquez-de Turco, and N. G. Bazan).

The toxicity and lipid metabolism studies of PLA_2s effect of primary cortical neuronal cultures have been completed to the extent that this work has been published in a high priority scientific journal (Journal of Biological Chemistry, December, 1996). The calcium studies using PLA_2s will be published as a separate work and is still in progress, and has appeared in abstract form. The major finding from these studies was that the PLA_2s and glutamate work at the level of toxicity and lipid metabolism by different mechanisms and can show a synergistic effect when added together. The calcium studies are consistent with this so far, and will be guided by these soon to be

published results. **Other Projects**

Ongoing research projects at the Medical Education Building

a) Dr. Cindy Linn is studying calcium channels in catfish retinal cells. She is combining electrophysiology techniques with fluorescent calcium indicator measurements. Several successful experiments have been done using both ratio imaging and the continuous "Ratio Over Time" capability of the InterVision system.

b) Drs. Fu-Sun Lo and Bill Guido have been studying synaptic transmission in the rat LGN during early postnatal development. They find that the onset of EPSP's, IPSP's and LTP/LTD are developmentally regulated.

Ongoing research projects at the Eye Center

a) (Drs. M. A. DeCoster and N. G. Bazan). 3D reconstructions and animated movies of neurons and astrocytes from primary cell cultures, as well as brain tissue sections, continue to be used to model methods for scanning and analyzing cellular association and orientation via the confocal microscope.

b) (Drs. M. A. DeCoster, D. Linn, and N. G. Bazan). Fluorescent dyes have been injected into intact retinal tissue and imaged and analyzed using the confocal microscope. Calcium dynamics in stimulated retinas have been established both in control tissues as well as in retinas treated with calcium channel blockers and other antagonists. In addition, work is now being carried out to analyze calcium responses in retinas from different genetically engineered rodent models.

c) (Drs. M. A. DeCoster, Ying Tao, H. Bazan, and N. G. Bazan). Fluorescent calcium dyes have been loaded into primary cultured rabbit corneal epithelial cultures. It has been determined that

PAF (100 nM) induces a delayed, transient increase in intracellular calcium concentration ($[Ca^{2+}]_I$) in these cell cultures. The PAF receptor antagonist BN50730 blocks this calcium response to PAF. The PAF response is largely dependent upon extracellular calcium influx. Calcium channel blockers also block the response to PAF. This work has just been published in the journal *Investigative Ophthalmology and Visual Science* (November, 1997, Vol. 38, #12).

Goals for Year 5

Future goals at the Medical Education Building

Considerable progress has been made this year in acquiring new funding for research projects using CIF equipment. Dr. Mize submitted 2 NIH grant applications, one of which was funded in May '1996, the other to be funded in January 1997. Dr. Bobbin is currently resubmitting an NIH grant application, which if successful should start in mid 1997. All three of these grant applications have included preliminary data collected in the CIF, and they all fund continuing research requiring use of the CIF equipment. If all three projects are actively using the CIF, then together with Dr. Linn's project and Dr. Guido's, the Facility will be running at near capacity. There may be some time for short term research projects by other researchers. It is expected that the CIF will continue to play an important support role in the research projects of these LSUMC Neuroscientists. It is expected that the CIF users will continue to produce nationally recognized work that will enhance the reputation of LSUMC Neuroscience.

Future goals at the Eye Center

The imaging facility at the Neuroscience Center in the Lions Eye building is at a stage of rapid progress both physically and scientifically. More investigators are using the facility now for a wide array of projects from calcium imaging of living cells to cellular quantification and morphometric measurements of variously stained tissues and cell cultures. The computer processing and storage needs and capabilities have grown in tandem, and many of the workstations are now interconnected via networking utilities. The imaging facility has been successfully moved to the new 8th floor of the Lions Eye building in late September 1997, as coordinated by Dr. DeCoster. Dr. DeCoster will continue to be the coordinator for the imaging facility, managing computer and confocal microscope usage for the Neuroscience Center; these facilities will also be used in his own research. Technical support will most likely be retained to help with data analysis, file management, and presentation production associated with the imaging facility.

Publications

Cork, R.J., Lo, F-S., and Mize, R.R (1996) Postnatal development of synaptic plasticity in the rat superior colliculus: Long term depression in the superficial layers. *Soc. Neurosci. Abstr.* **22(1)** p.761.

Cork, R.J., Baber, S.Z. and Mize, R.R (1996) $Calbindin_{D28k}$ and parvalbumin in the rat superior colliculus. Exp. Brain Res. (to be submitted)

Cork, R.J., Baber, S.Z. and Mize, R.R (1995) $Calbindin_{D28k}$ and parvalbumin are expressed in complementary patterns in the rat superior colliculus. *Soc. Neurosci. Abstr.* **21** p. 656.

Lo, F-S, Cork R.J. and Mize. R.R. (1995) A high-frequency burst firing mode in neurons of the rat superior colliculus. *Soc. Neurosci. Abstr.* **21** p.655.

Mize, R.R., Banfro, F.T. and Scheiner, C.A. (1996) Pre- and post-natal expression of amino acid neurotransmitters, calcium binding proteins, and nitric oxide synthase in developing superior colliculus. Prog. Brain Res. (In Press)

Mize, R.R., Scheiner, C.A., Salvatore, M.J., and Cork, R.J. (1996) Inhibition of nitric oxide synthase fails to disrupt the development of cholinergic fiber patches in the rat superior colliculus. Dev. Neuroscience (Submitted)

Scheiner, C.A., Cork, R.J., and Mize, R.R. (1996) Inhibition of nitric oxide synthase fails to disrupt the development of cholinergic fiber patches in the rat superior colliculus. *Soc. Neurosci. Abstr.* **22(1)** p.761.

DeCoster, M. A. and Bazan, N. G.: Modulation of intracellular calcium dynamics in rat hippocampal neurons by platelet-activating factor. XV th Washington International Spring Symposium Abstracts, (1995) 82.

Kolko, M., DeCoster, M. A., and Bazan, N. G.: Neurotoxicity and modulation of calcium dynamics in rat cortical neurons by phospholipases. XV th Washington International Spring Symposium Abstracts, (1995) 106.

Kolko, M., DeCoster, M. A., Lambeau, G., Lazdunski, M., and Bazan, N. G.: Effect of secretory phospholipases A_2 on viability of rat cortical neurons and calcium dynamics. Soc. Neurosci. Abstr., 21 (1995) 608.

DeCoster, M. A., Bazan, H. E. P., and Bazan, N. G.: Platelet-activating factor induced intracellular calcium oscillations in rat hippocampal neurons. Soc. Neurosci. Abstr., 21 (1995) 1127.

Kolko, M., Rodriguez de Turco, E.B., DeCoster, M.A., and Bazan N.G.: Modulation of calcium, neurotoxicity and arachidonic acid release by phospholipase A type II and glutamate *in vitro*. FASEB Abstr., 1478 (1996) A1255.

Cinar, H., DeCoster, M.A., and Bazan, N.G.: Modulation of chronic neurotoxicity by combined kainate and glutamate treatment of hippocampal neurons. FASEB Abstr., 1646 (1996) A1285.

DeCoster, M.A. and Bazan, N.G.: Platelet-activating factor modulates intracellular calcium dynamics in rat hippocampal neurons. FASEB Abstr., 2153 (1996) A1373.

Kolko, M., DeCoster, M.A., Rodriguez de Turco, E.B., and Bazan, N.G.: Synergy by Secretory Phospholipase A_2 and Glutamate on Inducing Cell Death and Sustained Arachidonic Acid Metabolic Changes in Primary Cortical Neuronal Cultures. J. Biol. Chem. In press.

In addition to the above scientific publications, several images produced in the CIF have been published in different places. Two images are being used by Noran Instruments in their literature on confocal microscopes, and two images have been selected for the LSUMC 1996 'Art of Healing Exhibition'.

304.3

ON/OFF SUBLAMINATION IN THE FERRET LGN IS INDEPENDENT OF SYSTEMIC CHANGES IN BLOOD PRESSURE AND REQUIRES NEURONAL NOS. K. S. Cramer* and M. Sur, Department of Brain & Cognitive Sciences, M.I.T., Cambridge, MA 02139.

Blockade of nitric oxide synthase (NOS) with N-Nitro-L-Arginine (L-NoArg) during the third and fourth postnatal weeks in the ferret disrupts the formation of ON/OFF sublaminae (Cramer and Sur, 1994). Because NO is a potent vasodilator, we examined the role of systemic changes in blood pressure on sublamination during systemic treatment with L-NoArg. Mean arterial blood pressure (MAP) was measured during the fourth postnatal week in four animals treated with 40 mg/kg/day i.p. L-NoArg from postnatal day 14 (P14) and in four normal, age-matched controls. MAP ($\pm$ s.e.m.) increased from 57.6 $\pm$ 4.6 mmHg to 83.1 $\pm$ 4.8 mmHg following L-NoArg treatment. When animals received the antihypertensive calcium channel blocker verapamil, 5 mg/kg/day i.p., together with L-NoArg, blood pressure was normal (60.0 $\pm$ 1.6; n = 4). In these animals, sublamination was assessed in sections of LGN contralateral to an intraocular injection of WGA-HRP; disruption of sublamination was similar to that seen in animals treated with L-NoArg alone, suggesting that NOS blockade-induced changes in retinogeniculate projections occur independently of changes in MAP.

Sublamination in the LGN relies at least in part on the neuronal form of NOS. Neuronal NOS immunohistochemistry was similar to NADPH-diaphorase histochemistry in its transient expression during retinogeniculate segregation. In addition, ON/OFF sublamination was disrupted by blockade of the neuronal form of NOS from P14 to P26 with 7-nitroindazole, which appears not to produce hypertension. While systemic changes in blood pressure are not involved in the segregation of sublaminae, further experiments are necessary to examine the role of local changes in cerebral blood flow produced by NO release. *Supported by EY07023*

304.4

ROLE OF SPONTANEOUS RETINAL ACTIVITY IN REORGANIZATION OF RETINOGENICULATE CONNECTIONS DURING DEVELOPMENT. P.M. Cook*, G. Prusky and A.S. Ramoa Dept. of Anatomy, Virginia Commonwealth Un., Richmond, VA 23298 and Dept. of Psychology, Un. of Lethbridge, Lethbridge AB T1K3M4.

The adult form and function of the lateral geniculate nucleus (LGN) arise after extensive modifications in circuit organization that include segregation of axonal arbors from the two eyes into eye-specific layers. Previous studies have shown that intracranial infusion of tetrodotoxin (TTX) in fetal cats prevents segregation (Shatz and Stryker, 1988), suggesting that spontaneous action potential activity contributes to remodeling of the retinogeniculate pathway. We have examined the activity-dependent mechanisms of eye-specific segregation using a technique which allows direct inferences about the role of spontaneous retinal activity. Our method uses continuous intraocular application of TTX to block spontaneous discharge of retinal ganglion cells in newborn ferrets, which display retinogeniculate remodeling during the first 2 weeks of postnatal life. After a 2 week infusion, intraocular injection of horseradish peroxidase (HRP) revealed the projection pattern contralateral and ipsilateral to the HRP injected eye. Eye-specific segregation of retinogeniculate projections was observed at postnatal day 14 in controls as well as in ferrets that received monocular (n=3) or binocular (n=1) injection of TTX. However, segregation was aberrant in the monocularly injected animals. First, projections from the untreated eye occupied an approximately 50% larger volume of both LGNs than those from the TTX-treated eye. The total size of the LGN, however, remained unaltered and this suggests that the normal eye invaded territory normally occupied by the TTX treated eye. Moreover, a low density of afferents from the contralateral eye were observed to terminate in layer A1, which normally receives only ipsilateral eye input. These results suggest that binocular competition modulates rearrangements in retinogeniculate projections. Additionally, they are consistent with the hypothesis that spontaneous retinal activity may fine-tune segregation of retinal afferents into eye-specific layers. (Supported by NSF IBN-9421983)

304.5

POSTNATAL DEVELOPMENT OF SYNAPTIC PLASTICITY IN THE RAT SUPERIOR COLLICULUS: LONG-TERM DEPRESSION IN THE SUPERFICIAL LAYERS. R. J. Cork*, F-S. Lo and R. R. Mize. Anatomy Department and Neuroscience Center of Excellence, LSU Medical Center, New Orleans, LA 70112.

We have been studying the development of the synaptic circuitry in the rat superior colliculus (SC) between ages P1 and P10. Using an in-vitro brainstem preparation, we have measured extracellular field potentials, and made whole-cell recordings of postsynaptic potentials, from the superficial layers of SC. We have also used immunocytochemistry and NADPH-histochemistry to map the development of various molecules thought to be involved in modulating synaptic transmission (i.e. NMDAR1, and NOS). Field potentials or post-synaptic potentials were measured following stimulation of optic tract (OT) fibers. Whole cell recordings showed EPSPs with two components. The later component was blocked by APV, suggesting that it was mediated by the NMDA receptor. NMDAR1 antibody also intensely labeled the neuropil of the superficial layers at P1. From P3 some neurons also showed an IPSP following the EPSP. The IPSP could be blocked by bicuculline, an antagonist of $GABA_A$ receptors. Between ages P1 and P8, tetanic stimulation (50 Hz, 20 s, submaximal intensity) induced a long-term (>90 min.) depression (LTD) of the field potential and the EPSP. Neither APV (10 μM or 50 μM) nor bicuculline (10 μM) could prevent LTD, suggesting that it is independent of either NMDA or $GABA_A$ receptor activation. Nitrendipine (5 μM), an L-type Ca^{2+}-channel blocker that blocks induction of LTD in the hippocampus, also failed to prevent LTD induction in the SC. The magnitude of the LTD decreased steadily from P1 to P8 and at P9/P10 tetanic OT stimulation induced a mixture of depression and long-term potentiation (LTP). Consistent with the idea that NOS promotes LTP, significant NOS expression was first observed in cells of the superficial layers at P9.

Supported by DOD cooperative agreement DAMD 17-93-V-3013, NIH grant EY02973, and the LSUMC Neuroscience Center.

304.6

INHIBITION OF NITRIC OXIDE SYNTHASE FAILS TO DISRUPT THE DEVELOPMENT OF CHOLINERGIC FIBER PATCHES IN THE RAT SUPERIOR COLLICULUS. C.A. Scheiner*, R.J. Cork and R.R. Mize. Dept. of Anatomy and the Neuroscience Center, Louisiana State University Medical Center, New Orleans, LA 70112

Nitric oxide (NO) has been proposed to be a retrograde messenger involved in synaptic refinement during development. The patch-cluster system in the intermediate gray layer (IGL) of the superior colliculus (SC) is an excellent model for studying the role of NO because both the clustered neurons and one of the fiber systems (ACh) that form the patches contain NOS during development. We have used Nω-nitro-L-arginine, an inhibitor of nitric oxide synthase (NOS), to determine if inhibition of NOS disrupts the formation of the ACh patches. Sprague-Dawley rats received 1-100 μM of NoArg from birth until sacrifice at P10, P14, P18, P21-22, or P28. Control animals were litter mates of the experimental animals plus other younger and older animals. ACh fibers were identified using choline acetyltransferase (ChAT) immunocytochemistry and NOS containing cells were labelled with nicotinamide adenine dinucleotide phosphate diaphorase (NADPH-d) histochemistry. NADPH-d was expressed in cells within the periaquaductal gray (PAG) and the deep gray layer (DGL) of the SC by P4, the earliest age examined. By P9, many cells in the IGL expressed NADPH-d, while few in the superficial layers were labeled. Some of these neurons in the IGL formed obvious clusters, while others were loosely scattered throughout the layer. NADPH-d labeling in IGL cells declined by P14-P18 and virtually absent in the adult. ChAT labeled fibers first appeared in the IGL at P10 and were readily visualized by P14. At this age, the ChAT fibers were fairly uniformly distributed through the IGL, but by P18 they had a patch like distribution with as many as five patches spaced at 250-300 μM intervals. Inhibition of NOS from birth produced no qualitative differences in the distribution or density of ChAT labeled fibers at any of the ages examined. We therefore conclude that NO does not contribute to the refinement of cholinergic fiber patches in the rat SC, probably because the fiber system is not glutamatergic. Supported by NIH NEI-02973, DOD cooperative agreement DAMD 17-93-V-3013,a Louisiana State Board of Regents Graduate Student scholarship, and the LSUMC Neuroscience Center.

304.7

ROLE OF RETINAL ACTIVITY IN MATURATION OF ELECTROPHYSIOLOGICAL MEMBRANE PROPERTIES AND SYNAPTIC RESPONSES OF FERRET LGN A.S. Ramoa* and G. Prusky Dept. of Anatomy, Virginia Commonwealth University, Richmond, VA 23298 and Dept. of Psychology, University of Lethbridge, AB T1K3M4.

The adult form and function of the lateral geniculate nucleus (LGN) arise after extensive modifications in circuit organization that, in the ferret, occur during the first postnatal month. We have shown that electrophysiological membrane properties and synaptic responses in LGN neurons of the ferret change markedly during this critical period of development (J. Neurosci. 14:2089, 1994; J. Neurosci. 14:2098, 1994; J. Neurosci. 15:5739, 1995). These changes, which appear to be coordinated to facilitate circuit remodeling of LGN neurons, include: late maturation of low-threshold Ca++ spikes and inhibitory potentials as well as developmental switches in the expression of NMDA receptor isotypes. We examined whether these changes are regulated by retinal activity. Our method uses continuous intraocular application of tetrodotoxin starting as early as the day of birth to block spontaneous discharge of retinal ganglion cells. Whole-cell recordings in the LGN slice preparation revealed that maturation of low-threshold calcium spikes and hyperpolarization-activated currents was unaltered by a 3 to 4-week binocular infusion of tetrodotoxin. In contrast, synaptic properties were markedly affected. Treated animals at P40 were found to display long duration NMDA-EPSCs that resembled those present in normal newborn animals rather than the shorter-duration EPSCs seen in normal animals at similar age ($P<0.01$). Additionally, application of ifenprodil, which binds with higher affinity to heteromeric receptors containing the NR-2B subunit, blocked more potently NMDA-EPSCs in newborn and TTX-treated animals animals at P40 than in normal P40 animals ($p<0.01$), suggesting that a developmental switch in the subunit composition of the NMDA receptor is prevented by intraocular TTX. In conclusion, retinal activity may regulate developmental changes in synaptic properties of LGN neurons (NSF IBN-9421983).

304.8

CHOLINERGIC PROCESSES IN XENOPUS TECTUM. M.J. Titmus*, L. Pleban, R. Lima & S.B. Udin, Dept. of Physiology & Biophysics, SUNY, Buffalo, NY 14214.

The ipsilateral visual input to Xenopus tectum comes into register with the contralateral map during development. The major transmitter for the contralateral (retinotectal) input is glutamate, and the major transmitter for ipsilateral input, relayed via the nucleus isthmi, is probably acetylcholine. The role of NMDA receptors in the activity-dependent process of organization of the ipsilateral map is demonstrated by the ability of NMDA receptor blockers to prevent matching of the ipsilateral map to the contralateral map during the critical period, but little is known about the role of acetylcholine.

Immunohistochemistry indicates that nicotinic receptors are located in the layers of the tectum that receive binocular inputs; unilateral eye enucleation indicates that most of those receptors are located on retinotectal axons. Receptor binding using tritiated cytisine also indicates the presence of nicotinic receptors in the tectum. Muscarinic receptors are located on cells and dendrites located appropriately to receive isthmotectal input.

Calcium imaging using Fura-2 in tectal slices demonstrates no measurable response to nicotinic agonists alone, but shows significant synergism when nicotine or cytisine are applied with NMDA. In contrast, muscarinic agonists decrease calcium influxes elicited with NMDA. These results suggest that activity of isthmotectal axons can significantly modulate the effects of glutamate released from retinotectal axons.

Supported by USPHS Grant EY-10690 to M.J.T and S.B.U.

Calbindin$_{D28k}$ and Parvalbumin in the Rat Superior Colliculus.

R. John Cork, Sayed Z. Baber and R. Ranney Mize

Department of Anatomy, and Neuroscience Center of Excellence, LSU Medical Center, New Orleans, Louisiana LA 70112.

ABSTRACT

We have mapped the distributions of two calcium binding proteins (CaBP), calbindin$_{D28k}$ (CB) and parvalbumin (PV) in the rat superior colliculus (SC). The dominant feature of the distributions was a band of strongly labelled medium-sized CB cells centered on the optic layer (ol). Parvalbumin cells were found predominately in the intermediate gray layer (igl) where they were clustered in patches of PV labelled fibers. The superficial gray layer (sgl) could be divided into two sublaminae based upon CaBP expression. CB-labeled cells were found mostly in the dorsal half of the sgl, many of them being vertically oriented small bipolar cells. PV-labeled cells were generally found in the ventral part of the sgl and dorsal ol. Some of the sgl PV cells had morphologies similar to those of the small vertical CB-cells, but there were also horizontally oriented cells. Overall, the CaBP cells are distributed in complementary tiers that are not restricted to the traditional laminae. This suggests that there are functional sublaminae in the colliculus.

INTRODUCTION

The calcium binding proteins (CaBP), calbindin$_{D28k}$ (CB) and parvalbumin (PV) have been used as anatomical markers for functional groups of neurons (Celio, 1990). They are often expressed in discrete populations of neurons with complementary distributions, and in some parts of the brain they are found in subpopulations of GABAergic neurons (e.g. Celio, 1986; Hendry, et al, 1989; Miettinen, et al., 1996).

The physiological relevance of the two CaBP is unclear. The superfamily of CaBP comprises many molecules with one or more "EF-hand" calcium binding sites. Those members of the family whose function is known (e.g. calmodulin) are regulatory proteins that undergo conformation changes upon calcium binding and then affect the activity of other proteins. Neither CB nor PV have any known regulatory function. It has been suggested that they act as calcium buffers, dampening cytoplasmic calcium transients, and possibly protecting neurons against any toxic effects mediated by elevated calcium levels. This possibility is not, however, supported by some of the bichemical studies of CB structure. CB appears to have 6 calcium-binding sites of which maybe 4 are active(Ref). The binding constants for these sites vary but the apparent calcium binding constant for CB is about 10^{-8} M (Ref) suggesting that all the calcium binding sites would be fully occupied at physiological levels, and that transient changes in calcium would not have any effect on the calcium binding status of CB. If the other possibility, that these CaBP have some regulatory role, is true then by analogy with calmodulin it might be expected that CB would undergo a conformation change upon calcium binding Leathers & Norman (1993) have found that CB does indeed undergo calcium-dependent conformational changes that affect its binding to several membrane bound proteins, however the details of what it binds to, and what effects it might have, are not known. Although there is this uncertainty about the *in vivo* functions for these proteins, it is clear that excess CB or PV introduced into cells can buffer calcium transients induced by

depolarization (Chard et al., 1993). Whether they are simply passive calcium buffers, or whether they might regulate the activity of specific proteins, depending on $[Ca^{2+}]_i$, remains to be determined.

Attempts to identify physiological roles for these CaBP have concentrated mainly on correlating CaBP content with cell location, morphological characteristics, or different physiological properties of the cells. As it has been suggested that a major function of these CaBP is to protect neurons from the damaging effects of excess calcium influx, whether due to repeated stimulation, ischemia, or neuropathological diseases, the presence of CaBP has often been correlated with neuronal survival after different insults that cause elevation of cytoplasmic calcium levels. CB is found specifically in two types of rat hippocampal neurons, dentate granule cells and CA1 pyramidal neurons, that are relatively resistant to excitotoxic damage. CB expression in the dentate gyrus granule cells is increased in response to repeated stimulation, suggesting that CB expression is regulated by $[Ca^{2+}]_i$ (Lowenstein et al., 1991), and Iacopino & Cristakos (1990) reported that CB expression in these cells could be upregulated by corticosterone although this effect might also be due to an increase in $[Ca^{2+}]_i$ rather than direct gene regulation. The situation with protection against ischemic damage is less clear. The dentate gyrus granule cells are vulnerable to ischemic damage until CB-IR has developed in the cells (Goodman et al. 1993) but vulnerability to ischemic damage in different neuronal populations is not well correlated with CB-IR. The CA1 pyramidal neurons are the most susceptible to damage while the CA3 pyramidal neurons that do not contain CB are less vulnerable (Goodman et al., 1993). CA1 interneurons which contain CB or PV are mostly protected against the damaging effects of ischemia (Johansen et al., 1990).

While these correlational anatomical studies have not been very successful in elucidating functions for CaBP, several studies have begun to look for physiological correlates of CaBP expression. Because of the co-expression of PV and GABA in some cells it has been proposed that PV cells should be highly active neurons with high firing rates (Celio, 1986). When Kawaguchi & Kubota (1993) correlated the morphology and electrophysiology of GABAergic nonpyramidal cells in the rat neocortex with their CaBP content, they did find that PV cells were fast spiking, while CB cells had low threshold calcium spikes. However, Li et al. (1995) reported that endogenous CB controlled the firing mode of neurons in the rat supraoptic nucleus by affecting calcium dependent depolarizing after-potentials, and excess CB shifted neurons from a phasic firing pattern to a fast continuous firing mode.

The superior colliculus (SC) should prove to be a productive structure in which to study the possible functions of CaBP. The mammalian superior colliculus is structurally multilayered and, at least in the intermediate layers, is compartmentalized into functional units. This compartmentalization is reflected in both the distributions of various biochemical constituents of the collicular cells, as well as specific arrangments of afferent fibers. The SC contains multiple populations of cells that can be grouped together on the basis of neuronal class, morphology, location, biochemical content, synaptic contacts or projection site. One of the biochemical markers of these compartments is PV (Illing, 1992), and CB is known to be expressed in specific subpopulations of the cells in the SC (Lane et al., 1993). In his major survey of CB and PV in the rat brain, Celio (1990) stated that the distributions of CB and PV are similar " in the upper two layers and complementary in the lower four layers." In the cat SC the distribution of PV is complementary to that of CB neurons, with two tiers of PV neurons lying between three tiers of CB cells (Mize et al. 1992). Thus establishing correlations between their CaBP content and the morphology and physiology of the cells in the different SC subpopulations should help to establish what the functions of CB and PV are.

Although several investigators have looked at different aspects of PV and/or CB in the rat SC, there have been no detailed studies comparing the distributions of these two CaBP in the rat. Celio's (1990) survey gave only a brief description of their distributions. Illing et al.(1990) described the distribution of PV in rat SC, and Illing (1992) reported that PV expression correlated with the compartmental architecture of the intermediate SC layers. Schmidt-Kastner et al.(1992) made a cursory examination of PV and CB staining patterns in the rat SC during their study of the effects of SC deafferentation. Lane et al. (1993) described a population of calbindin-immunoreactive (CB-IR) cells in the optic layer of the rat SC.

Some reports have described CaBP-distributions in the colliculi of other species. Mize et al. (1991) described the distribution and morphology of CB cells in the cat SC. They found three laminar tiers of CB cells. Most of the CB cells were interneurons but only a very small percentage of them contained GABA. Behan et al. (1992) studied the localization of CB in the hamster SC and they also concluded that CB was not co-localized with GABA in the SC. In 1992, Mize et al. reported that CB and PV are expressed in complementary sublaminar patterns in the cat SC. In this report we extend these observations to the rat SC with the intent of developing the rat SC as a model system in which to investigate the physiology of the CaBP containing cells.

MATERIALS AND METHODS

Male Sprague Dawley rats (250-300g; n=6) were anesthetized with Halothane or Ketamine/Xylocaine and perfused intracardially with ~400 ml of 4% paraformaldehyde in phosphate buffered saline (PBS) (pH 7.4). The brain was removed and the midbrain was blocked coronally and mounted on the stage of a vibratome with cyanacrylate glue. Serial sections, 50 μm thick, were cut through the SC.

CaBP Immunocytochemistry

In most experiments, alternate sections were labeled for either CB or PV. Sections were incubated in 1% $NaBH_4$ for 30 min. followed by 4% Normal Horse Serum (NHS) for 30 min. Sections were then labeled with primary antibody (1:400 Mouse anti-CB (Sigma) or 1:500 Mouse anti-PV (Sigma)) for 8- 16 hrs.. After another 30 min incubation in 4% NHS, sections were treated with a biotinylated secondary antibody, (1:200 Horse anti-Mouse (Sigma)) for 30 min. Antibody labelling was visualized using Vectastain Avidin-Biotin Complex (ABC) or ABC Elite (Vector Laboratories, Burlingame, CA). After a 1 hr incubation sections were stained by treatement with Diaminobenzidine hydrochloride (0.005%) and hydrogen peroxide (0.003%) for 1-3 min. Sections were given multiple rinses with PBS between each step. Antibody dilutions were made in 1% NHS in PBS.

In experiments to determine if cells co-expressed CB and PV, sections were double labelled with Mouse anti-CB (Sigma) and Rabbit anti-PV (Swant) primary antibodies. Normal Goat serum was substituted for the NHS used in single antigen lebeling experiments. Instead of ABC/DAB staining sections were incubated in a mixture of fluorescently tagged secondary antibodies; 1:150 FITC Goat anti-Rabbit, or BODIPY-FL Goat anti-Rabbit, and 1:150 R-Phycoerythrin (PE) Goat anti-Mouse (Molecular Probes). Images were collected with the Noran Odyssey laser scanning microscope using the 488 nm laser line for excitation. Separate images were collected simultaneously at 510 - 545 nm for Bodipy/FITC and 555-625nm for PE.

NTS Plotting

Cell locations were mapped using a Eutectic Neuron Tracing System, marking the positions of all labeled cell bodies in a dorsal quadrant of the SC sections, and outlining the surface of the midbrain. The NTS software calculated the depth of each cell as the shortest (airline) distance between the cell and the dorsal edge of the colliculus. Data was collected from 9 representative sections; three sections (caudal, central, and rostral SC) from 3 different rats.

Cell Body Morphologies and Locations

Drawings of CaBP labeled cell bodies were made using a Zeiss microscope with a drawing tube. Cell locations were determined by making drawings at 4x, cell bodies and proximal dendrites were drawn at 60x or 100x. The montage of cell bodies (Fig. X) was constructed by placing the center of each cell soma at the appropriate distance from the dorsal surface of the SC. Cells were oriented in the montage so that the angle between the proximal dendrites and the closest part of the dorsal surface was correct.

Cell Densities and Soma Areas.

Numerical densities (Number of cells per unit volume) were determined using the method described in Albers et al. (1988). As we cut 50 μm thick sections, and the equations used by Albers et al. (1988) are based on assumptions that are most reliable for infinitely thin sections, we reduced the effective section thickness by determining the number of nuclei per unit area in a single focal plane (approx 2.5 μm thick).

The average area of cell bodies were obtained using a Joyce-Loebl Magiscan image analyzer. Representative sections were scanned for complete cell body profiles lying within selected layers of cells. Complete profiles were defined as those with a well defined nucleus and a clearly visible nucleolus. Only cell profiles containing a nucleus and nucleous were included in this analysis. Acceptable profiles were outlined on the video monitor with a light pen, and the computer calculated areas. Statistical analysis of the area data was all done with the Magiscan system.

3D Reconstruction.

The three dimensional distribution of the CB-containing cells in the optic layer was examined by reconstructing the immunocytochemically labeled sections. Images of all the sections from 1 rat were collected with a JVC high resolution video camera. Outlines of the midbrain surface, central aqueduct, and the outer limits of the CB labeling were digitized from these images with a digitizing tablet. Digital data was then transferred to a SGI workstation, running Skandha 3D-reconstruction software. After aligning the sections, a 3-D model of the colliculus and CB cell layer was constructed in the computer. This model could be displayed on a computer monitor. To examine the shape of the CB-cell layer, the reconstruction could be rotated about any of 3 orthogonal axes and the opacity of the outer surface could be reduced.

RESULTS

Distribution of labeled cells in the SC.

The most distinctive feature in all the CaBP labeled sections was a band of CB-immunoreactivity (CB-IR) in the ol and dorsal igl. (Figure 1. a. low power CB-DAB and b. low power Fluorescence) containing densely labeled, medium-sized cell-bodies in a meshwork of labeled fibers. Smaller lightly labeled neurons were distributed throughout the sgl (Fig 1c) and in

the deeper layers there were the occasional larger cell bodies (Fig 1d). *[Description of neuropil labeling]*

The pattern of PV staining was rather featureless. There was light uniform staining of the sgl neuropil, (Fig. 1e) and medium to large labeled cells scattered throughout the deeper collicular layers. Some lightly stained, small to medium sized cells were seen in the superficial layers. In most sections there were so few PV cells that a pattern of labelling was not discernable, however in some sections through the caudal half of the colliculus, two features of the PV distribution were evident. There was a thin band of medium sized cells in the ventral sgl just dorsal to the ol, and a thicker band of cells and labelled fibers in the igl. In the igl the pattern of labelling was patchy with cell somas and labelled fibers occuring in clusters.(Fig 1f)

The layer of heavily labeled CB cells was so obvious in the sections that it could be mapped into a 3-D reconstruction of the SC (Fig. 2). It was present throughout the SC with a relatively uniform mediolateral width along the anteroposterior axis. The layers are thicker along their medial edges giving the overall impression of two wings. (Figure 2. 3-D image of CB layer). As the PV cellular labeling was less clearly defined, it was not so obvious where the edges of any PV lamellae were. Nevertheless, a 3-D reconstruction suggested that there was a band of PV cells that lay ventral to the CB "wings", and that this band was thicker laterally (data not shown).

When the locations of all the CaBP-IR cells in sections through the SC were plotted most CB cells were distributed in two bands in the superficial layers (Fig 3). In addition to the band of cells in the ol there was a more diffuse band of cell bodies scattered throughout the sgl. This upper band of cell bodies was concentrated in the dorsal two thirds of the sgl. In some sections there was also a thin line of CB cells in the zonal layer (zl). CB cells were scattered throughout the deeper SC layers without any obvious pattern. Between the two superficial CB layers there was a clear gap that was mostly empty of cells. Although it was not confirmed by any quantitative analysis, cells in the ol sometimes seemed to form clusters giving the band of cells a "patchy" appearance.

There were fewer PV-IR cells than CB-IR ones in the SC (Fig 4). The plots of PV cell locations showed cells scattered throughout the intermediate and deep layers with some cells in the superficial layers. There was little evidence of any laminar pattern of PV distribution except in caudal sections, where the cells in the ventral sgl lay in an obvious band (Fig . 4).

Depths and thickness' of the cell layers

As the laminae of the colliculus have often been defined in terms of their depth below the surface of the tectum we collected data on the depths of Cb and PV cell bodies. Data was collected from several sections from 3 different rats. The sections chosen were of similar shape and size, and were taken from similar locations along the rostral-caudal axis of the midbrain e.g. the central region of the SC. The NTS software calculated the depth of each cell from the data files of cell distributions. Depth was defined as the shortest distance between the cell body and the dorsal surface of the colliculus. In total, depths were calculated for 3947 CB-cells from 7 sections, and 1200 PV-cells from 6 sections.

The peaks in the cell-depth histograms illustrate the relative densities and thickness' of the various tiers of cells. Three peaks are seen in the CB cell distribution (Fig 5A). Most CB cells are in the sgl between 100 - 300 μm from the dorsal surface. The heavily stained cells in the ol lie in a band between 300 - 600 μm. There is then a dispersed population of cells in the dgl at depths ranging from 1200 - 2000 μm. The peaks in the PV histogram (Fig 5B) are less distinct, but there is a clear peak centered at 300 μm and a broad peak between 700 - 1200 μm.

Superimposing the two depth distributions (Fig 5C) shows that the patterns of CaBP expression are complementary, with the PV tiers centered between the CB tiers. The approximate boundary depths of the superficial SC layers are shown for reference. The depths of these particular layers were compiled as averages from several studies of the rat SC laminae (e.g. Albers et al., 1988, Lane et al. 1993). It should be noted that the deep SC laminae, below the ol, are not uniform in thickness mediolaterally, nor are they parallell to the dorsal surface of the SC as are the superfical layers. The combination of these two factors means that there is only an approximate correspondence between depth and a particular cell layer, and the distributions of cell depths are broader (e.g. Fig. 5C) than the thickness' of the layers they represent. There is always some overlap of the depth values of cells in a particular deep layer with those for adjacent layers.

If the depth distributions are plotted as percentages of the total number of CaBP-containing cells, instead of as percentages of CB- or PV-cells, the relative densities of the two CaBP in the different layers are revealed (Fig 5D). CB cells predominate in most regions of the colliculus, even at some of the depths where the PV laminae are. The only SC layer where there are more PV cells than CB ones is in the igl between 800 μm and 1200μm.

Cell size and morphology in the different layers

Having determined that there are alternating bands of CaBP immunoreactivity in the SC, we wanted to determine if the populations of cells in particular tiers had any distinguishing morphological characteristics. We determined the average size of the cell body profiles in the individual tiers (Table 1).

Tier	Mean Area of Cell body (μm^2)	s.d. (μm^2)
Calbindin: sgl	84	21.5
Parvalbumin: sgl/ol	151	31.2
Calbindin: ol/igl	184	53.1
Parvalbumin: igl/dgl	211	95.1

Table 1. Mean area of cell bodies in specified tiers. Data was collected using the Magiscan Image Analyzer, scanning along specific cell tiers.

The results of the cell area measurements show that CaBP content is not correllated with cell size, as neither CB nor PV are confined to cells in a particular size range. However, cell size is correlated with depth in the SC. There is a steady increase in cell size from the small cells near the dorsal surface to the much larger cells in the deep layers. Instead of being correlated with cell size CaBP content seems rather to be a function of location in the SC. Thus a cell's location in the ol is a better predictor of its CaBP content than its size. It is nonetheless true that cells in particular tiers fall within characteristic size ranges. Thus the CB cells in the sgl and ol/igl belong to statistically different populations of cells.

The determination of which cell morphologies were represented in the different CaBP layers was done by drawing well labelled cells, and proximal dendrites, and compiling a montage of the cells at their appropriate depths (Fig 6). We concentrated on the morphologies of the cells in the superficial collicular layers as these have been described in detail (e.g. Langer & Lund, 1974 ;

Labriola & Laemle, 1977; Wharton & Jones, 1985) and little is known about the cell types in the deeper layers. The CaBP-labeled material contained examples of all the major cell types described in Golgi stained sections (Langer & Lund, 1974; Labriola & Laemle, 1977). *Marginal cells were found in both the CB and PV-labelled sections*, as were vertical fusiform cells and horizontal cells. Two of the cell types appeared to be confined to one or other CaBP. Most, if not all, of the CaBP-containing wide-field vertical cells were CB-cells, and all the stellate cells we observed contained PV. However, as the sample of cell drawings is rather small, we cannot say definitely that either CaBP is found exclusively in a particular cell type.

Double label results

Fluorescently labeling both CB and PV in the same sections enabled us to determine if any cells expressed both CaBP. Low magnifications views of the SC, confirmed the complementary patterns of CaBP distribution (Fig 7A). At higher magnifications, confocal microscopy of the double labeled sections revealed that almost all CaBP-cells contained only PV or CB, but not both proteins. A few cells were seen that might have contained both proteins, but we could not rule out the possibility that these examples were due to overlap of two cells in different focal planes, or that they were due to "bleed-through" of signal from one fluorescent label into the channel for the other label's signal.

DISCUSSION

Distribution of CB and PV in the superior colliculus

Our results show that PV and CB are distributed in alternating tiers of cells that form sublaminae of the traditional divisions of the SC. There are three layers of CB cells with two PV layers interspersed between them. The upper band of CB cells occupies the dorsal two-thirds of the sgl and is mainly composed of vertically-oriented lightly labeled cells. Most of the cells are bipolar with small fusiform cell bodies (*cell sizes*). There are also vertically oriented pyriform cells and horizontal bipolar cells. The middle band of CB cells overlays the optic layer and consists of heavily labeled medium-sized cells in a mesh work of labelled fibers. Most of the cells appear to be wide field vertical cells with laterally oriented proximal dendrites projecting up into the superficial layers.

Two distinct populations of CB-cells have previously described in the upper layers of the SC. Schmidt-Kastner et al. (1992) briefly described, a layer of medium-sized CB cells with predominately vertically oriented dendrites in the ventral sgl, and a plexus of strongly stained neurons just ventral to the ol. Although the locations of these CB cells are ventral to those we assigned the cells, we assume that these two populations correspond to the upper two CB tiers described in this paper. Lane et al. (1993) presented a more detailed picture of CB distribution in the superficial layers of the rat SC. They found an upper band of small fusiform cells in the dorsal half of the sgl, and a heavily labeled band of medium-sized cells in the ol. Cells in the latter band were mostly wide-field vertical or medium-sized stellate cells. Using retrograde labeling, they also determined that the majority, if not all, of the CB-cells in this band projected to the lateral posterior nucleus (LP) of the thalamus. The majority (80%) of the LP projecting neurons contained CB and about 15% contained both CB and adenosine deaminase.

Between the two CB layers lies a band of PV cells. Its dorsal edge overlaps with the superficial CB tier and contains a similar mix of cell types plus some stellate cells. Cells in the ventral part of this PV layer lie in a narrow band where there are few CB cells. This band is more

distinct in the caudal colliculus and many of the cell somas appear to be medium sized horizontal cells. Schmidt-Kastner et al. (1992) reported seeing PV neurons scattered throughout the sgl but make no mention of their morphology or sublaminar distribution. The distribution of PV in the rat SC was more fully described by Illing et al.(1990). They observed two populations of PV neurons. One, consisting of vertically oriented cells of similar morphology, was located in the ventral half of the sgl, the other was composed of many neurons of differing size and morphology widely distributed throughout the igl and deeper layers. They also observed patches of PV-IR in the igl, and found that a subpopulation of small neurons were clustered in the patches (Illing et al., 1990).

Ventral to the optic layer there are a few scattered CB cells in the igl and greater numbers of scattered CB cells in the deeper layers. The igl is the only layer where PV cells outnumber CB cells, most of the cells have medium to large somas. There is some evidence of clustering of neurons in the igl.

Comparison with other species

As far as we are aware the only other species in which the distributions of CB and PV have been compared, is the cat (Mize et al. 1992). In the cat, the CaBP are distributed in a pattern of alternating sublaminar tiers, very similar to that seen in the rat. The uppermost tier consisted of small CB-IR cells of varying morphologies. Three cell types were identified in this layer, horizontal fusiform cells, pyriform neurons with vertically oriented dendrites, and stellate cells (Mize et al., 1991). Retrograde filling studies showed that some of the pyriform and stellate cells cells projected to the lateral geniculate nucleus but the horizontal cells did not.

Ventral to the upper CB tier was a dense band of PV labelled cells (Mize et al., 1992) occupying the ventral sgl and the upper ol. Most of these cells were small round neurons, stellate neurons, or vertical bipolar neurons with fusiform cell bodies. They constituted more than 80% of the neurons retrogradely labelled by an injection into the lateral posterior nucleus (LP), although less than 50% of the PV-cells in this tier projected to the LP.

The middle CB tier straddled the border between the ol and the igl. The major cell type in this band had a stellate cell body and, in many cases, varicose dendrites that projected into the upper ol or deep SC layers but not into the sgl (Mize et al. 1991). The vast majority of the CB cells in this middle tier appeared to be interneuons that did not contain GABA.

Below the ol the CaBP tiers were less obvious with lower cell densities. PV cells predominated in the igl and below them was a region with mostly CB-cells. The PV-neurons were mostly medium-sized stellate cells or large multipolar neurons. Many of these PV cells projected to the dorsal lateral pontine gray nucleus or the predorsal bundle (Mize et al. 1992). CB-cells in the deeper regions of the cat SC were also scattered throughout the deep gray and deep white laminae. They varied considerably in size and morphology, but mostly appeared to be various types of stellate neuron. Some of the largest CB-cells were found in the deepest parts of the colliculus bordering the dorsal edge of the periaqueductal gray (Mize et al., 1991). These CB cells also seemed to be mostly interneurons.

Possible functional consequences of CaBP distribution

Although the observed patterns of immunohistochemical staining were fairly consistent between animals, it is possible that they could have been influenced by the functional state of the colliculus. Winsky and Kuznicki (1996) reported that the binding of CaBP antibodies to their antigens varied depending on whether the CaBP were in a calcium-bound or -unbound state. Given

that calcium levels in neurons can fluctuate greatly some of the patterns we have seen may reflect variations of calcium levels rather than CaBP.

The functions of these CaBP remain unknown. CB and PV do not seem to be selective for any one cell type, yet their pattern of expression appears to be related to the functional organization of the colliculus. There appear to be several functional domains in the colliculus and it seems that different groups of cells have different requirements for CaBP.

REFERENCES

Albers, F.J., Meek, J. and Nieuwenhuys, R. (1988) Morphometric parameters of the superior colliculus of albino and pigmented rats. J. Comp. Neurol. *274:*357-370.

Behan, M., Jourdain, A., and Bray, G.M. (1992) Calcium binding protein (calbindin D28k) immunoreactivity in hamster superior colliculus: ultrastructure and lack of co-localization with GABA. Exp. Brain Res. *89:*115-124.

Bennett-Clarke, C.A., Chiaia, N.L., Jacquin, M.F., and Rhoades, R.W. (1992) Parvalbumin and calbindin immunocytochemistry reveal functionally distinct cell groups and vibrissa-related patterns in the trigeminal brainstem complex of the adult rat. J. Comp. Neurol. *320:*323-338.

Celio, M.R. (1986) Parvalbumin in most γ-Aminobutyric acid-containing neurons of rat cerebral cortex. Science *230:*995-997

Celio, M.R. (1990) Calbindin D28k and parvalbumin in the rat nervous system. Neuroscience *35:*375-475

Dun, N.J., Huang, R., Dun, S.L., and Förstermann, U. (1994) Infrequent co-localization of nitric oxide synthase and calcium binding proteins immunoreactivity in rat neocortical neurons. Brain Res. *666:*289-294.

Gross, M.D., Gosnell, M., Tsarbopoulos, A. and Hunziker, W. (1993) A functional and degenerate pair of EF hands contains the very high affinity calcum-binding site of calbindin-D28k. J. Biol. Chem. *268:*20917-20922.

Hendry, S.H., Jones, E.G., Emson, P.C., Lawson, D.E., Heizmann, C.W., and Streit, P. (1989) Two classes of cortical GABA neurons defined by different calcium binding protein immunoreactivities. Exp. Brain Res. 76:467-472

Iacopino, A.M. and Christakos, S. (1990) Corticosterone regulates Calbindin-D28k mRNA and protein levels in Rat Hippocampus. J. Biol. Chem. *265*: 10177-10180.

Illing, R.-B., Vogt, D.M., and Spatz, W.B. (1990) Parvalbumin in rat superior colliculus Neurosci. Letts. 120:197-200

Illing, R.-B. (1992) Association of efferent neurons to compartmental architecture of the superior colliculus. Proc. Natl. Acad. Sci. USA *89:*10900-10904.

Ingersoll, R.J. and Wasserman R.H. (1971) Vitamin D_3-induced calcium binding protein. Binding characteristics, conformational effects, and other properties. J. Biol. Chem. *246:*2808-2814.

Johansen, F.F., Tønder, N., Zimmer, J., Baimbridge, K.G., and Diemer, N.H. (1990) Short-term changes of parvalbumin and calbindin immunoreactivity in the rat hippocampus following cerebral ishemia. Neurosci. Letts. *120:*171-174.

Labriola, A.R. and Laemle, L.K. (1977) Cellular morphology in the vissual layer of the developing rat superior colliculus. Exp. Neurol. 55:247-268.

Lane, R.D., Bennett-Clarke, C.A., Allan, D.M., and Mooney, R.D. (1993) Immunochemical heterogeneity in the tecto-LP pathway of the rat. J. Comp. Neurol. *333:*210-222.
Langer, T.P., and Lund, R.D. (1974) The upper layers of the superior colliculus of the rat: A Golgi study. J. Comp. Neurol. *158:*405-436.
Leathers, V.L., Linse, S., Forsen, S., and Norman, A.W. (1990) Calbindin-D28k, a 1α,25-dihydoxyvitamin D_3-induced calcium-binding protein, binds five or six Ca^{2+} Ions with high affinity. J. Biol. Chem. *265:*9838-9841.
Leathers, V.L., and Norman, A.W. (1993) Evidence for calcium-mediated conformational changes in calbindin-D_{28K} (the vitamin D-nduced calcium binding protein) interactions with chick intestinal brush border membrane alkaline phosphotase as studied via photoaffinity labeling techniques. J. Cell. Biochem. 52:243-252.
Li, Z., Decavel, C. and Hutton, G.I. (1995) Calbindin-D_{28K}: role in etermining intrinsically generated firing patterns in rat supraoptic neurones. J. Physiol. (Lond) 488: 601-608.
Lowenstein, D.H., Miles, M.F., Hatam, F., and McCabe, T. (1991) Up regulation of calbindin-D28k mRNA in the rat hippocampus following focal stimulation of the perforant path. Neuron *6:*627-633.
Miettinen, M., Koivistovo, E., Riekkinen, P.and Miettinen, R. (1996) Coexistence of parvalbumin and GABA in nonpyramial neurons of the rat entorhinal cortex. Brain Res. 706:113-122.
Mize, R.R., Jeon, C-J., Butler, G., Luo, Q., and Emson P.C. (1991) The calcium binding protein calbindin-D28k reveals subpopulations of projection and interneurons in the cat superior colliculus. J. Comp. Neurol. *307:*417-436.
Mize, R.R., Luo, Q., Butler, G., Jeon, C-J., and Nabors, B. (1992) The calcium binding proteins parvalbumin and calbindin-D28k form complementary patterns in the cat superior colliculus. J. Comp. Neurol. *320:*243-256.
Schmidt-Kastner, R., Meller, D. and Eysel, U.T. (1992) Immunochemical changes of neuronal calcium-binding proteins parvalbumin and calbindin-D-28k following unilateral deafferentation in the rat visual system. Exp. Neurol. *117:*230-246.
Seress, L., Gulyás, A.I., Ferrer, I., Tunon, T., Soriano, E. and Freund, T.F. (1993) Distribution, morphological features, and synaptic connections of parvalbumin- and Calbindin D28k-immunoreative neurons in the human hippocampal formation. J. Comp. Neurol. *337:*208-230.
Wharton, S.S. and Jones, D.G. (1985) Postnatal development of the superficial layers in the rat superior colliculus: a study with Golgi-Cox and Klüver-Barrera techniques. Brain Res. 58: 490-502.
Winsky, L. and Kuznicki, J. (1996) Antibody recognition of calcium-binding proteins depends on their calcium binding status. J. Neurochem. 66:764-771.

265.13

NEONATAL DECORTICATION IN CAT: EFFECTS ON MULTISENSORY INTEGRATION IN SUPERIOR COLLICULUS (SC) NEURONS. B.E. Stein*[1], M.T. Wallace[1] and L.K. Wilkinson[2] Dept. Neurobiol. and Anatomy[1], Bowman Gray Sch. Med./Wake Forest Univ., Winston-Salem, NC 27157 and Dept. Psychology[2], Virginia Commonwealth Univ., Richmond, VA 23298

Many SC neurons respond to stimuli from two or more modalities, and synthesize this information to alter the salience of events. Physiological and behavioral data are remarkably parallel: the same multisensory stimulus combinations that enhance neuronal responses enhance orientation behaviors, whereas stimulus combinations that depress neuronal responses depress these behaviors. In the vast majority of SC neurons multisensory integration involves inputs from an area of association cortex, the anterior ectosylvian sulcus (AES). Deactivation of AES compromises multisensory integration in SC neurons and eliminates multisensory orientation behaviors. An adjacent cortical area (rostral lateral suprasylvian cortex—rLS) is a small contributor to this function and is normally inadequate to support these behaviors. In mature animals in which AES was ablated neonatally, the situation is quite different. The proportion of multisensory SC neurons is high (even higher than normal, 67% vs 58%), and a sizable, although smaller (43% vs 79%) percentage synthesize multisensory information. Cortical deactivation in a small sample of these neurons suggest that they depend on rLS for their cross-modal integration. These data, coupled with the previous abstract (Wilkinson, Wallace, and Stein 1995), indicate that loss of AES is likely to initiate a process whereby rLS corticotectal influences are significantly expanded. Although not complete, this compensation is sufficient to support SC-mediated multisensory behaviors. Supported by NIH grant EY06562.

265.14

VISUAL ORIENTING RESPONSES IN THE HEMIANOPIC VISUAL FIELD OF THE CORTICALLY BLIND CAT CAN BE RESTORED BY SITE-SPECIFIC GABA-ERGIC DISINHIBITION OF THE SUPERIOR COLLICULUS

V.Ciaramitaro*, J.S. Durmer, W.E. Todd & A.C. Rosenquist
Dept. of Neuroscience, Univ. of Penn, Phila., PA 19104

Following unilateral removal of all known visual cortical areas, a cat is rendered hemianopic in the contralateral visual field as measured by visual perimetry and other behavioral tests. One mechanism mediating reversible recovery of visual orienting in the previously blind hemifield is GABAergic disinhibition of the superior colliculus (SC) ipsilateral to a cortical lesion. (Ciaramitaro et.al., Society for Neuroscience Abstracts, vol 20(2): p 1186,1994)

SC disinhibition is effective in mediating recovery when injections of bicuculline methiodide, a GABAa antagonist, are made into the *medial* and *rostral* areas of the deeper layers of the SC. Immediate post-injection effects endure for approximately one hour and include a defensive reaction and strong motor biases of the eyes, head and body contralateral to the injection site. Subsequent recovery of visual orienting behavior endures for several hours, depending on the concentration and volume of the drug. Although similar injections of more *lateral* or *caudal* SC regions elicit the same immediate post-injection effects, there is no subsequent recovery of visual orienting behavior.

Thus, recovery of visual orienting in the cortically blind cat appears to be mediated by a *site-specific* GABA-ergic mechanism which is *dissociable* from immediate post-injection motor effects.
(*Supported by EY02654 , 2 T32 EY07035 and 2 PO1 EY01583*)

265.15

CALBINDIN$_{D28k}$ AND PARVALBUMIN ARE EXPRESSED IN COMPLEMENTARY PATTERNS IN THE RAT SUPERIOR COLLICULUS.

R.J. Cork*, S.Z. Baber & R.R. Mize. Department of Anatomy and Neuroscience Center, LSU Medical Center, New Orleans, LA 70112.

We have examined the distributions of two calcium binding proteins, calbindin$_{D28k}$ (CB) and parvalbumin (PV), in the rat superior colliculus (SC). Sections, cut from the brains of adult Sprague Dawley rats, were labeled using fluorescence- or DAB- immunohistochemistry. The distributions of labeled cells were plotted using a Eutectics NTS system, and cell size data was collected using a Joyce-Loebl Magiscan image analyzer. CB was expressed in cells found in three sublaminar tiers. The most dorsal tier consisted of lightly labeled cells that were scattered at 100-250 μm deep in the superficial gray layer (*sgl*). The second tier consisted of a dense band of intensely labeled cells in the optic layer (*ol*), at depths between 300 μm and 500 μm. The third tier consisted of cells widely distributed throughout the deep gray layer (*dgl*), between 1 mm to 2 mm deep. PV was found in the somas of cells in two tiers that lay between the CB bands. An upper band was concentrated at about 300 μm, occupying the ventral *sgl* and dorsal *ol*. The remainder of the PV cells formed a thick wedge with cells concentrated along the dorsal lateral edge of the intermediate gray layer (*igl*) (900 ± 300 μm) but extending into the *dgl* to about 1600 μm. Labeled cell size increased with depth throughout the SC. Cell size bore no apparent relationship to CB or PV expression, however, average labeled cell-body areas were different in different tiers. For example, the mean cell-body area was 83.7±21.5 μm^2 for the upper CB tier, and 184.4±53.1 μm^2 for the *ol* CB tier. Fluorescence double-labeling showed that a few cells expressed both CB and PV but that, overall, the calcium binding proteins were expressed in alternating tiers superimposed on the traditional laminated structure. Supported by Department of the Army, Cooperative Agreement DAMD17-93-V-3013, and NIH EY02973.

265.16

EFFECT OF NEONATAL EYE REMOVAL ON EXPRESSION OF mRNAs FOR GAD, PPT, CCK, PENK AND SOM IN RAT SUPERIOR COLLICULUS

A.R.Harvey*[1], L.Tang[1] and D.J.S.Sirinathsinghji[2]. [1]Dept. of Anatomy and Human Biology, The University of Western Australia, Perth, WA 6907 and [2]Neuroscience Research Centre, Merck Sharp and Dohme Research Laboratories, Harlow, UK

This study used the technique of *in situ* hybridization histochemistry to study the expression of mRNAs for glutamic acid decarboxylase (GAD), preprotachykinin (PPT), preprocholecystokinin (CCK), preproenkephalin (PENK) and preprosomatostatin (SOM) in the adult rat superior colliculus (SC), and to determine how mRNA expression was altered in the SC in rats unilaterally enucleated at birth. Hybridization was carried out on cryostat sections (10μm) using ^{35}SdATP-labelled synthetic oligonucleotide probes (45 mer). In the superficial layers of normal SC, large numbers of GAD mRNA expressing cells were found in stratum zonale (SZ) and stratum griseum superficiale (SGS). PPT mRNA expressing cells were mainly found in the upper two-thirds of SGS while CCK mRNA expression was prominent in the middle third of this layer. PENK mRNA expression was mostly found in lower SGS and stratum opticum (SO). Cells containing SOM mRNA formed a conspicuous band in the lower third of SGS and upper SO. In the superficial tectal layers contralateral to eye removal, quantitative analysis revealed a significant decrease in GAD, PPT, CCK and PENK mRNA expression. For all 4 probes, both the number of cells expressing these mRNAs and the level of expression per cell was decreased in visually deprived SC. By comparison, neonatal enucleation resulted in only a slight fall in the level of SOM mRNA expression in SGS and upper SO. The data show that removal of the major source of primary sensory input to the superficial layers of rat SC leads to a long-lasting reduction in the synthesis (and presumably turnover) of GAD and the neuropeptides PPT, CCK and PENK.

265.17

NEUROACTIVE SUBSTANCES IN THE PARABIGEMINAL NUCLEUS OF THE THIRTEEN-LINED GROUND SQUIRREL. R.J. Garcia-Mercado and N. Lugo*. Dept. Anatomy and Inst. of Neurobiology, Univ. of Puerto Rico, MSC, San Juan, P.R. 00901.

The parabigeminal nucleus (Pb) has extensive reciprocal connections with the superior colliculus (SC) in the thirteen-lined ground squirrel (*Spermophilus tridecemlineatus*). Immunohistochemical methods were employed to identify neurotransmitters and/or neuromodulators implicated in these projections. Animals were intracardially perfused with 4% paraformaldehyde or 4% paraformaldehyde-2.5% glutaraldehyde in PB (pH 7.4), depending on the antibody to be used. Brain sections 40 μm thick were processed for immunofluorescence or with a DAB-nickel enhanced avidin-biotin complex (ABC) method. Immunoreactive cells and/or fibers were identified in Pb after incubations with antisera against choline acetyl transferase (ChAT), gamma-aminobutyric acid (GABA), tyrosine hydroxylase (TH), substance P (SP), somatostatin (SS), neuropeptide Y (NPY) and serotonin. Cells positive for ChAT appear to constitute most of the neuronal population of Pb. Small GABA-like cells scattered throughout the nucleus were less abundant, as were fusiform cells positive for TH or for SP. Few neurons exhibited SS-like and NPY-like immunoreactivity. These cells formed clusters in the lateral portion of Pb. Serotonin-like fibers were abundant in this nucleus, yet no cell bodies were detected. Fibers positive for TH, SP and NPY were also found in the superficial and deep layers of SC. Pb has only been found to connect with SC in the thirteen-lined ground squirrel. Thus, our observations suggest that some of the substances detected in Pb may be involved in its connections with SC. Our results also imply that some of the neuroactive substances might be colocalized within a single Pb cell. (Supported by ONR Grant N00014-89-J-3070 and NIH Grant MH-48190).

265.18

VISUOCORTICAL PROJECTIONS TO THE MACAQUE MONKEY BASAL PONTINE GRAY. R.A. Giolli*, K.M. Gregory, F. L. Lui and R.H.I. Blanks. Dept. Anat. & Neurobiol., Univ. Calif. Coll. Med. Irvine, CA 92717.

Projections to the basal pontine gray were studied after injections of ^{3}H-leucine restricted to one of each of the following cytoarchitecturally defined cerebrocortical areas: 17, OA, caudal PGa, caudal OAa, POa, and 7. All corticopontine projections are divergent as they terminate as dense patches of silver grains distributed over multiple zones of basal pons arranged as lamellae. The data also suggest some convergence of terminal pontine fields from different visuocortical areas. We find that: area 17, in which central visual field is represented, does not project to the basal pons (area 17 representing peripheral visual field was not studied). Area OA has a limited projection targeting the dorsolateral (DL) and lateral (L) pontine gray. Area PGa projects widely to DL, L, dorsal (D) and peduncular (P) pontine gray, whereas the area OAa projection is limited to DL and P pontine gray. Area POa targets DL, L, and P pontine gray while area 7 projects widespread to the DL, L, D, P, and ventral pontine gray. Area 7b, alone provides a small input to the dorsomedial pontine gray. Supported by NSF grant IBN 9121376. F. L. was supported by the Fidia Foundation.

265.7

REFLEXIVE SHIFTS OF ATTENTION: FACILITORY AND INHIBITORY EFFECTS OCCUR AT ISOLUMINANCE. S. Danziger, R. Fendrich*, A. Kingstone[1] and R. Rafal. Center for Neuroscience, Univ. of California Davis, [1] Dept. of Psychology, Univ. of Alberta, Canada

When attention is summoned reflexively by a peripheral cue, an initial facilitation of detection reaction time (RT) to targets appearing at the cued location is followed by a slowing of RT to such targets. This slowing has been termed Inhibition of Return (IOR). The superior colliculus (SC) has been implicated as a potential source of these effects, since (1) they are reduced in PSP patients with midbrain degeneration, and (2) they are generated more effectively in normal humans by cues in the temporal hemifield. The latter effect correlates with the larger direct innervation of the SC by the nasal hemiretina.

This study exploited the lack of color opponent cells in the SC. Using a flicker nulling technique, we determined the green luminance that was isoluminant with a grey background for each subject. Manual RT was measured for a subject's monocular detection of a peripheral target. An uninformative precue preceded the target by 75-125 or 600-1000 ms. In alternating blocks the cue was isoluminant with or brighter than the background. Isoluminant and non-isoluminant cues produced equivalent facilitation at short intervals and IOR at long intervals. Effects did not differ between the nasal and temporal hemifields. These results suggest that the effects of reflexive attentional orienting may not require the retino-tectal pathway. Supported by PHS MH41544 and NINDS PO1 NS17778.

265.8

DIRECT RETINAL PROJECTIONS TO THE OLFACTORY BULB AND INFERIOR COLLICULUS (IC) IN THE HAMSTER. L.P. Morin* and J. Blanchard. Dept. Psychiatry, Stony Brook University, Stony Brook, NY 11794.

Three divisions of the visual system have been well studied. These consist of a) the classical image forming and analysing areas, b) those nuclei concerned with oculomotor regulation, and c) the circadian rhythm system. Retinal projections have also been reported in areas (e.g., dorsal midline thalamus or olfactory tubercle) not belonging to the above. Here, cholera toxin-β fragment (CT-β) was injected intraocularly (5 µl of 0.2% CT-β in 2% DMSO in 0.9% saline) and CT-β immunohistochemistry was performed on brains taken from anesthetized, perfused adult male hamsters about 48 hr later.

CT-β-IR fibers exit the contralateral basal hypothalamus over the supraoptic nucleus into anterior amygdala. Fibers continue rostro-laterally, through the nucleus of the lateral olfactory tract (NLOT), into the LOT. They extend rostrally in the LOT to the rhinal fissure and turn medially. Numerous fibers with terminals are present in the caudal part of the dorsal anterior olfactory nucleus.

Fibers are also found in a superficial lamination near the midline of the contralateral inferior colliculus (IC). Fibers and terminals are evident spreading across the caudal pole of the IC. The IC results are similar to reports in other species [Brain Res. 233, 45-52, '82], but a retinal projection in the LOT has not previously been documented. Supported by NS22168 to LPM.

265.9

VELOCITY SELECTIVITY OF NEURONS IN THE PIGEON'S TECTUM CAN BE MODULATED BY MANIPULATION OF OBJECT'S RETINAL IMAGE SIZE. B.J. Sun and B. J. Frost*. Visual and Auditory Neurosciences Laboratory, Dept. Psychol., Queen's Univ., Kingston, Ont. K7L 3N6, Canada.

An object's velocity appears constant even with variations in viewing distance. Such velocity constancy can be achieved through utilizing distance cues and/or scaling of retinal velocity relative to object size or other reference scales in the visual scene. Little is known about the neural mechanism of such *velocity constancy* especially at the single cell level. We have developed visual stimuli using a Silicon Graphics IRIS computer graphics system, which presents moving objects within the context of a rather realistic 3-D environment. Apparent distance of an object relative to the pigeon was manipulated through presentation of perspective depth cues in the background. Retinal image size of an object could also be manipulated in order to simulate the difference in apparent size of an object at different viewing distances. The neural responses of pigeon's tectal neurons to objects moving in the tangent screen were recorded extracellularly. Magnitude of the responses as the function of object velocity and object size were analyzed. It was found that the velocity tuning curve of the recorded neurons shifted towards slower retinal velocity when that object was made to appear farther away from the pigeon. This effect is most prominent when the retinal image size exceeds that of the cell's receptive field. The effect of manipulation of distance through perspective depth cues alone (while maintaining same retinal image size for different viewing distances) were not as strong as those produced by combining the manipulation of retinal size and viewing distance. These results suggest that these neurons may be involved in the processing of velocity constancy, i.e. extracting information about the object velocity through incorporating retinal velocity with information about object size (and possibly object distance) rather than solely relying on retinal velocity.

Supported by an NSERC grant OGP0000353 to BJF and an NSERC Postgraduate Scholarship to HS.

265.10

A HIGH-FREQUENCY BURST FIRING MODE IN NEURONS OF THE RAT SUPERIOR COLLICULUS F-S Lo*, R.J. Cork & R.R. Mize. Dept. of Anatomy and Neuroscience Center, LSU Medical Center, New Orleans, LA 70112.

We have shown elsewhere that in the optic layer of the rat superior colliculus there is a tier of cells containing the calcium binding protein calbindin$_{D28k}$. Using an *in vitro* slice preparation, together with intracellular recording techniques and iontophoretic injection of biocytin we are characterizing the membrane properties and morphology of these cells. Recordings were obtained from 29 neurons in the region of the optic layer. They had an average resting potential of -62±7.6 mV and a mean resting input resistance of 41.8±12.8 MΩ. The large (73.2±8.5 mV) overshooting sodium spikes were followed by two after-hyperpolarizations (AHP) and showed frequency accommodation. An inward rectifying current (I_h) that was blocked by 10 mM CsCl, was observed during hyperpolarizing current pulses. If cells were depolarized to about -60 mV from hyperpolarized potentials a relatively short (20-30 ms) low-threshold calcium spike (LTS) with 1-2 Na-spikes riding on it was observed. The LTS was reversibly blocked by 1mM $NiCl_2$. Upon further depolarization, some cells fired a train of single Na-spikes after the LTS, while others (11/29) exhibited repetitive bursting behavior within a limited range of depolarized potentials (-47 to -53 mV). The inter-burst frequency increased with greater depolarization, reaching a maximum at about 50 Hz. The degree of burst frequency accommodation was also voltage dependent, decreasing as the potential approached the Na-spike threshold. During these experiments we noted that pyramidal cells in the hippocampal CA1 region had many similar membrane properties, e.g. I_h, short LTS, 2 AHPs, and also expressed calbindin. Double labeling experiments are underway to determine if the cells that have been recorded from do contain calbindin.

Supported by Department of the Army, Cooperative Agreement DAMD17-93-V-3013, and NIH EY02973.

265.11

SENSORY RESPONSE PROPERTIES IN THE SUPERIOR COLLICULUS (SC) OF THE NEWBORN RHESUS MONKEY M.T. Wallace*, J.G. McHaffie and B.E. Stein. Dept. of Neurobiology and Anatomy, Bowman Gray School of Medicine, Wake Forest Univ., Winston-Salem, NC 27157

Unlike altricial species such as carnivores and rodents, the monkey is born capable of attending and orienting to a variety of sensory cues. Presumably, a high proportion of SC sensory and sensorimotor neurons are sufficiently mature to support these behaviors in the absence of postnatal sensory experience. Indeed, in the superficial SC of the newborn monkey a well-ordered visual map was found. Although response selectivities clearly resembled those in adults, receptive fields were 2-4 times larger and latencies were significantly longer (X=161 vs. 93 ms). In deep layers, visual neurons were also topographically organized and had immature latencies (X=185 vs. 98 ms), as did auditory neurons (X=45 vs. 18 ms). In contrast, somatosensory neurons seemed most mature: they were predominantly cutaneous, high velocity, rapidly adapting, short latency (8-28 ms) and were organized into a well-ordered body map. The immaturity of the SC was most apparent in its multisensory neurons. Such neurons were much less common than in adults (7% vs. 25%), and they lacked the adult capacity to integrate cross-modal information (Wallace and Stein 1994). Nevertheless, and in contrast to observations in other species, no postnatal experience was necessary for alignment of their receptive fields. It seems likely that the monkey SC, like the cat SC, undergoes a developmental chronology in which somatosensory processing matures first, followed by auditory, visual, and finally multisensory. Most protracted is the development of the ability to synthesize cues from the different sensory modalities. Supported by NIH EY06562 and NS22543.

265.12

EFFECTS OF NEONATAL DECORTICATION ON MULTISENSORY ORIENTATION BEHAVIOR L.K. Wilkinson*[1], M.T. Wallace[2] and B.E. Stein[2] Dept. Psychology[1], Virginia Commonwealth Univ., Richmond, VA 23298 and Dept. Neurobiology and Anatomy[2], Bowman Gray School of Medicine/Wake Forest Univ., Winston-Salem, NC 27157

The ability of superior colliculus (SC) neurons to integrate information from different senses is critical to its role in attentive and orientation behavior. In cat, this ability is dependent on inputs from an area of association cortex , the anterior ectosylvian sulcus (AES). Deactivation of AES eliminates multisensory integration in the majority of SC neurons (Wallace and Stein 1994) and markedly degrades an animal's ability to use multiple sensory cues to facilitate attentive and orientation behaviors (Wilkinson, Meredith and Stein 1992). Furthermore, SC neurons develop the capacity for multisensory integration only after AES corticotectal projections become functional (Wallace and Stein 1993). In the present experiments the behavioral consequences of neonatal AES ablation were examined. AES was removed at 7 dpn and following maturation each animal (n=3) was trained to approach a near threshold visual stimulus presented either: (a) alone (b) accompanied by a spatially coincident auditory cue, or (c) accompanied by a spatially disparate auditory cue. Surprisingly, the behavior of these animals was indistinguishable from normal adults: spatially coincident multisensory cues dramatically enhanced correct responses, whereas spatially disparate cues significantly depressed these behaviors. Apparently, there are developmental mechanisms that allow for compensation following loss of AES. Presumably its loss initiates processes which enable neighboring cortical areas to take over these functions. Supported by NIH grant EY06562.

Pre- and postnatal expression of amino acid neurotransmitters, calcium binding proteins, and nitric oxide synthase in the developing superior colliculus

R. Ranney Mize, Francis T. Banfro, and Christopher A. Scheiner

Departments of Anatomy and Ophthalmology and the Neuroscience Center of Excellence, Louisiana State University Medical Center, 1901 Perdido Street, New Orleans, LA 70112

Key words: GABA, glutamate, nitric oxide, calbindin, parvalbumin, synapse formation, axon pathfinding

Send proofs to: Dr. R. Ranney Mize
Professor and Head
Department of Anatomy
LSU Medical Center
1901 Perdido Street
New Orleans, LA 70112
Tele: (504) 568-4012
Fax: (504) 568-4392
Email: rmize@lsumc.edu

Introduction

The mammalian superior colliculus (SC) is an excellent model for developmental studies because it is multi-laminated, has well-defined and segregated afferent inputs, and contains specific output neurons which project to both ascending and descending targets in the brain. The receptive field properties of its neurons have been studied extensively and it has a relatively refined topographic map of the visual world that is conveyed by inputs from both th retina and the visual cortex. Finally, the specific neurotransmitters of many of its intrinsic an projection neurons have been identified and some of its synaptic circuits are well-established (see Huerta and Harting, 1984; Chalupa, 1984; Mize, 1992, 1996, for reviews).

Much less is known about how these features develop. Retinotectal pathway development has been studied in great detail, particularly in lower vertebrates (see Constantine-Paton et al.. 1988; Udin and Fawcett, 1988, for reviews), and more recently in rats (Simon and O'Leary, 1992; Simon et al., 1992). Studies in rat and other rodents demonstrate that there are at least two distinct and well-defined periods of growth in this structure. During early stages of development, neurons divide, migrate to specific laminae, begin to establish dendritic branching patterns, and send their axons to specific targets (Mustari et al., 1979; Altman and Bayer, 1981; Cooper and Rakic, 1981; Edwards et al., 1986a). Extrinsic afferents also grow into SC during this period and at least those from the retina establish a rough topographic order (Edwards et al., 1986b; Udin and Fawcett, 1988; Sanes, 1993), which has been referre to as the 'prepattern' (Simon and O'Leary, 1992). Most of these events are 'activity independent' in the sense that visually driven or patterned electrical activity is presumed to be absent or limited during this prenatal stage of development.

In later stages of development, this 'prepattern' of cellular lamination, afferent fiber innervation, and topographic order is further developed and refined. Permanent synapses are formed, stabilized, and strengthened while others are eliminated by cell death and fiber retraction (Lund and Lund, 1972; Mize and Sterling, 1977; Finlay et al., 1982; Cooper and Rakic, 1983; Simon et al., 1992). The physiological receptive field properties of individual cells are first recorded and stimulus induced electrical responses mature (Stein, 1984 for review). Many of these later events are activity or experience dependent and can be modified by alterations of the visual environment or changes in the patterning of extrinsic afferents (Shatz, 1990; Goodman and Shatz, 1993). Although many of the factors underlying these developmental events have been studied, remarkably little is known about the onset of expression of neurotransmitters and other neurochemicals that occurs during these two stages of development in the mammalian SC.

As a consequence, we have examined the onset of expression of three types of neurochemical in the cat superior colliculus: the amino acid neurotransmitters GABA and glutamate; the calcium binding proteins calbindin and parvalbumin; and the synthetic enzyme of nitric oxide, nitric oxide synthase (NOS). In some cases, we have compared the time course of expression with the development of cellular lamination and the growth of afferents into the SC. Our results show that some neurochemicals, especially GABA and calbindin, are expressed in the very earliest stages of development as neurons are migrating from the subventricular zone to the tectal plate. Others, particularly parvalbumin and glutamate, are expressed much later in development, during the period of synaptogenesis and fiber refinement. Finally, we show that nitric oxide synthase, which has recently been identified as a potential retrograde messenger during synapse stabilization (Gally et al., 1990), is expressed transiently at a time which correlates with the refinement of the axonal connections that are

formed with neurons that express it.

Development of the amino acid neurotransmitters in cat SC

Organization: Gamma aminobutyric acid (GABA) is a key inhibitory neurotransmitter in the mammalian SC (Okada, 1992). Immunocytochemical studies have shown that GABA containing neurons account for up to 40% of all cells in SC. Most of these are small to moderate in size and the vast majority are interneurons (Mize, 1992 for review). They are most densely distributed within the zonal, superficial gray, optic, and intermediate gray layers but they are also found in fewer numbers in the deepest layers of SC (Mize, 1988). Electron microscopy studies show that GABA immunoreactive processes contain primarily pleomorphic or flattened synaptic vesicles and form microcircuits that likely mediate several different types of inhibition (Mize et al., 1982; Mize, 1988;1992;1994). Developmental studies in vitro suggest that GABA is first effective at generating inhibitory post-synaptic potentials only in postnatal tissue (Warton et al., 1990; Kraszewski and Grantyn, 1992) and that GABA containing synapses increase dramatically in number for 2-3 weeks after birth (Warton et al., 1990). Thus, GABA mediated inhibition develops relatively late in the mammalian SC.

Development: Despite the late postnatal onset of GABAergic inhibition, GABA antibodies label cells within this structure as early as the end of the first trimester before birth. We examined the expression of GABA in fetal tissue ranging in age from E24-E59 and at postnata ages P1 to P60. GABA content was localized using standard immunocytochemistry techniques. The distribution of antibody labeled neurons was plotted with a computer-based microscope tracing system and cell size measured with an image analyzer.

By E24, the earliest age examined, GABA immunoreactivity is found in both the neuropil and in some cell bodies throughout the tectal plate. Cell bodies and processes are also labeled within the subventricular zone (SVZ) at this age. By E30-36, a distinct bi-laminar distribution of GABA immunoreactivity is present. Both cell bodies and processes are intensely labeled within the superficial layers at E30 (Figure 1A), and an obvious dense band of label in the upper one-half of the cat SC is visible (Figure 1B). Labeled cell bodies in this dense band are mostly small cells with few or no labeled processes. By contrast, GABA-ir in the deep layers is very sparse due both to the small number of labeled neurons and very limited neuropil labeling. Those cells that are labeled are mostly bipolar neurons with vertical fusiform cell bodies and vertically oriented dendrites (Figure 1C). This cell type is also seen in the SVZ (Figure 1A), where the dendrites of some cells extend into the deep layers of SC. This morphology is characteristic of neurons in the process of migration (see Edwards et al., 1986a). The pattern of labeling seen at E30-36 suggests that: 1) many GABA containing neurons have already reached the superficial layers by E30; 2) neurons destined for the superficial layers of SC express GABA while still in the SVZ; 3) GABA is expressed in SC neurons both during and after migration; 4) the deep bipolar neurons represent a transient cell morphology in the process of migration.

By E40-46, the pattern of anti-GABA labeling is nearly identical to that found in the adult, although many more cells are labeled than at later stages of development. Well-labeled neurons are now densely distributed throughout the superficial and intermediate gray layers of SC (Figure 2A). There are fewer labeled neurons in the deepest layers, but these also are intensely labeled by the antibody (Figure 2A). Labeled cell bodies in the superficial layers have characteristics similar to those in the adult, with small round or sometimes ovoid cell bodies and short dendritic processes (Figure 2B). Cell bodies in the intermediate layers are

also mostly small round cells (Figure 3C), as are most of those in the deepest layer. Only a few cells retain a bipolar morphology (Figure 3D), suggesting that few if any GABA containing cells are still migrating by E46. Neuropil labeling is also quite prominent at this age (Figures 2B-D).

Labeling at later ages produces a similar laminar pattern, but many fewer cells are labeled. We plotted the distribution and number of GABA-ir neurons from one animal in each of four age groups (E30, E46, P1, P60) to determine quantitatively the reduction in GABA labeled cell number. Computer counts show a 2.5 fold decrease in GABA-ir cells between E46 and P60, despite the significant increase in overall SC volume that occurs at later ages. Thus, the maximum number of GABA containing cells is reached around the end of the second trimester (E40-46) with significant cell death or loss of expression occurring by P60.

To date, we have examined glutamate immunoreactivity in the prenatal SC in only six prenatal age groups (E41, E46, E51, E53, E58). Our preliminary data suggests that intense glutamate immunoreactivity develops much later in the prenatal kitten than does GABA. At E41-46, only a few darkly labeled neurons are found within the optic and intermediate gray layers, regions that are known to contain many glu-ir cells in the adult. A larger number of intensely labeled neurons are found at E51-53, most within the deeper layers of SC. By E58, a number of large neurons and some medium sized cells within the deep superficial gray and optic layers are now well-labeled but their number is less than that seen in the adult. Further development in the number and density of glu labeled cells occurs postnatally.

Functional Considerations: GABA is also one of the earliest neurotransmitters to be expressed in other regions of the CNS. In rat visual cortex, for example, GABA immunoreactivity is

seen as early as E13 (Lauder et al., 1986; Van Eden et al., 1989). It appears first in neurons within the marginal and subplate zones and somewhat later in cell groups throughout the cortical plate (Luskin and Shatz, 1985). Very early expression of GABA-ir has also been found in the spinal cord, brainstem, and diencephalon (Lauder et al., 1986), so GABA must be important to developmental processes that occur very early, including mitosis, migration, and neurite outgrowth.

Studies that have specifically examined the relationship between GABA expression and cell migration have shown that GABA is not expressed until after cells have reached their final destinations, at least in visual cortex (Miller, 1986). On the other hand, many studies have shown that GABA is important in neurite outgrowth. GABA and it's agonists increase the length, number, and branching of neurites in cultured cerebellar granule cells (Hansen et al., 1987), in cortical neurons (Spoerri, 1987), and in chick optic tectum cells (Michler-Stuke and Wolff, 1987). GABA also increases the density of the rough endoplasmic reticulum, suggesting that it promotes protein synthesis and incorporation of receptor protein into the plasma membrane (Hansen et al., 1987; Spoerri, 1987). GABA application in culture can also enhance low and high affinity GABA receptor binding (Meier et al., 1984; Redburn, 1992). Thus, one key function of GABA early in development may be to promote neurite extension, possibly by binding to GABA receptors.

Another early effect of intracellular GABA may be to alter ion concentrations and the membrane potential. Increases in potassium concentration in culture have been shown to stimulate neurite outgrowth in dorsal root ganglia (Chalazonitis and Fischbach, 1980) and high calcium concentrations in chick tectal cultures increase the number of neurites if GABA is also present in the medium (Michler-Stuke and Wolff, 1987). Similarly, intracellular calcium

mobilization promotes neurite outgrowth in vitro (Anglister et al., 1982). Thus, the ionic conductance and membrane potential properties of neurons may be important to their growth well before cells are innervated by afferents or form synapses. However, GABA has also been shown to promote synaptogenesis in both retinal and cerebral neurons (Spoerri, 1987; Messersmith and Redburn, 1993). It is therefore not surprising that GABA in SC neurons continues to be expressed at postnatal ages when synapse formation is occurring (Lund and Lund, 1972; Sterling and Mize, 1977). In summary, GABA probably plays different roles at different stages of development and is likely involved both in neurite outgrowth and synaptogenesis.

Development of calcium binding proteins in cat SC

Organization: Calcium binding proteins (CaBPs) in the CNS regulate intracellular calcium by buffering cytoplasmic Ca++, by controlling Ca++ transport across the cell membrane, and by regulating Ca++ dependent second messenger systems (Heizmann and Hunziker, 1990; Celio, 1990; Braun, 1990; Baimbridge et al., 1992). Two of the most frequently studied CaBPs in the CNS are calbindin (CB) and parvalbumin (PV). CB is a 28kD calcium binding protein that is co-localized in some GABAergic interneurons (Baimbridge et al., 1992; Kawaguchi et al., 1987) and is often present in neurons that have low threshold calcium spikes (Kawaguchi, 1993; Lo et al., 1995). PV is a 12 kD calcium binding protein that is found in both projection and interneurons and has been associated with cells that are fast spiking (Kawaguchi et al., 1987; Kawaguchi and Kubota, 1993).

In the cat superior colliculus, these two calcium binding proteins are found in complementary sublaminar tiers and in different cell types (Mize et al., 1991; 1992; Mize and

Luo, 1992). CB neurons form three sublaminar tiers, one within the upper superficial gray layer (sgl), a second within the deep optic and dorsal intermediate gray layers (igl), and a third consisting of cells scattered within the deep gray layer (dgl) of SC (Mize et al., 1991; 1992; Mize and Luo, 1992). The vast majority of CB cells are small interneurons, some of which contain GABA (Mize et al., 1991). By contrast, PV labeled neurons in cat SC form a single dense band of medium to large sized cells that overlap the deep sgl and upper optic layers. PV cells are also distributed throughout the deeper layers of SC, but virtually no PV neurons are present within the upper sgl (Mize et al., 1991). The vast majority of PV neurons are projection cells that send their axons to a variety of extrinsic targets, including the lateral posterior nucleus and a number of descending brainstem sites (Mize et al., 1992).

Development: CB and PV have very different developmental histories in the kitten SC. We have examined the expression of CB and PV in fetal tissue ranging in age from E24-E59 and at postnatal ages P1 to P60. CB is expressed at the earliest prenatal age examined - E24. At this age, most CB neurons are located within the subventricular zone (SVZ), but others are sparsely scattered throughout the tectal plate. By E28, CB positive neurons are found throughout the dorsal-ventral extent of the tectal plate, but cells at different depths differ in morphology (Figure 3A). The most dorsal neurons are small cells with few or no dendritic processes (Figure 3A,B). Intermediate depth cells have multipolar morphologies with short dendrites (Figure 3B). Many of the deeper cells have bipolar morphologies with vertically oriented dendrites (Figure 3C), similar to those that contain GABA at this stage of development and which are believed to be in the process of migrating.

The three sublaminar tiers of CB cells are barely visible at E34, and many deeper cells retain a bipolar shape (Figure 4A). Labeled CB cells in the SVZ at E34 also have

morphologies typical of migrating neurons. By contrast, the three tiers of CB neurons are well segregated by E40-46, labeled bipolar cells are no longer present, and no CB labeling is found within the SVZ at these later ages (Figure 4B,C). As with GABA labeled neurons, the highest density of CB neurons is found at E40-46. Cell counts from tissue aged E40-P60 show that the density of CB cells at E40 is three times higher than that found at P60.

This reduction in cell density is due primarily to cell death in the prenatal kitten but is also due to loss of expression of CB after birth. This conclusion is based upon two lines of evidence. First, overall neuronal density as measured in thionin stained sections decreases progressively from E41 to P21. Thus, the overall loss of neurons is similar to that of CB containing cells, suggesting that CB cells die in proportion to the total population. Secondly, pyknotic neurons with eccentric nucleoli, typical of dying cells, are observed in the late prenatal period and are especially numerous between E51 and E59, a period in which the number of CB cells declines rapidly. Very few pyknotic profiles are observed after P7, which indicates that there is little cell death after birth. Because the density of CB cells continues to decrease until P60, the postnatal decrease in CB neurons must be due to a loss of expression.

PV expression has a dramatically different developmental time course. PV immunoreactivity is not observed prior to P1 and there is a continuous increase in the number of PV labeled cells until P35 with a slight decline thereafter. PV labeled neurons at P1 are few in number, but by P7 the dense band of PV neurons in the deep superficial gray and upper optic layers is already visible (Figure 5A). The number of PV cells increases in density by P21, and is fully developed by P35 (Figure 5B-C). PV cell morphology is like that of the adult by the time PV is first expressed. At all ages, PV neurons are medium to large sized cells, usually with stellate-like morphologies and multiple dendrites radiating from the soma

(Figure 5A-C). In summary, PV is expressed late in development, well after cells have migrated and lamination is well-developed.

Functional Considerations: The roles that CB and PV play in brain development are largely unknown. CB expression occurs very early in prenatal development in many brain regions, often at a time when both cell generation and migration are still in process. In SC, CB is unlikely to be involved in mitosis because no CB cells are found within the ventricular zone where SC cells divide (Edwards et al., 1986a). On the other hand, CB may well be involved in cell migration. Bipolar neurons with morphologies typical of migrating cells are CB ir in the kitten SC until around E40, the time at which migration ends. We also found many CB neurons in the SVZ that had bipolar dendrites and crossed into the deep layers of the tectum. Thus, CB appears to be an important molecule for at least some neurons that are in the process of migration.

Its role may be to regulate intracellular calcium in migrating cells. Calcium levels are reportedly high in migrating neurons. Actively elongating growth cones have higher levels of intracellular calcium than do inactive cones (Kater et al., 1988), while excessive calcium can inhibit growth cone motility and neurite extension (Mattson and Kater, 1987). In addition, N-type calcium channels are first expressed in cerebellar granule cells as they begin to migrate and the calcium channel blocker omega conotoxin retards migration (Komuro and Rakic, 1992). Thus, regulation of intracellular calcium is essential to migrating neurons and CB could well serve to buffer or otherwise regulate calcium levels in these developing cells.

Although it is not clear from our studies whether CB is expressed in all migrating neurons, there is evidence in other brain regions that CB is transiently expressed in many cells that do

not contain it in the adult. In striatum, aspiny neurons in the dorsal caudate-putamen express CB intensely in the prenatal but not the adult rat (Liu and Graybiel, 1992). CB is also intensely expressed in layer 4 and 6 cortical neurons in the prenatal monkey that do not express this protein in the adult (Hendrickson et al., 1991). Thus, several lines of evidence suggest that many neurons express CB during migration while only a subset of these cells retain the protein once migration has ceased.

PV must play a very different role in developing neurons and possibly the same role which it plays in the adult. PV immunoreactivity does not occur in cat SC until after birth and is maximal between P7 and P35, a period during which stimulation evoked neuronal activity is first recorded (Stein, 1984; Kao et al., 1993). Most synaptogenesis also occurs during this postnatal period (Mize and Sterling, 1977). For these reasons, PV is more likely to be involved in regulating intracellular calcium influx produced by receptor and electrical activity. Consistent with this, PV has been localized in fast spiking neurons in both the hippocampus (Kawaguchi et al., 1987) and cortex (Kawaguchi, 1993) and PV may be essential in regulating calcium influx that occurs when cells are firing at very high frequencies.

Cells containing PV may also be specifically associated with the NMDA receptor (Andressen et al., 1993; Celio, 1990). Fast spiking cells are selectively activated by NMDA receptor agonists (Kawaguchi, 1993) and the development of NMDA receptors correlates roughly with the time of initial PV expression in visual cortex (Kleinschmidt et al., 1987; Bode-Greuel and Singer, 1989; Braun, 1990; Reynolds and Bear, 1991). Thus, peak NMDA receptor and PV function may be related.

Development of Nitric Oxide Synthase in the cat SC

Organization: Nitric oxide (NO) is a free radical gas that has been implicated as a retrograde messenger in both long term potentiation and synapse stabilization in the developing brain (Gally et al., 1990; Garthwaite, 1991). NO is diffusible and membrane permeant and does not require synaptic vesicle packaging for release. It is produced in postsynaptic cells by activation of excitatory amino acid receptors (NMDA) that increase intracellular Ca++. This increase activates NO's synthetic enzyme, nitric oxide synthase (NOS), which leads to the production and release of NO (Bredt and Snyder, 1990; Garthwaite, 1991). According to the Gally hypothesis (Gally et al., 1990), post-synaptic release of NO activates guanylate cyclase-cGMP in presynaptic axons, thus enhancing neurotransmitter release and strengthening or stabilizing the synapses which contact NO containing cells (Bredt and Snyder, 1989; Gally et al., 1990). NO is a good candidate as a retrograde messenger both because of its diffusion characteristics and because the NMDA receptor is also known to be involved in synapse stabilization.

If NO is involved in the process of axon stabilization, then NOS should first be expressed at a time when synapses are being established and axons refined. To test this, we have examined the expression of NOS in the pre- and postnatal kitten SC using a histochemical reaction specific to nicotinamide adenine dinucleotide phosphate diaphorase (NADPHd), a byproduct of NO synthesis that is a marker of NOS containing neurons. These results have also been confirmed using antibodies directed against neuronal NOS.

NOS is found in very specific groups of neurons and fibers in the adult SC (Arceneaux et al., 1995). NADPH and bNOS immunoreactivity are found in cells within the dorsolateral

periaquaductal gray (pag), within cells and fibers in the deep gray layer, and within fibers and in a few neurons within the intermediate gray layer (igl). A few labeled neurons are also scattered in the superficial layers of SC. The igl labeling is of particular interest because it is primarily confined to a group of fibers and cells that we call the patch-cluster system (Figure 6)(Jeon and Mize, 1993). These fiber patches were first described by Graybiel (1978b, 1979) who showed that they contained acetylcholine. More recently, the patches have been shown t include afferent fibers from at least three sources (Figure 6): the pedunculopontine tegmental nucleus which contain acetylcholine (ACh) (Illing and Graybiel, 1985; Beninato and Spencer, 1986; Hall et al., 1989; Illing, 1990; Harting and Lieshout, 1991; Jeon and Mize, 1993); the substantia nigra which contain GABA (Graybiel, 1978a; Harting and Lieshout, 1991; Ficalor and Mize, 1989); and the frontal eye fields (Illing and Graybiel, 1985) which probably contai glutamate (Dori et al., 1992).

These fiber patches precisely overlap clusters of neurons that project to the region of the cuneiform nucleus (CFR; Jeon and Mize, 1993). The cell clusters consist of closely apposed groups of 3-20 neurons. There are 4-7 clusters per section, mostly located in the dorsal igl of the caudal SC. The correspondence between the clustered cells and fiber patches has been shown directly by double labeling experiments in which the fibers were labeled by antibodies to choline acetyltransferase (ChAT) and the cells by retrograde transport of horseradish peroxidase injected into the CFR (Jeon and Mize, 1993).

Development: This patch-cluster system is an exciting model for studying fiber-target interactions in the developing CNS for several reasons. First, the system receives fiber input from three sources, each of which uses a different neurotransmitter. These fibers must somehow establish patches during development, probably either by forming well-demarcated

bundles during outgrowth or by a process of fiber pruning as the fibers contact the clustered cells. The time at which the three fiber systems reach the igl is for the most part not known. Markers of acetylcholine do not reveal ACh containing fiber patches prior to P14 (McHaffie et al., 1991). SN fibers traced by anterograde transport of DiI reach the igl as early as P51, but a patch-like pattern of innervation has not been observed until after birth (Banfro et al., 1994). Thus, patch formation probably occurs gradually sometime between P1 and P14.

We have shown that the clustered pattern of neurons forms earlier. Clustered cells can be identified in the igl as early as P51 when DiI is injected into the CFR (Banfro and Mize, 1996). Thus, the clustered cells must either migrate from the SVZ in a clustered pattern or group into clusters before their axons reach the CFR. We do not yet know whether the clustered neurons establish this identify before or after they have migrated into the igl, but we do know that the clusters are formed well before fibers from the SN or PPTN establish obvious patches within this layer.

Figure 7 illustrates the possible steps involved in formation of the patch-cluster system in the cat SC. In the first panel (E40), neurons in the igl have migrated and formed a layer, but the clusters have not yet been established. Axons from the PPTN (red), substantia nigra (green) and frontal eye fields (yellow) are growing towards the igl but have yet to form patches. The second panel (E51) shows that some neurons in the igl have achieved an identity as 'cluster' neurons (red circles), either by selective migration, target site recognition, or the onset of some chemical substance. At this same stage the axons from all three afferent sources have reached their target field but are still distributed diffusely within the igl. The third panel (P7) suggests that another molecule (dark blue circles) is expressed in the 'cluster' cells that promotes or strengthens synaptic contacts with the three afferents. The final panel (P21)

suggests that the fibers not contacting the clustered neurons retract and die, so that only the clustered neurons and fiber patches remain.

Is nitric oxide involved in this process? We have begun to examine this hypothesis by studying the onset of expression of NOS in the developing SC. Our results show that the earliest expression of NOS occurs by E28, the earliest age examined. At this age, cells within the SVZ are well-labeled by NADPH but no NADPH positive cells are found within the tectal plate. By E36, NADPH cells with radial processes can be seen extending into the deep layers of SC. By E41, NADPHd labeled cells in the SVZ form a well-demarcated wedge and those in the deep gray layer form a dense band of neurons that extend throughout the layer (Figure 8A). The bipolar morphology of some cells in both the SVZ and dgl suggests that these cells are still migrating into the tectal plate (Figure 8A).

Although NADPH labeled cells in the dgl are well developed by E41, the earliest appearance of labeled neurons within the igl does not occur until E51-E58. Even at E58, only scattered single neurons in the igl are NADPH positive (Figure 8B). Nevertheless, these labeled cells have a periodicity characteristic of the cell clusters found in the adult igl. By P3, NADPH positive neurons form obvious clusters (Figure 9A) and as many as 20 neurons can b seen in a single cluster by P7 to P14 (Figure 9B). Although the cell clusters are well-labeled by P7 to P14, NADPH positive fiber patches are not readily visible until P35 (Figure 9C), an age at which the numbers of NADPH labeled cells begins to decline. Thus, NOS expression in 'clustered' cells in the igl occurs just prior to birth, reaches a maximum between P3 and P21, then declines gradually by the third postnatal month. The 'window' of maximal expression of NOS thus matches the time at which the afferent fibers in the igl form patches. There is thus a clear temporal correlation between NOS expression and afferent-target

matching in this system.

Whether NO is essential to this process is yet to be determined. We have recently begun experiments in which we have injected both Nw-nitro-L-arginine methyl ester (L-NAME) and Nw-nitro-L-arginine (L-NA) intraperitoneally into rat pups aged P1-P21. If NOS is involved in patch-cluster development, these NOS synthesis inhibitors should disrupt the development of the patches in this species. Our preliminary results are negative. PPTN fibers, labeled both by anti-choline acetyltransferase and NADPH, form normal appearing patches between P14 and P21 in both control and experimental groups (Scheiner and Mize, unpublished observations). We have not yet determined whether fibers from the SN and FEF are effected by these inhibitors or whether formation of the ACh fiber patches is delayed by inhibition of NOS.

Functional Considerations: Evidence that NO plays a role in synapse stabilization or pruning in other regions of the CNS is mixed. NO appears to be involved in both fiber retraction and topographic refinement in some species. In the chick optic tectum and rat superior colliculus, for example, peak NOS expression occurs in superficial layer cells at about the time at which retinal fibers reach this structure or synapses begin to form (Williams et al., 1994; Vercelli et al., 1995). Similarly, monocular enucleation either reduces NOS expression (Williams et al., 1994) or delays its expression in these neurons (Vercelli et al., 1995). More importantly, blockade of NO production using NOS inhibitors alters retinal topography in that the ipsilateral retinal-tectal pathway fails to retract in chicks (Wu et al., 1994) and the ipsilateral and contralateral retinal afferents fail to segregate in rats that have been treated with L-NA (see Wu et al., this volume).

Similar effects have been shown in the ferret lateral geniculate nucleus, where NOS inhibitors block segregation of the "on" and "off" sublaminae during a critical period (Cramer and Sur, 1994). By contrast, NO is apparently not involved in the development of other pathways. The segregation of contralateral and ipsilateral afferents is not disrupted by NOS inhibitors in the ferret LGN (see Cramer and Sur, this volume); topographic refinement of the ipsilateral and contralateral retinal afferents in SC is not disrupted in genetic "knockout" mice that presumably lack neuronal NOS (Frost et al., 1994); and infusion of NOS inhibitors into visual cortex does not block formation of ocular dominance columns in cat (Gillespie et al., 1993). Thus, NO has different effects in different species with the best evidence suggesting that NO is involved in fiber retraction in chick SC and some but not all types of fiber segregation in ferrets LGN and rat SC.

Study of the mechanisms underlying the role of NO in development is in its infancy, and many components of the process have not yet been examined. Nevertheless, the hypothesis tha a free radical gas serves as a retrograde messenger is a highly attractive and potentially important advance in our understanding of brain development and worthy of further study. Our patch-cluster model will be particularly illuminating in this regard in that it will be possible for us to examine whether NOS inhibition effects different fiber pathways, one of which uses glutamate and two of which do not. The system is also unique in that NOS is expressed in both post-synaptic clustered neurons but also in one set of afferent fibers which innervate these cells.

Summary and Conclusions

Neurons within the superior colliculus (SC) contain a variety of neurochemicals, including the amino acid neurotransmitters GABA and glutamate, the calcium binding proteins calbindin and parvalbumin, and the neuromodulator nitric oxide. We have examined the development of expression of these substances using antibody immunocytochemistry. These results are summarized in Figure 10. GABA and calbindin are expressed very early in development, at a time when cells are still dividing and migrating from the subventricular zone. The expression of both GABA and CB is maximal at around E40-46, the age at which these cells have just established their adult lamination and extrinsic afferents have begun to grow into the tectum. GABA and CB likely play diverse roles during this stage of development, including the regulation of intracellular calcium during cell migration and neurite outgrowth.

Glutamate is expressed somewhat later in development while parvalbumin immunoreactivity does not appear until shortly after birth. These two substances continue to increase in density throughout the period of postnatal growth, at a time when synapse formation and evoked electrical activity are beginning to develop. Both PV and glutamate may be involved in one or both of these activity-dependent processes.

Nitric oxide synthase (NOS) is expressed at different times in different cell groups. NOS appears very early in prenatal development in cells within the SVZ and in the deep gray layer of SC. On the other hand, cells within the intermediate gray layer of SC do not express NOS until shortly before birth. The igl cells that express NOS at this age are clustered neurons similar to those that project to the CFR in the adult. NOS expression occurs in these cells at precisely the time when axons begin to form patches that innervate these clusters. Based upon

this temporal correlation, we hypothesize that nitric oxide may regulate synapse formation in this cell group.

REFERENCES

Altman, J. and Bayer, S.A. (1981) Time of origin of neurons of the rat superior colliculus in relation to other components of the visual and visuomotor pathways. *Exp. Brain Res.*, 42:424-434.

Andressen, C., Blumcke, I. and Celio, M.R. (1993) Calcium-binding proteins: selective markers of nerve cells. *Cell Tissue Res.*, 271:181-208.

Anglister, L., Farber, J.C., Shadar, A. and Grinvald, A. (1982) Localization of voltage-sensitive calcium channels along developing neurites: Their possible role in regulating neurite elongation. *Dev. Biol.*, 94:351-365.

Arceneaux, R.D., Barnes, P.A., Scheiner, C.A., Kratz, K.E., Guido, W. and Mize, R.R. (1995) NADPH-diaphorase histochemistry reveals specific cell types in the cat superior colliculus that contain nitric oxide synthase. *Invest. Ophth. Vis. Sci.*, 36/4:1345.

Baimbridge, K.G., Celio, M.R. and Rogers, J.H. (1992) Calcium-binding proteins in the nervous system. *TINS*, 15:303-308.

Banfro, F.T. and Mize, R.R. (1994) Substantia Nigra afferents innervate the cat superior colliculus during the second half of gestation. *Soc. Neurosci. Abs.*, 20(1):187.

Banfro, F.T. and Mize, R.R. (1996) The clustered cell system is present before formation of the Ach patches in the intermediate gray layer of the cat superior colliculus. *Brain Res.*, submitted.

Beninato, M. and Spencer, R.F. (1986) Cholinergic projections to the rat superior colliculus demonstrated by retrograde transport of horseradish peroxidase and choline acetyltransferase immunohistochemistry. *J. Comp. Neurol.*, 253:525-538.

Bode-Greuel, K.M. and Singer, W. (1989) The development of N-methyl-d-aspartate receptors in cat visual cortex. *Dev. Brain Res.*, 46:197-204.

Braun, K. (1990) Calcium-Binding Proteins in Avian and Mammalian Central Nervous System: Localization, Development and Possible Functions. *Prog. Histochem. Cytochem.*, 21:1-64.

Bredt, D.S. and Snyder, S.H. (1989) Nitric oxide mediates glutamate-linked enhancement of cGMP levels in the cerebellum. *Proc. Natl. Acad. Sci. USA*, 86:9030-9033.

Bredt, D.S. and Snyder, S.H. (1990) Isolation of nitric oxide synthase, a calmodulin-requiring enzyme. *Proc. Natl. Acad. Sci. USA*, 87:682-685.

Celio, M.R. (1990) Calbindin D-28K and parvalbumin in the rat nervous system. *Neuroscience*, 35:375-475.

Chalazonitis, A. and Fischbach, G. (1980) Elevated potassium induces morphological differentiation of dorsal root ganglionic neurones in dissociated cell culture. *Dev. Biol.*, 78:173.

Chalupa, L.M. (1984) Visual physiology of the mammalian superior colliculus. In Vanegas, H. (Ed), *Comparative Neurology of the Optic Tectum,* Plenum, New York, pp. 775-818.

Constantine-Paton, M., Cline, H.T. and Debski, E. (1988) Patterned activity, synaptic convergence, and the NMDA receptor in developing visual pathways. In Cowan, W.M., Shooter, E.M., Stevens, C.F. and Thompson, R.F. (Eds.) *Annual Reveiws of Neuroscience, Vol. 11,* Annual Reviews, Inc., Palo Alto, pp.129-154.

Cooper, M.L. and Rakic, P. (1981) Neurogenetic gradients in the superior and inferior colliculi of the *Rhesus* monkey. *J. Comp. Neurol.*, 202:309-334.

Cooper, M.L. and Rakic, P. (1983) Gradients of cellular maturation and synaptogenesis in the superior colliculus of the fetal *Rhesus* monkey. *J. Comp. Neurol.*, 215:165-186.

Cramer, K.S. and Sur, M. (1994) Inhibition of nitric oxide synthase disrupts on/off sublamination in the ferret lateral geniculate nucleus. *Soc. Neurosci. Abs.*, 20(2):1470.

Cramer, K.S. and Sur, M. (1996) The role of NMDA receptors and nitric oxide in retinogeniculate development. In *Progress in Brain Research*, present volume.

Dori, I., Dinopoulos, A., Cavanaugh, M.E. and Parnavelas, J.G. (1992) Proportion of glutamate- and aspartate-immunoreactive neurons in the efferent pathways of the rat visual cortex varies according to the target. *J. Comp. Neurol.*, 319:191-204.

Edwards, M.A., Caviness, V.S. and Schneider, G.E. (1986a) Development of cell and fiber lamination in the mouse superior colliculus. *J. Comp. Neurol.*, 248:395-409.

Edwards, M.A., Schneider, G.E. and Caviness, Jr.,V.S. (1986b) Development of the crossed retinocollicular projection in the mouse. *J. Comp. Neurol.*, 248:410-421.

Ficalora, A.N. and Mize, R.R. (1989) The neurons of the substantia nigra and zona incerta which project to the cat superior colliculus are GABA immunoreactive: a double-label study using GABA immunocytochemistry and lectin retrograde transport. *Neuroscience*, 29:567-581.

Finlay, B.L., Berg, A.T. and Sengelaud, D.R. (1982) Cell death in the mammalian visual system during normal development: II. Superior colliculus. *J. Comp. Neurol.*, 204:318-324.

Frost, D.O., Zhang, X.-F., Huang, P.L. and Fishman, M.C. (1994) Effect of Nitric oxide synthase gene knockout or blockade on the develpoment of retinal projections. *Soc. Neurosci. Abs.*, 20(2):1318.

Gally, J.A., Montague, P.R., Reeke, Jr., G.N. and Edelman, G.M.(1990) The NO hypothesis: Possible effects of a short-lived, rapidly diffusible signal in the development and function of the nervous system. *Proc. Natl. Acad. Sci. USA*, 87:3547-3551.

Garthwaite, J. (1991) Glutamate, nitric oxide and cell-cell signalling in the nervous system. *TINS*, 14(29): 60-67.

Gillespie, D.C., Ruthazer, E.S., Dawson, T.M., Snyder, S.M. and Stryker, M.P. (1993) Nitric oxide synthase inhibition does not prevent ocular dominance plasticity in cat visual cortex. *Soc. Neurosci. Abs.*, 19:893.

Goodman, C.S. and Shatz, C.J. (1993) Developmental mechanisms that generate precise patterns of neuronal connectivity. *Cell/Neuron Suppl.*, 10:77-98.

Graybiel, A.M. (1978a) Organization of the nigrotectal connection: an experimental tracer study in the cat. *Brain Res.*, 143:339-348.

Graybiel, A.M. (1978b) A stereometric pattern of distribution of acetylcholinesterase in the deep layers of the superior colliculus. *Nature*, 272:539-541.

Graybiel, A.M. (1979) Periodic-compartmental distribution of acetycholinesterase in the superior colliculus of the human brain. *Neuroscience*, 4:643-650.

Hall, W.C., Fitzpatrick, D., Klatt, L.L. and Rackowski, D. (1989) Cholinergic innervation of the superior colliculus in the cat. *J. Comp. Neurol.*, 287:495-514.

Hansen, G.H., Meier, E., Abraham, J. and Schousboe, A. (1987) Trophic effects of GABA on cerebellar granule cells in culture. In Redburn, D.A. and Schousboe, A. (Eds.), *Neurotrophic Activity of GABA During Development,* Alan R. Liss, New York, pp. 109-138.

Harting, J.K. and Lieshout, D.P.V. (1991) Spatial relationship of axons arising from the substantia nigra, spinal trigeminal nucleus and pedunculopontine tegmental nucleus within the intermediate gray of the cat superior colliculus. *J. Comp. Neurol.*, 305:543-558.

Heizmann, C.W. and Hunziker, W. (1990) Intracellular calcium-binding molecules. In Bronner, F. (Ed.), *Intracellular Calcium Regulation*, Alan R. Liss, New York, pp.211-248.

Hendrickson, A.E., Van Brederode, J.F., Mulligan, K.A. and Celio, M.R. (1991) Development of the calcium binding protein parvalbumin and calbindin in the monkey striate cortex. *J. Comp. Neurol.*, 307:626-646.

Huerta, M.F. and Harting, J.K. (1984) The mammalian superior colliculus: Studies of its morphology and connections. In H. Vanegas (Ed.), *Comparative Neurology of tthe Optic Tectum*, Plenum, New York, pp. 687-773.

Illing, R.B. (1990) Choline acetyltransferase-like immunoreactivity in the superior colliculus of th cat and its relation to the pattern of acetylcholinetransferase staining. *J.Comp. Neurol.*, 296:32-46.

Illing, R.B. and Graybiel, A.M. (1985) Convergence of afferents from frontal cortex and substantia nigra onto acetylchoilinesterase-rich patches of the cat's superior colliculus. *Neuroscience*, 14:455-482.

Jeon, C.-J. and Mize, R.R. (1993) Choline acetyltransferase immunoreactive patches overlap specific efferent cell groups in the cat superior colliculus. *J.Comp. Neurol.*, 337:127-150.

Jeon, C.-J., Spencer, R.F. and Mize, R.R. (1993) Organization and synaptic connections of cholinergic fibers in the cat superior colliculus. *J.Comp. Neurol.*, 333: 360-374.

Kao, C.-Q., Stein, B.E. and Coulter, D.A. (1993) Postnatal development of synaptic responses ir deep layers of superior colliculus slices studied using whole cell patch techniques. *Soc. Neurosci. Abs.*, 19(1):768.

Kater, S.B., Mattson, M.P., Cohan, C. and Connor, J. (1988) Calcium regulation of the neuronal growth cone. *TINS*, 11:315-321.

Kawaguchi, Y. (1993) Groupings of nonpyramidal cells with specific physiological and morphological characteristics in rat frontal cortex. *J. Neurophysiol.*, 69:416-431.

Kawaguchi, Y. and Kubota, Y. (1993) Correlation of physiological subgroupings of nonpyramidal cells with parvalbumin and Calbindin D-28K-immunoreactive neurons in layer V of rat frontal cortex. *J. Neurophysiol.*, 70:387-374.

Kawaguchi, Y., Katsumaru, H., Kosaka, T., Heizmann, C.W. and Hama, K. (1987) Fast spiking cells in rat hippocampus (CA1 region) contain the calcium binding protein parvalbumin. *Brain Res.*, 416:369-374.

Kleinschmidt, A., Bear, M.F. and Singer, W. (1987) Blockade of "NMDA" receptors disrupts experience-dependent plasticity of kitten striate cortex. *Science*, 238:355-358.

Komuro, H. and Rakic, P. (1992) Selective role of N-type calcium channels in neuronal migration. *Science*, 257:806-809.

Kraszewski, K. and Grantyn, R. (1992) Unitary, quantal and miniature GABA-activated synaptic chloride currents in cultured neurons from rat superior colliculus. *Neuroscience*, 47:555-570.

Lauder, J.M., Han, V.K.M., Henderson, P., Verdoorn, T. and Towle, A.C. (1986) Pre-natal ontogeny of the GABAergic system in the rat brain: an immunocytochemical study. *J. Neurosci.*, 19:465-493.

Liu, F. C. and Graybiel, A.M. (1992) Transient calbindin -D 28k -positive systems in the telencephalon: ganglionic eminence, developing striatum and cerebral cortex. *J. Neurosci.*, 12:674-690.

Lo, F.-S., Cork, R.J. and Mize, R.R. (1995) A high-frequency burst firing mode in neurons of the rat superior colliculus. *Soc. Neurosci. Abs.*, 21:655.

Lund, R.D. and Lund, J.S. (1972) Development of synaptic patterns in the superior colliculus of the rat. *Brain Res.*, 42:1-20.

Luskin, M.B. and Shatz, C.J. (1985) Studies of the earliest generated cells of the cat's visual cortex: Cogeneration of subplate and marginal zones. *J. Neurosci.*, 5:1062-1075.

Mattson, M.P. and Kater, S.B. (1987) Calcium regulation of neurite elongation and cone motility *J. Neuroscience.*, 7:4034-4043.

Meier, E., Drejer, J. and Schousboe, A. (1984) GABA induces functionally active low-affinity GABA receptors on cultured cerebellar granule cells. *J. Neurochem.*, 43:1737-1744.

Messersmith, E.K. and Redburn, D.A. (1993) The role of GABA during development of the oute retina in the rabbit. *Neurochem. Res.*, 18:463-470.

McHaffie, J., Beninato, M., Stein, B.E. and Spencer, R.F. (1991) Postnatal development of acetylcholinesterase and cholinergic projections to the cat superior colliculus. *J.Comp. Neurol.*, 313:113-131.

Michler-Stuke, A. and Wolff, J.R. (1987) Facilitation and inhibition of neurite elongation by GABA in chick tectal neurons. In Redburn, D.A. and Schousboe, A. (Eds.), *Neurotrophic Acitivity of GABA During Development,* Alan R. Liss, New York, pp.253-266.

Miller, M.W. (1986) The migration and neurochemical differentiation of gamma-aminobutyric acid (GABA)-immunoreactive neurons in rat visual cortex as demontrated by a combined immunocytochemical-autoradiographic technique. *Dev. Brain Res.*, 28:41-46.

Mize, R.R. (1988) Immunocytochemical localiztion of gamma-aminobutyric acid (GABA) in the cat superior colliculus. *J.Comp. Neurol.*, 276:169-187.

Mize, R.R. (1992) The organization of GABAergic neurons in the mammalian superior colliculus. In Mize, R.R., Marc, R.E. and Sillito, A.M. (Eds.), *GABA in the Retina and Central Visual System, Progress in Brain Research, Vol.90,* Elsevier, Amsterdam, pp.219-248.

Mize, R.R. (1994) Conservation of basic synaptic circuits that mediate GABA inhibition in the subcortical visual system. In Bloom, F. (Ed.), *Neuroscience: From the Molecular to the Cognitive, Progress in Brain Research, Vol.100*, Elsevier, Amsterdam, pp.123-132.

Mize, R.R. (1996) Neurochemical microcircutry underlying visual and oculomotor function in the cat superior colliculus. *Progress in Brain Res. (In press)*

Mize, R.R. and Sterling, P. (1977) Synaptic development in the superficial gray layer of the cat superior colliculus. *Ant. Rec.*, 187:658.

Mize, R.R. and Luo, Q. (1992) Visual deprivation fails to reduce calbindin 28kD or GABA immunoreactivity in the *Rhesus* monkey superior colliculus. *Vis. Neurosci.*, 9:157-168.

Mize, R.R., Spencer, R.F. and Sterling, P. (1982) Two types of GABA-accumulating neurons in the superficial gray layer of the cat superior colliculus. *J.Comp. Neurol.*, 206:180-192.

Mize, R.R., Jeon, C.-J., Butler, G.D., Luo, Q. and Emson, P.C. (1991) The calcium binding protein calbindin-D28K reveals subpopulations of projections and interneurons in the cat superior colliculus. *J. Comp. Neurol.*, 307:417-436.

Mize, R.R., Luo, Q., Butler, G., Jeon, C.-J. and Nabors, B. (1992) The calcium binding proteins parvalbumin and calbindin-D28K form complementary patterns in the cat superior colliculus. *J. Comp. Neurol.*, 320:243-256.

Mustari, M.J., Lund, R.D. and Graubard, K. (1979) Histogenesis of the superior colliculus of the albino rat: A tritiated thymidine study. *Brain Res.*, 164:39-52.

Okada, Y. (1992) The distribution and function of gamma-aminobutyric acid (GABA) in the superior colliculus. In Mize, R.R., Marc, R.E., and Sillito, A.M. (Eds.), *GABA in the Retina and Central Visual System, Progress in Brain Research, Vol. 90*, Elsevier, Amsterdam, pp.249-262.

Redburn, D.A. (1992) Development of GABAergic neurons in the mammalian retina. In Mize, R.R., Marc, R.E., and Sillito, A.M. (Eds.), *GABA in the Retina and Central Visual System, Progress in Brain Research, Vol. 90*, Elsevier, Amsterdam, pp. 133-147.

Reynolds, I.J. and Bear, M.F. (1991) Effects of age and visual experience on [^{3}H]MK801 binding to NMDA receptors in the kittens visual cortex. *Exp. Brain Res.*, 85:611-615.

Sanes, J.R. (1993) Topographic maps and molecular gradients. *Curr. Opin. Neurobiol.*, 3:67-74.

Shatz, C.J. (1990) Impulse activity and the patterning of connections during CNS development. *Neuron*, 5:745-756.

Simon, D. K. and O'Leary, D.D.M. (1992) Development of topographic order in the mammalian retinocollicular projection. *J.Neurosci.*, 12:1212-1232.

Simon, D.K., Prusky, G.T., O'Leary, D.D.M. and Constantine-Paton, M. (1992) N-Methyl-D-aspartate receptor antagonists disrupt the formation of a mammalian neural map. *Proc. Natl. Acad. Sci. USA*, 89:10593-10597.

Spoerri, P.E. (1987) GABA-mediated developmental alternation in a neuronal cell line in cultures of cerebral and retinal neurons. In Redburn, D.A. and Schousboe, A. (Eds.), *Neurotrophic Activity of GABA During Development,* Alan R. Liss, New York, pp. 189-220.

Stein, B.E. (1984) Development of the superior colliculus. In Cowan, W.M., Shooter, E.M., Stevens, C.F., and Thompson, R.F. (Eds.), *Annual Reveiws of Neuroscience, Vol. 7,* Annual Reviews, Inc., Palo Alto, pp.95-125.

Udin, S.B. and Fawcett, J.W. (1988) Formation of topographic maps. In Cowan, W.M., Shooter, E.M., Stevens, C.F. and Thompson, R.F. (Eds.), *Annual Review of Neuroscience, Vol. 11,* Annual Reviews, Inc., Palo Alto, pp. 289-327.

Van Eden, C.G., Mrzljak, L., Voorn, P. and Uylings, H.M.B. (1989) Prenatal developments of GABAergic neurons in the neocortex of the rat. *J. Comp. Neurol.*, 289:213-227.

Vercelli, A., Biasiol, S. and Jhaveri, S. (1995) Development of NADPH-diaphorase activity in the superficial layers of the rat superior colliculus (SC): Effects of eye enucleation and of activity. *Soc. Neurosci. Abs.*, 21:817.

Warton, S.S., Perouansky, M. and Grantyn, R. (1990) Development of GABAergic synaptic connections in vivo and in cultures from the rat superior colliculus. *Dev. Brain Res.*, 52:95-111.

Williams, C.V., Nordquist, D. and McLoon, S.C. (1994) Correlation of nitric oxide synthase expression with changing patterns of axonal projections in the developing visual system. *J. Neurosci.*, 14(3):1746-1755.

Wu, H.H., Williams, C.V. and McLoon, S.C. (1994) Involvement of nitric oxide in the elimination of a transient retinotectal projection in development. *Science*, 265:1593-1596.

Wu, H.H., Waid, D.K. and McLoon, S.C. (1996) Nitric oxide and the developmental remodeling of retinal connections in the brain. In *Progress in Brain Research*, present volume.

Figure Captions

Figure 1. GABA immunoreactivity in the prenatal kitten superior colliculus at E30. (A) Dense immunoreactivity is already present in the superficial layers (SL) of the tectal plate. Scattered labeled cells are also found within the deep layers (DL) and the subventricular zone (SVZ). (B) SL labeling consists of densely labeled cell bodies and neuropil. Most cells in the DL and SVZ have a bipolar morphology typical of migrating neurons; (C) Higher magnification view of vertical fusiform cell bodies and vertically oriented dendritic processes (arrows). Asterisk in A marks sites shown at higher magnification in B,C. VZ = ventricular zone; CA = Cerebral aqueduct. Scale bars: A = 200 μm; B = 50 μm; C = 20 μm.

Figure 2. GABA immunoreactivity in the prenatal kitten superior colliculus at E46. (A) The distribution of cells is like that of the adult, with large numbers of cell bodies in the superficial (SL) and intermediate layers (IL) and fewer neurons in the deep layers (DL). Note that labeled cells are also present in the dorsal periaquaductal gray (PAG). Well-labeled cell bodies and punctae in the neuropil in the SL (B), IL (C), and DL (D). Asterisks in A mark locations illustrated in panels B,C, and D. Scale bars: A = 100 μm; B-D = 20 μm.

Figure 3. Calbindin (CB) immunoreactivity in the prenatal kitten superior colliculus (SC) at E28. (A) CB neurons are distributed throughout the tectal plate and within the dorsal subventricular zone (SVZ). The morphology of these cells differs in different regions. (B) CB neurons near the surface of SC are small with few or no dendritic processes. Cells within the intermediate region of the tectal plate are larger and have multipolar processes. (C) CB labeled neurons within the deepest region of SC and within the SVZ have bipolar morphologies with vertically ascending dendrites typical of migrating cells (small arrows). Asterisks and large arrows in A mark the location of regions illustrated in B and C. CA = cerebral aqueduct; VZ = ventricular zone. Scale

bars: A = 100 μm; B-C = 20 μm.

Figure 4. Calbindin (CB) immunoreactivity in the prenatal kitten superior colliculus (SC) at E34, E40, and E46. (A) CB labeled cells are found throughout the tectal plate as well as within the subventricular zone (SVZ) at E34. Many cells in the deep layers and SVZ have a bipolar morphology. Arrowheads mark the superficial, intermediate, and deep layers of SC at this age. (B-C) Three tiers of CB neurons are visible by E40 (B) and well-developed by E46. (C). Most cells are small, but a few have larger cell bodies (arrows). sdt = superficial dense tier; idt = intermediate dense tier; ddt = deep dense tier; pag = periaquaductal gray; CA = cerebral aqueduct; VZ = ventricular zone. Scale bar: A,B,C = 100 μm.

Figure 5. Parvalbumin (PV) immunoreactivity in the postnatal kitten superior colliculus (SC) at P7, P21, and P35. (A) PV immunoreactivity is present in medium and large sized cells at P7. The dense band is not yet visible. There are no cells in the superficial gray layer (sgl). (B) By P21, a dense band of labeled neurons is visible within the ol (optic layer) and scattered PV neurons are seen deep. (C) An obvious dense band of PV immunoreactivity in neurons and neuropil is visible at P35. Scattered cells in the intermediate gray layer (igl) and deeper layers (dl) are intensely labeled. Scale bar. A-C = 200 μm.

Figure 6. The patch-cluster system in the intermediate gray layer of the cat superior colliculus. Clustered neurons project to the cuneiform region (CFR) of the caudal midbrain. Clustered neurons overlap patches of afferent fibers from the pedunulcopontine tegmental nucleus (PPTN) that contain acetylcholine (ACh), from the substantia nigra (SN) that contain GABA, and from the frontal eye fields (FEF) that probably contain glutamate (Glu). Synaptic contacts involving various receptors are suggested but have not yet been demonstrated experimentally. Evidence suggests that the clustered neurons express nitric oxide synthase (NOS) transiently during

development.

Figure 7. Development of the patch-cluster system in the intermediate gray layer (igl) of the cat superior colliculus. Early in prenatal development (E40), neurons within the igl (blue circles) have no identifiable neurochemical characteristics that distinguish the clustered neurons. Extrinsic axons from the pedunculopontine tegmental nucleus (PPTN, red), the substantia nigra (SN, green), and frontal eye fields (FEF, yellow) have not reached the SC at this age. By E51, the clustered neurons (red circles) are labeled by DiI injected into the cuneiform region (CFR), indicating that the clusters are established at the time their axons reach the CFR. Axons from the SN (green), and possibly from the PPTN (red) and FEF (yellow), have reached the igl, but no patches are present. By P7, clustered cells avidly express NOS (dark blue circles). Our hypothesis predicts that the patches are beginning to form and that axons not contacting NOS containing neurons are retracting from the igl. By P21, the adult patch cluster system has been established and NOS expression is reduced (light blue circles).

Figure 8. Nicotinamide adenine dinucleotide phosphate diaphorase (NADPHd) labeling in the prenatal kitten superior colliculus (SC) at E41 and E58. (A) At E41, NADPHd labeled neurons form a wedge of cells in the dorsal subventricular zone. Labeled cells are also present in the deep layer (dgl) of SC. A few bipolar neurons extend from the deep layer towards the intermediate layer of SC at this age (arrows). (B) By E58, single neurons labeled by NADPHd (arrows) can be seen in the intermediate gray layer (igl). The periodicity of these cells is similar to that of clustered neurons in the igl. Scale bars; A-B = 100 μm.

Figure 9. Nicotinamide adenine dinucleotide phosphate diaphorase (NADPHd) labeling in the postnatal kitten superior colliculus (SC) at P3, P14, and P35. (A) Two clusters (arrows) of NADPHd labeled neurons are visible in the intermediate gray layer (igl) by P3. Labeled cells are

also seen in the deep gray layer (dgl) and the periaquaductal gray (pag). (B) By P14, the NADPHd clusters (arrow) contain more labeled neurons and a few fibers. (C) By P35, the number of NADPHd labeled clustered cells has decreased, but fiber labeling is intense (arrow). Scale bar: A-C = 100 μm.

Figure 10. Summary diagram showing the time course of pre- and postnatal development of the cat superior colliculus. The time scale is indicated by the large central arrow. Developmental events, including cell generation, migration, lamination, afferent innervation, synaptogenesis, and the onset of neuronal activity are shown above that line. Mitosis, migration, and lamination occur early and are largely complete by E40-46. Synaptogenesis and neuronal activity occur later, usually at or shortly after birth. Afferent innervation occurs at different times for different afferents. The time of onset and maximal expression of gamma aminobutyric acid (GABA), calbindin (CB), glutamate (GLU), parvalbumnin (PV), and nitric oxide synthase (bNOS) are shown below the time line arrow. GABA and CB are expressed early, GLU and PV later, and bNOS at various times during pre- and postnatal development.

Acknowledgments

Foremost, we thank Grace D. Butler for her continuous technical support of these projects, particularly her expertise in immunocytochemistry. We also thank Dr. John Cork for his contribution to the digital graphics illustrated in this paper. Many student collaborators contributed to the data analysis reported in this review: Mike Tamberella, John Hewitt, Monica Simon, Renee Arceneaux, and Paul Barnes. This research was supported by USPHS Grant EY-02973 from the National Eye Institute, U.S. Army Research and Development Grant DAMD 17-93-V-3013-P40001, a Louisiana Educational Quality Support Fund Enhancement Grant LEQSF-ENH TR-20, and the Neuroscience Center of Excellence at LSU Medical Center. Chris Scheiner is a Board of Regents Fellow supported by LEQSF grant (95-00)-GF-12.

Rev. 10/08/96 1:27 PM

Inhibition of Nitric Oxide Synthase Fails to Disrupt the Development of Cholinergic Fiber Patches in the Rat Superior Colliculus.

R.R. Mize
C.A. Scheiner
M.F. Salvatore
R.J. Cork

Departments of Anatomy, Ophthalmology, and the Neuroscience Center
Louisiana State University Medical Center, 1901 Perdido Street, New Orleans, LA 70112
USA

Key words:
nitric oxide
synapse formation
axon pathfinding
Nω-nitro-L-arginine
acetylcholine
visual system

Short title: NOS inhibition and development of rat SC

Send proofs to:

Dr. R. Ranney Mize
Department of Anatomy
LSU Medical Center
1901 Perdido Street
New Orleans, LA 70112
Tele: 504-568-4012
Fax: 504-568-4392
Email: rmize@lsumc.edu

Abstract

Nitric oxide (NO) may serve as a retrograde messenger to refine or stabilize synapses in the developing nervous system. Whether this action is dependent upon glutamate and the N-Methyl-D-Aspartate (NMDA) receptor is not yet established. We have used the patch-cluster system in the intermediate gray layer (IGL) of the rat superior colliculus (SC), a system receiving both glutamatergic and cholinergic input, to study this question. The normal distribution and development of nitric oxide synthase (NOS) in SC was examined using nicotinamide adenine dinucleotide phosphate diaphorase (NADPHd) histochemistry in Sprague-Dawley rats aged P4 to adulthood. Fibers containing acetylcholine (ACh) were identified using choline acetyltransferase immunocytochemistry. In addition, Nω-nitro-L-arginine (NoArg), an inhibitor of NOS, was injected intraperitoneally from birth until P10, P14, P18, or P21-22 to determine if NOS inhibition would disrupt the formation of the ACh patches. Control animals were studied from the same age groups. Our results show NADPHd labeled cells within the periaqueductal gray (PAG) and the deep gray layer (DGL) of SC by P4, the earliest age examined. By P8-P9, cells in the IGL were well labeled by NADPHd, while few in the superficial layers (SL) were labeled. SL cells were visible by P10 and were intensely labeled by P14. IGL cells transiently expressed NADPHd in that the number of labeled cells increased from P8-P35, then decreased in the adult. ChAT labeled fibers first appeared in the IGL at P10, formed a characteristic two-tier pattern by P14, and established obvious patches by P21. Inhibition of NOS from birth produced no qualitative differences in the distribution or density of either ChAT labeled fibers or NADPHd labeled cells and fibers at any of the ages examined. We therefore conclude that NO does not contribute to the refinement of cholinergic fiber patches in the rat SC, probably because the fiber system is not glutamatergic.

Introduction

Nitric oxide (NO) is a free radical gas with diffusion properties that make it an excellent candidate for a retrograde messenger in the central nervous system. Release of NO is thought to start with an influx of calcium through the N-Methyl-D-Aspartate receptor which activates nitric oxide synthase (NOS) to produce NO that diffuses from the postsynaptic cell into presynaptic terminals. NO is then thought to act upon the presynaptic guanylate cyclase-cGMP system to enhance neurotransmitter release, probably glutamate[1,2]. This process has been implicated in the synaptic plasticity that occurs during long term potentiation (LTP)[3-8] and in axon refinement during development [7,9].

Evidence for this hypothesis in development is, to date, scanty. In the visual system, NO appears to be involved in both fiber retraction and the refinement of topographic maps. Peak NOS expression occurs in cells at the time at which axons from the retina are retracting in both the chick optic tectum [10] and the rat superior colliculus (SC) [11]. Monocular enucleation reduces NOS expression during this period [10] and interruption of NO release using inhibitors of NOS disrupts topographic refinement of both the ipsilateral and contralateral retino-tectal pathways in chicks [11,12]. A similar effect has been shown in the lateral geniculate nucleus of the ferret where NOS inhibitors block segregation of the "on" and "off" sublaminae of this nucleus [13,14]. On the other hand, the eye-specific segregation of ipsilateral and contralateral retinal input to the ferret LGN is not disrupted by inhibition of NOS [14] and the topography of ipsilateral and contralateral retinal afferents projecting to the SC is not altered in nNOS genetic knockout mice that presumably lack NO [15]. Our understanding of the role of NO in fiber refinement is, therefore, in its formative stages.

A number of questions remain unanswered. For example, it is not yet established whether NO affects only glutamatergic synapses or whether it can also enhance transmitter release or otherwise

affect synapses that use other neurotransmitters [16,17]. Nor is it known whether the NMDA receptor is the only source of Ca^{2+}-influx that regulates the production of NOS. Other sources of increased calcium could include the inositol trisphosphate (IP_3)-dependent release of intracellular calcium stores after activation of the G-protein linked ACh receptor or calcium influx through various voltage-gated calcium channels.

The model that we have chosen to address these questions is the patch-cluster system in the mammalian SC. This system in cat consists of 'clusters' of neurons within the intermediate gray layer (IGL) that project through the tectopontobulbar pathway to the region of the cuneiform nucleus [18]. These cell clusters precisely overlap fiber patches in the IGL that arise from mesencephalic tegmental nuclei and that contain acetylcholine [19,20]. Fibers from the substantia nigra that contain GABA [21], and those from the prefrontal eye fields that probably contain glutamate, also form patches that overlap those containing ACh [22,23]. The patch-cluster system is not as well defined in the rat, but fiber patches in the rat SC also arise from brainstem nuclei and contain ACh [20].

The patch-cluster system is of particular interest because we have shown that neurons that form clusters in the cat IGL first express NOS [24,25] at about the time that the ACh afferents innervate the IGL [26]. These ACh afferents then establish their characteristic patch-like distribution during the time at which clustered cells are heavily labeled by NADPHd [24]. In the present study, we have determined whether the patch-cluster system in rat is disrupted by inhibition of NOS. In addition, we have examined the normal distribution and onset of expression of NOS in this species.

Materials and Methods

Animals and drug treatment

We examined the distribution of nitric oxide synthase (NOS) and choline acetyltransferase (ChAT) in normal adult and postnatal rats and in rats in which NOS was inhibited. Adult rats were obtained from Harlan Sprague Dawley (Indianapolis, IN). Timed pregnancies were also obtained from this supplier. Birth dates were determined to within 24 hours. All procedures involving the use of experimental animals were approved by the LSU Medical Center IACUC office.

Rat pups from newly born litters were divided randomly into experimental and control groups. Experimental animals received intraperitoneal injections of 1, or 3 μmol/g body weight Nω-Nitro-L-arginine (NoArg, Sigma, St. Louis) daily from P1 (the day after birth) until day of sacrifice. Control animals received injections of comparable volumes of normal saline. Control and inhibited animals were perfused at postnatal ages P8 (N=2) , P10-11(N=6), P14(N=6), P18(N=3), P21-22(N=6), and P28(N=3). At least one additional rat from ages P4, P5, P9 and P35 was used to examine the normal development of NADPH labeling. The P28 case was discarded because of poor fixation.

Animals were anesthetized with a Ketamine hydrochloride/xylazine mixture (80 mg/kg body weight) and perfused transcardially with 4% paraformaldehyde, 0.1% glutaraldehyde in phosphate buffer at pH 7.4 . Glutaraldehyde was omitted in the normal rats aged P4-P9 and in one adult. After perfusion, all brains were removed, post-fixed in the same fixative for 4-18 hr., and placed in a phosphate buffer at pH 7.4 with 8% dextrose added. The following day, the brains were blocked, cut on a vibratome into 50-100 μm sections, and treated for histochemistry or immunocytochemistry. All sections were then mounted on glass slides, dehydrated in alcohol/xylene, and coverslipped.

Histochemistry procedures

Sections treated to identify NOS were reacted with nicotinamide adenine dinucleotide phosphate diaphorase (NADPHd) histochemistry. Sections were first rinsed in tris buffer and placed in a NADPH solution containing 50mg NADPH, 12.5 mg nitro blue tetrazolium, and 50ml 0.3% Triton X-100, tris buffer, pH 7.1 at 37 °C for 1-3 hrs. The sections were then rinsed in phosphate buffer, dehydrated, and coverslipped. Sections treated for choline acetyltransferase (ChAT) immunocytochemistry were prepared using the ABC technique (Vector Laboratories, Burlingame CA). Sections were rinsed in phosphate buffered saline (PBS) and incubated in blocking serum (4% normal rabbit serum) for 1 hr. They were then incubated in a 1:500 dilution of goat anti-ChAT (Chemicon International, Temecula, CA) for 44-48 hrs, rinsed, and incubated with secondary antisera (rabbit anti-goat, 1:100 in PBS), rinsed again, then incubated with avidin biotin complex (ABC) for one hour. Sections were then rinsed and reacted with 0.05% 3,3'-diaminobenzidine (DAB) in tris buffer with 0.003% H_2O_2. Sections from most experiments were enhanced with 0.005% nickel chloride/cobalt acetate [27] for 90-150 sec, rinsed and treated as above.

Determination of NOS inhibition in brain

We examined the amount of NOS inhibition produced by Nω-Nitro-L-arginine in P14, P18, and P22 rat pups. Two P14, one P18 and seven P22 rats received daily injections of 1 μmol/g body weight NoArg, and two P14 and one P18 rat received 3 μmol/g body weight daily injections prior to sacrifice. Each age group was compared with at least one saline injected pup of the same age. Rat pups were decapitated, their brains rapidly removed and homogenized in 20 mM Hepes containing 0.32 M sucrose, 1mM dithiothreitol (DTT), and 0.5 mM EGTA for 1 minute [28]. The homogenate was centrifuged for 15 minutes at 4°C and then the supernatant was removed and centrifuged again for an additional 15 min. The cytosolic homogenate (supernatant) was removed and applied to 1 ml columns of Dowex AG50W-X8 (Na^+ form) to remove endogenous arginine. The protein content of the arginine-free homogenate was determined. Aliquots containing 300 mg

of protein were then incubated for 15 minutes at 37 °C with buffer containing 20 mM Hepes, 0.32 mM sucrose, 1mM DTT, 0.5 mM EGTA, 0.5 mM $CaCl_2$, 200 μM NADPH, 1μM L-arginine, and 0.1 μCi/ml [^{3}H]L-arginine. The reaction was stopped by adding 2 ml of 20 mM Hepes containing 2mM EDTA (pH=5.5). Samples were applied to Dowex AG50W-X8 (Na^+ form) to remove [^{3}H]L-arginine and elute any [^{3}H]L-citrulline. The columns were then washed with 3.0 ml of water and the [^{3}H]L-citrulline content was quantified by liquid scintillation spectroscopy of the flow-through and water rinse. DPM's were calculated and the data expressed as pmoles of L-citrulline/min/mg protein for each animal. From this data we calculated the percent inhibition compared to the age group control.

Data Analysis

Coronal sections through the rostral-caudal extent of SC were examined with the light microscope from at least one control and one experimental animal at ages P10-11, P14, P18, and P21-22. Both NADPH and ChAT labeled sections were examined and photographic records taken using a Zeiss Universal camera system. We also examined and photographed sections from normal animals aged P4, P5, P8, P9 and P35 that were labeled only with NADPH. The laminar distribution of NADPH labeled neurons in normal control animals was examined quantitatively by use of a computer based Neuron Tracing System (NTS; Eutectic Electronics, Rayleigh NC). Between 3 and 6 sections from at least one animal aged P4,P5,P8,P9,P10,P11, P14, P18, P21, and one adult, were plotted. Plots were produced by outlining the surface of SC by moving a screen cursor with a joystick. The position of each NADPH labeled neuron was also recorded. Histograms were generated from these plots to illustrate the relative number of cells at different depths within the SC at different ages.

We also estimated quantitatively the number of NADPH labeled neurons within the IGL of SC at different ages. Cell counts were made manually at 20X magnification from 3-10 sections from control animals at ages P4, P5, P8, P9, P14, P18, P21, P35, and from two adult rats. These counts were expressed as number of cells within the IGL for each section at each age.

Results

Distribution of NOS and ChAT in the adult rat SC

NOS was present in only a small subset of neurons within the juvenile (P35) and adult rat superior colliculus, as revealed by NADPHd histochemistry. In addition, selected fiber pathways were intensely labeled by NADPH. The densest concentration of NADPHd positive neurons was found within the zonal (ZL) and superficial gray (SGL) layers of SC. These neurons formed a dense band that extended from the surface of SC to the ventral border of the SGL. The band consisted of intensely labeled cell bodies, dendrites, and axon-like fibers that extended throughout the rostro-caudal axis of SC (fig. 1A-C).

Many fewer NADPHd positive neurons were found below the SGL. Only a few lightly labeled neurons were seen within the optic layer (OL) and no labeled fibers were found in that layer (fig. 1A-C). Scattered well-labeled neurons were present within the intermediate gray (IGL) layer. These neurons were mostly located within NADPH labeled fiber patches within the IGL (fig. 1B-C, arrows). NADPH positive fibers in this layer also had a characteristic distribution. Within the rostral SC, they formed a single continuous band (fig. 1A). In the middle and caudal SC, they were distributed in two separate tiers, one within the dorsal IGL, the other within the ventral IGL (fig. 1B-C). Both tiers had patches of heavy fiber labeling (fig. 1B,C, arrows) with interpatch intervals that contained many fewer fibers. NADPH labeled fibers also formed bridges between the two tiers (see fig. 1B,C).

The remaining cellular and fiber labeling in SC was distributed primarily within columnar streams within the deep gray (DGL) layer. Most of the labeled fibers projected vertically towards the IGL and most of the labeled cells were located within these fiber streams (fig. 1B,C). NADPH positive fibers and cells were also found within a dorsolateral wedge of the periaqueductal gray (PAG).

Some cells within this wedge had dendrites that projected into the deep layers of SC (fig. 1A-C). Finally, NADPH labeling was found within the mesencephalic tegmentum where it intensely labeled cells within three nuclei: the parabigeminal nucleus (PBG), the pedunculopontine tegmental nucleus (PPTN), and the lateral dorsal tegmental nucleus (LDTN). All three of these nuclei send projections to the rat SC [20].

Labeling by antibodies directed against choline acetyltransferase (ChAT) showed a very similar pattern to the fiber labeling seen using NADPHd histochemistry. A dense band of ChAT labeled fibers was present in the ZL-SGL (fig. 2A-B). ChAT labeling within the rostral IGL formed a single tier of fibers while more caudal labeling revealed two tiers of ChAT labeled fibers, each with densely labeled patches (fig. 2A,B). Labeling of adjacent sections for ChAT and NADPH at P35 showed that this two tier fiber pattern was identical using both labels. This result coupled with previous reports [29,30,20] provide strong evidence that ChAT and NOS are contained in the same fiber groups throughout the IGL.

In summary, the juvenile and adult rat SC has a distinct pattern of cells and fibers that contain NOS. These cells and fibers are found primarily within the SGL, IGL, and DGL. The NADPH labeled fibers also contain ChAT and arise from cell groups within the mesencephalic tegmentum.

Development of NADPH labeling in the postnatal rat

NADPH labeling in SC at P4-P5 was confined primarily to small cells within the dorsolateral wedge of the PAG and in neurons scattered within the DGL (fig. 3A). Only a few lightly labeled neurons were seen within the IGL at P4 and none within the more superficial layers. In the P5 case, a cluster of lightly labeled cells was seen within the lateral IGL in caudal sections (fig. 3,5). No NADPH labeling was resolved within axon-like fibers at P4-P5, but many blood vessels did contain NADPH labeling (fig. 3A).

By P8-P10, the number of labeled cells in the PAG wedge had increased, and many more labeled cells were present in SC (figs. 3A,5). Some neurons within the PAG had vertically oriented dendrites which projected into the DGL and appeared to be migrating from the PAG (fig. 3B). Labeled cells within the IGL were now found at both rostral and caudal levels and in both the medial and lateral SC. In caudal sections, these cells were often grouped into clusters (fig. 3B-D). Some very lightly labeled neurons were also scattered within the SGL by P9 (fig. 5). However, no labeled axons were seen in any layer of SC between P8 and P10. Blood vessel labeling was still prominent.

By P14, clustered neurons in the IGL were quite well labeled by NADPH and these cells were found in both the superficial and deep tiers of this layer (figs. 4A,C, 5). In addition, neuropil labeling within the IGL was now visible (fig. 4A), and a few axon-like fibers and boutons could be resolved (fig. 4C). Cellular labeling within the SGL at P14 was intense and many more cells were labeled than at P8-P10. Cell labeling in the PAG wedge and DGL was similar to that seen earlier.

By P18-P21, NADPH labeling was intense in neurons in both the IGL and SGL (fig. 5). Fiber labeling was also dramatically increased. By P21 fibers formed a typical two-tier patch-like pattern similar to that seen in the juvenile and adult. Within these patches, cells were darkly stained and many axon-like fibers with varicosities and terminal boutons were also well labeled by NADPH (fig. 4B,D).

Fig. 5 summarizes the development of NOS cells within SC. NADPH labeled neurons were present in the PAG and DGL and scattered within the lateral IGL by P4-5. Significant NOS expression in IGL cells occurred by P8-9 and reached a maximum between P14-P35. SGL cellular labeling was first seen at P9-P10 but was not prominent until P14.

NADPH expression in the IGL

In an effort to determine the time-course of NOS expression in IGL neurons, we counted the number of NADPH labeled neurons within the IGL at different ages. No more than 10 labeled neurons were found in any section at P4, while an average of 20 was found by P5 (fig. 6). By P8-9, the number of NADPH labeled neurons in the IGL ranged from 26 to 75 with a mean of 43.4. This is a two fold increase from that seen at P5. The average number found between the ages of P18-21 ranged from 40-45 and peaked at 56.3 at P35. This number decreased significantly in adults (fig. 6), despite a substantial increase in the area of the IGL. These data thus confirm quantitatively that the number of NADPH positive neurons increases during the period of fiber development in the IGL, and then decreases in the adult.

Distribution of ChAT labeled fibers in normal development and after NOS inhibition

We examined the distribution of fibers labeled by anti-choline acetyltransferase and by NADPHd, in both control and NOS inhibited rats between the ages of P8 and P21. ChAT fiber labeling in control animals developed between P8-P21. No ChAT fiber labeling was found at P8, even when we prolonged the DAB reaction to overstain the tissue. At P10-11, anti-ChAT fibers were visible in the IGL, but there were relatively few fibers at this age and most were lightly labeled. The density of ChAT labeled fibers in the IGL was much higher at P14, as was the intensity of labeling within individual fibers. The two tier pattern was visible, although the tiers were not as well segregated as at later ages (fig. 7A). ChAT labeled fibers had a nearly continuous distribution across the IGL and few or no obvious patches were present at this age (fig. 7A). ChAT fiber labeling at P18 showed further differentiation of the tiers. The two tiers were thicker, there were some gaps within the tiers, and more fiber columns bridged the tiers (fig. 7B). By P21, ChAT labeling in the IGL was virtually identical to that seen in the P35 juvenile rat. Both fiber tiers were densely labeled and there were a number of fiber patches separated by interpatch intervals that had many fewer fibers (fig. 7C).

The pattern of ChAT labeling in the NoArg inhibited animals was virtually identical to that seen in controls (fig. 7D-F). Few fibers were present at P10 while the two-tier pattern was visible at P14 (fig. 7D). The tiers were further developed by P18 (fig. 7E) and patches were conspicuous by P21 (fig. 7F). Virtually no qualitative differences could be detected at any age. We thus conclude that inhibition of NOS has no affect on ACh fiber development in the rat SC.

NADPHd labeling also appeared to be unaltered by inhibition of NOS. Intense cellular, and light fiber labeling were observed in the IGL by P14. As in normal animals, labeled cells in the IGL sometimes appeared in clusters (fig. 8A). More obvious fiber labeling was observed in the IGL by P18 and many cells were labeled at this age as well (fig. 8B). By P21, NADPHd labeled fibers in the IGL formed two obvious tiers (fig. 8C), just as seen in normal P21 rats (see fig. 4B). The pattern of NADPHd labeling in the SGL and DGL was also similar to that seen in normal animals. We thus conclude that NOS inhibition, in the ranges we have tested, has no discernible effect upon NADPHd labeling in the developing rat SC.

Amount of NOS inhibition determined by biochemical assay

We also performed biochemical assays for NOS in additional experimental and control animals sacrificed at P14, P18, and P22. The assay results revealed a substantial reduction in NO synthase activity in all age groups after daily injections of NoArg. The L-citrulline produced in P14 homogenates after 1 μmol/g body weight injections ranged from 3.42 - 3.64 pmoles/min/mg protein compared to 14.16 pmoles/min/mg protein in the saline control. The percent inhibition was 74.3 to 75.9%. The reduction after 3μmol/g body weight injections was greater; L-citrulline ranged from 2.30-2.78 pmoles/min/mg protein, an 80.4-83.8% inhibition compared to control.

A similar dose dependency was found in the P18 rats. NOS activity after daily injections of 1 μmol/g body weight was reduced by 72.1% to 3.10 pmoles/min/mg protein, while after 3μmol/g body weight injections it was reduced by 91.0% to 1.0 pmoles/min/mg protein. Results from seven P22 rats were similar. Injections of 1μmol/g body weight reduced L-citrulline production from

17.38 pmoles/min/mg protein in the saline control to 1.95-3.19 pmoles/min/mg protein. This corresponded to an 81.6 to 88.8% inhibition of NOS activity. No correlation was found between the degree of inhibition and the pattern or density of labeling by either ChAT or NADPHd.

Discussion

Our results lead to the following conclusions: 1) the patch/cluster system exists in the IGL of the rat SC as it does in cat; the system appears to contain both acetylcholine and NOS; 2) the pattern of cellular labeling by NADPH develops in a ventral to dorsal sequence and is essentially adult-like by P21; 3) there is a transient expression of NOS in some neurons in the IGL. Maximal expression of NOS occurs during the period of fiber formation in the IGL and then declines in the adult; 4) this fiber pattern is neither altered nor delayed by inhibition of 72 to 91% of the endogenous NOS activity.

NOS distribution in the adult SC

Our results show that NO is a marker of the patch-cluster system in the rat SC as it is in the cat [24,25]. In both species NAPDHd intensely labels fibers within the IGL and these have a distribution virtually identical to those labeled by ChAT [20,28,30,31]. Like the cat, most NADPH labeled neurons within the rat IGL are found within the patches of labeled fibers. Although it has not been shown experimentally whether NOS containing cells are the same cells as the cluster neurons that project to the region of the cuneiform nucleus [18], the similarity in size and distribution of both cell groups makes this conclusion likely. This pattern of NADPH labeling in the IGL has also been found in the C57 wild type mouse [33, Scheiner and Mize, unpublished observations] and in the Cynomolgus monkey [34]. This system thus appears to be conserved across a variety of mammalian species.

The pattern of labeling within the other laminae of SC has been shown by others [33-39]. Much of the NADPH fiber labeling in SC is thought to arise from three nuclear groups within the

mesencephalic tegmental core: the pedunculopontine tegmental (PPTN) and lateral dorsal tegmental (LDTN) nuclei which give rise to the IGL fiber patches as well as some fibers within the DGL [19,20]; the parabigeminal nucleus (PBG) which projects principally to the SGL [19,20]; and the dorsolateral wedge of the periaqueductal gray (PAG) which apparently gives rise to fibers innervating the DGL [40, and present results]. These nuclear groups are intensely labeled by NAPDHd as well as by ChAT [29,30] and represent some of the major sources of NO in the brainstem [35].

The NADPH positive neurons within the ZL and SGL of the rat have varying morphologies that have been described by others [37,41]. These neurons overlap the retinal input to this region of SC [42,43] which is thought to be glutamatergic in both rat and cat [44-50]. Although the retinocollicular pathway in cat is also glutamatergic [50], the cat SC does not have a dense band of NADPH cells in the SGL [32,34]. Differences in NOS expression in the two species may be due to differences in the extent of binocular overlap or the functional types of retinal ganglion cell that project to the SGL. In any event, the pattern of NADPHd labeling in rat and cat is very similar in the IGL where inputs from the PPTN and SN in both species appear to be functionally similar.

Development of NOS expression in SC

Our results show that NADPH labeling develops in a ventral to dorsal sequence in the postnatal rat. In the first week after birth, NADPH positive cells are found only within the PAG and DGL and occasionally within the lateral IGL. Well labeled NADPH cells are first found in obvious IGL clusters only at P8-P10, a result previously reported [51]. The dense band of NADPH neuronal labeling in the SGL appears last, around P14-P15 [present results, 41,51].

Although the cells labeled by NADPH in the PAG, DGL, and SGL appear to retain NOS expression throughout life, the number of labeled cells in the IGL was substantially reduced in the adult. This suggests that some IGL cells express NOS transiently or that some NOS containing cells die during development. Transient expression is the more likely explanation given that there

appears to be little reduction in NOS cell number in the other layers. Transient expression as well as the time of onset suggest that NO could be involved in the retraction of IGL fibers into patches. Intensely labeled neurons in the IGL were visible by P10-P14, a time just preceding the development of ChAT and probably other fibers in this layer. The two tier pattern was seen by P14 while the patch-like distribution developed between P18 and P21. The ChAT labeled fibers thus appear to retract into patches during the time at which NOS expression is maximal in IGL neurons.

This phenomenon has also been seen in the cat SC. NAPDH labeled cells are first found in the IGL between E51-E58 and clusters of these neurons are not seen until P3-P7. The clustered neurons intensely express NOS by P10-P14 [24,25], the age at which ChAT first labels ACh fiber patches in the cat IGL [26, Scheiner et al., unpublished observations]. As ACh containing fibers from the PPTN and LDTN apparently arrive in the IGL after P1 [26], the onset of expression of NOS in the clustered neurons correlates well with the arrival of the fibers as well as their expression of ACh. However, this relationship between NOS expression and fiber segregation could involve fiber systems other than those containing ACh. Although fibers from the substantia nigra (SN) reach the SC of cat as early as E51, SN fiber patches in the IGL have not been observed earlier than P19 (Banfro, Scheiner and Mize, unpublished observations). Thus, NO could be influencing fiber segregation of this pathway instead of, or in addition to, that from the PPTN/LDTN.

A temporal correlation between NOS expression and fiber refinement has also been reported in other species and in other regions of the brain. NADPH labeling first appears in superficial layer cells of chick optic tectum at about the time that retinal axons innervate the tectum, and this expression is maximal during development and reduced in adults [10,11]. Neurons in the LGN of the cat [30,52] and ferret [13,14] also express NOS only during the first several weeks of life. This transient expression is apparently developmentally regulated by afferent input because monocular enucleation results in continuous expression of NADPH in the non-deprived laminae of the adult LGN [30] while bilateral enucleation eliminates NADPH labeling in cells in the superficial layers of the chick optic tectum [10,11]. Thus, both the correlation found between the onset of

expression of NOS and refinement of axons and the alterations in NOS levels produced by deafferentation suggest that NOS plays a role in axon fiber refinement or synapse stabilization in these structures.

Absence of an effect of NOS inhibitors on ChAT fiber development

The original hypothesis of Gally [7] predicted that NO could serve as a retrograde signal to 'instruct" presynaptic axons that they had established appropriate connections with their post-synaptic target. The hypothesis was explicit in stating that the post-synaptic release of NO depended upon the influx of Ca^{2+} and that this could occur through the NMDA receptor. Release of glutamate from a glutamatergic pathway was an implied component of the hypothesis.

A major purpose of the present study was to test whether NO might also serve as a retrograde messenger in the refinement of axons that utilize another neurotransmitter, in this case ACh. The patch-cluster system is an excellent model for studying this question because post-synaptic neurons in the patches express NOS, the ACh fibers in the system gradually retract into patches, and the two events are temporally correlated.

Our results, however, show that prolonged inhibition of NOS has no effect upon the pattern or time course of development of the ACh patches. The two tier pattern was visible by P14, and the patches were well demarcated by P21 in both experimental and control groups. Pilot studies in our laboratory have also shown that ChAT fibers develop normally in a neuronal NOS genetic knockout mouse [53]. Lower doses of NoArg than those used in our study are known to be effective in altering fiber refinement in the retinotectal pathway of the rat [11,McLoon, personal communication]. There is thus correlative evidence that the reduction or absence of bNOS has no effect on formation of the ACh patches.

Although our biochemical assay showed that NOS activity was being substantially reduced (72-91%) in the NoArg injected rats, NADPHd labeling was also not noticeably altered by inhibition of

NOS (fig. 8). This observation suggests to us that, while NADPHd labeling indicates the presence of the neuronal form of NOS [54], it does not depend upon NOS activity. Furthermore, it suggests that the lack of a NoArg effect on the ACh patches is not due to the disappearance of NOS containing cells in the target region.

To date, relatively few studies have, in fact, shown that NOS is involved in fiber refinement in developing CNS. The most complete studies have been performed in chick. The ipsilateral retinal projection, which is normally transient, is partially preserved by daily intraperitoneal injections of NoArg or NAME [11,12] and both of these inhibitors disrupt the topography of the contralateral retinotectal pathway [11]. McLoon and colleagues [11] have also shown that the ipsilateral and contralateral retinal afferents to the rat SC do not segregate completely after NoArg administration. A somewhat different effect has been reported in the ferret LGN, where the segregation of the 'on' and 'off' sublaminae is disrupted by either focal or systemic inhibition of NOS [13,14].

In both cases a glutamate pathway and the NMDA receptor are probably involved. The retinal pathways to SC and LGN are glutamatergic in all species studied [44 -47,49,55,56] and normal development of both pathways can be disrupted by NMDA antagonists [57,58]. In both ferret LGN and rat SC NOS inhibition and NMDA receptor blockade both appear to disrupt the retraction of axon arbors that would normally occur as a result of correlated electrical activity in other arbors [57,58]. The exact locus and mechanism of NO in these pathways is unknown and could include a presynaptic action such as an increase in guanylate cyclase-cGMP to promote enhanced release of neurotransmitter [1,2,5,59] or a post-synaptic action such as enhancement of an NMDA receptor mediated response [60]. These results suggest that NO may only play a role in fiber refinement in glutamatergic pathways involving the NMDA receptor. If this is so, then it remains possible that NO is involved in refinement of glutamatergic fibers that innervate the IGL, and this could explain the temporal correlation that was found between maximal NOS expression and fiber development in this region of the SC. We are currently conducting experiments to test this hypothesis.

On the other hand, it is worth noting that NO has been shown to affect synapse plasticity in non-glutamateric systems. Thus, NO donors suppress evoked presynaptic currents while NO-binding proteins and NOS inhibitors block this suppression induced by asynchronous firing in the neuromuscular junction of Xenopus [16]. In addition, NO donors have been shown to arrest or reversibly collapse growth cones in vitro in the dorsal root ganglion of the rat [17]. Thus NO can affect axon development in non-glutamatergic as well as glutamatergic synapses, but the mechanism appears to be one of suppression of non-correlated firing in the former and an enhancement of correlated firing in the latter.

References

1 Garthwaite J, Charles SL, Chess-Williams R: Endothelium derived relaxing factor release on activation of NMDA receptors suggests a role as intercellular messenger in brain. Nature 1988;336:385-388.

2 Bredt DS, Snyder SH: Nitric oxide mediates glutamate-linked enhancement of cGMP levels in the cerebellum. Proc Natl Acad Sci USA 1989;86:9030-9033.

3 Böhme GA, Bon C, Stutzmann JM, Doble A, and Blanchard JC: Possible involvement of nitric oxide in long-term potentiation. Europ J Pharmacol 1991;199:379-381.

4 Izumi Y, Clifford DB, Zorumski CF: Inhibition of long-term potentiation by NMDA-mediated nitric oxide release. Science 1992;257:1273-1276.

5 Schuman EM, Madison DV: A requirement for the intercellular messenger nitric oxide in long term potentiation. Science 1991;254:1503-1506.

6 Zhuo M, Small SA, Kandel ER, Hawkins RD: Nitric oxide and carbon dioxide produce activity dependent long-term synaptic enhancement in hippocampus Science 1993;260:1946-1950.

7 Gally JA, Montague PR, Reeke GN Jr, Edelman GM: The NO hypothesis: Possible effects of a short lived rapidly diffusible signal in the development and function of the nervous system.. Proc Natl Acad Sci USA 1990;87:3547-3551.

8 Garthwaite J: Glutamate nitric oxide and cell-cell signalling in the nervous system. Trends Neurosci 1991;14:60-67.

9 Bredt DS, Snyder SH Isolation of nitric oxide synthase a calmodulin-requiring enzyme. Proc Natl Acad Sci USA 1990;87:682-685.

10 Williams CV, Nordquist D, McLoon SC: Correlation of nitric oxide synthase expression with changing patterns of axonal projections in the developing visual system. J Neurosci 1994;14:1746-1755.

11 Wu HH, Waid DK, McLoon SC: Nitric oxide and the developmental remodeling of retinal connections in the brain. Prog Brain Res 1996;108:273-286.

12 Wu HH, Williams CV, McLoon SC: Involvement of nitric oxide in the elimination of a transient retinotectal projection in development. Science 1994;265:1593-1596

13 Cramer KS, Moore CI, Sur M: Transient expression of NADPH-diaphorase in the lateral geniculate nucleus of the ferret during early postnatal development. J Comp Neurol 1995;353:306-316.

14 Cramer KS, Sur M: The role of NMDA receptors and nitric oxide in retinogeniculate development. Prog Brain Res 1996;108:235-244.

15 Frost DO, Zhang X-F, Huang PL, Fishman MC: Effect of nitric oxide synthase gene knockout or blockade on the development of retinal projections. Soc Neurosci Abstr 1994;20(2):1318.

16 Wang TI, Xie Z, Lu B: Nitric oxide mediates activity-dependent synaptic suppression at developing neuromuscular synapses. Nature 1995:262-266.

17 Hess DT, Patterson, SI, Smith DS, Pate Skene JH: Neuronal growth cone collapse and inhibition of protein fatty acylation by nitric oxide. Nature 1993:366:562-565.

18 Jeon C-J, Mize RR: Choline acetyltransferase immunoreactive patches overlap specific efferent cell groups in the cat superior colliculus. J Comp Neurol 1993;337:127-150.

19 Hall WC, Fitzpatrick D, Klatt LL, Raczkowski D: Cholinergic innervation of the superior colliculus in the cat. J Comp Neurol 1989;287:495-514.

20 Beninato M, Spencer RF: Cholinergic projections to the rat superior colliculus demonstrated by retrograde transport of horseradish peroxidase and choline acetyltransferase immunohistochemistry. J Comp Neurol 1986;253:525-538.

21 Ficalora AN, Mize RR 1989) The neurons of the substantia nigra and zona incerta which project to the cat superior colliculus are GABA immunoreactive: a double label study using GABA immunocytochemistry and lectin retrograde transport. Neurosci 29 567-581.

22 Illing RB, Graybiel AM; Convergence of afferents from frontal cortex and substantia nigra onto acetylcholinesterase-rich patches of the cat's superior colliculus. Neurosci 1985;14:455-482.

23 Harting JK, Van Lieshout DP: Spatial relationship of axons arising from the substantia nigra spinal trigeminal nucleus and pedunculopontine tegmental nucleus within the intermediate gray of the cat superior colliculus. J Comp Neurol 1991;305:543-558.

24 Scheiner CA, Banfro FT, Arceneaux RD, Kratz KE, Mize RR: Nitric oxide synthase is expressed early in the prenatal development of the cat superior colliculus. Soc Neurosci Abstr 1995;21(2):817.

25 Mize RR, Banfro FT, Scheiner CA: Pre- and postnatal expression of amino acid neurotransmitters, calcium binding proteins, and nitric oxide synthase in the developing superior colliculus. Prog Brain Res 1996:108:313-332.

26 McHaffie J, Beninato M, Stein BE, Spencer RF: Postnatal development of acetylcholinesterase and cholinergic projections to the cat superior colliculus. J Comp Neurol 1991;313:113-131.

27 Nabors LB, Mize RR: A unique neuronal organization in the cat pretectum revelaed by antibodies to the calcium-binding protein calbindin-d 28k. J Neurosci 1991;11(8):2460-2476.

28 Iadecola C, Xiaohong X, Zhang F, Hu J, El-Fakahany EE: Prolonged inhibition of brain nitric oxide synthase by short-term systemic administration of nitro-L-arginine methyl ester. Neurochem. Res. 1994;19(4):501-505.

29 Butler GD, Scheiner CA, Whitworth RH, Mize RR: NADPH-diaphorase and choline acetyltransferase are colocalized in the fiber patches of the intermediate gray layer of the cat superior colliculus. Soc Neurosci Abstr 1996;22:635

30 Bickford ME, Gunluk, AE, Guido W, Sherman SM: Evidence that cholinergic axons from the parabrachial region of the brainstem are the exclusive source of nitric oxide in the lateral geniculate nucleus of the cat. J Comp Neurol 1993;333:2-22.

31 Mesulam M-M, Mufson EJ, Wainer BH, Levey AI: Central cholinergic pathways in the rat: an overview based on an alternative nomenclature. Neurosci. 1983;10(4):1185-1201.

32 Arceneaux RD, Barnes PA, Scheiner CA, Kratz KE, Guido W, Mize RR: NADPH-diaphorase histochemistry reveals specific cell types in the cat superior colliculus that contain nitric oxide synthase. Invest Ophth Vis Sci 1995; 36/4:1345.

33 Wallace MN: Spatial relationship of NADPH-diaphorase and acetylcholinesterase lattices in the rat and mouse superior colliculus. Neuroscience 1986;19:381-391.

34 Wallace MN: Lattices of high histochemical activity occur in the human, monkey, and cat superior colliculus. Neurosci 1988;25(2):569-583.

35 Vincent SR, Kimura H: Histochemical mapping of nitric oxide synthase in the rat brain. Neurosci 1992;14:1746-1755.

36 Leigh PN, Connick JH, Stone TW: Distribution of NADPH-diaphorase positive cells in the rat brain. Comp Biochem Physiol 1990;97C(2):259-264.

37 González-Hernández T, Conde-Sendín M, Meyer G: Laminar distribution and morphology of NADPH-diaphorase containing neurons in the superior colliculus and underlying periaqueductal gray of the rat. Anat Embryol. 1992;186:245-250.

38 Vincent SR, Hope BT: Neurons that say NO. Trends Neurosci 1992;15(3):108-113.

39 Bredt DS, Glatt CE, Hwang PM, Fotuhi M, Dawson TM, Snyder SH: Nitric oxide synthase protein and mRNA are discretely localized in neuronal populations of the mammalian CNS together with NADPH diaphorase. Neuron 1991;7:615-624.

40 Hamilton BL: Projections of the nuclei of the perioaquaductal gray matter in the cat. J Comp Neurol 1973;152:45-58.

41 Tenorio F, Giraldi-Guimaraes A, Mendez-Otero R: Developmental changes of nitric oxide synthase in the rat superior colliculus. J Neurosci Res 1995;42:633-637.

42 Lund RD, Lund JS: Modification of synaptic patterns in the superior colliculus of the rat during development and following deafferentation. Vision Res Suppl 1971;11:281-298.

43 Land PW, Lund RD: Development of the rat's uncrossed retinotectal pathway and its relation to plasticity studies. Science 1979;205:698-700.

44 Lund-Karlsen R, Fonnum F: Evidence for glutamate as a neurotransmitter in the corticofugal fibers to the lateral geniculate. Brain Res. 1978;151:457-467.

45 Kuale I, Fosse VM, Fonnum F: Development of neurotransmitter parameters in lateral geniculate body, superior colliculus and visual cortex of tha albino rat. Brain Res 1983;283:137-145.

46 Fosse VM, Heggelund P, Fonnum P: Postnatal development of glutamatergic GABAergic, and cholinergic neurotransmitter phenotypes in the visual cortex, lateral geniculate nucleus, pulvinar, and superior colliculus in cats. J. Neurosci 1989;9:426-435.

47 Sakurai T, Okada Y: Selective reduction of glutamate in rat superior colliculus and dorsal lateral geniculate nucleus after contralateral enucleation. Brain Res 1992;573:197-203.

48 Binns KE, Salt TE: Excitatory amino acid receptors participate in synaptic transmission of visual responses in the superficial layers of the cat superior colliculus. Eur J Neurosci 1994;6:161-169.

49 Sakurai T, Miyamoto T, Okada Y: Reduction of glutamate content in rat superior colliculus after retino-tectal denervation. Neurosci Lett 1990;109:299-303.

50 Mize RR, Butler GD: Postembedding immunocytochemistry demonstrates directly that both retinal and cortical terminals in the cat superior colliculus are glutamate immnunoreactive. J Comp Neurol 1996;371:633-648

51 González-Hernández T, Conde-Sendín M, González-González B, Mantolán-Sarmiento B, Pérez-González H, Meyer G: Postnatal development of NADPH-diaphorase activity in the superior colliculus and the ventral lateral geniculate nucleus of the rat. Dev Brain Res 1993;76:141-145.

52 Kratz KE, Banfro FT, Mize RR, Scheiner C, Guido W: Prenatal and early postnatal staining of NADPH-diaphorase in cortical and thalamic structures of the cat. Soc. Neurosci. Abs. 1994;20:466.

53 Huang PL, Dawson TM, Bredt DS, Snyder SH, Fishman MC: Targeted disruption of the neuronal nitric oxide synthase gene. Cell 1993;75:1273-1286.

54 Leonard CS, Kerman I, Blaha G, Taveras E, Taylor B: Interdigitation of nitric oxide synthase-tyrosine hydroxylase-, and serotonin-containing neurons in and around the laterodorsal and pedunculopontine tegmental nuclei of the guinea pig. J. Comp Neurol. 1995;362:411-432.

55 Montero VM: Quantitative immunogold analysis reveals high glutamate levels in synaptic terminals of retino-geniculate, cortico-geniculate, and geniculo-cortical axons in the cat. Visual Neurosci. 1990;4:437-443.

56 Montero VM, Wenthold RJ: Quantitative immunogold analysis reveals high glutamate levels in retinal and cortical synaptic terminals in the lateral geniculate nucleus of the macaque. Neuroscience 1989;31:639-647.

57 Hahm JO, Langdon RB, Sur M: Disruption of retinogeniculate afferent segregation by antagonists to NMDA receptors. Nature 351;568-570.

58 Simon DK, O'Leary DDM: Development of topographic order in the mammalian retinocollicular projection. J Neurosci 1992;12 :1212-1232.

59 Montague PR, Gancayco CD, Winn MJ, Marchase RB, Freidlander MJ: Role of NO production in NMDA receptor-mediated neurotransmitter release in cerebral cortex. Science 1994;263:973-977.

60 Murphy KPSJ, Williams JH, Bettache N, Bliss TVP: Photolytic release of nitric oxide modulates NMDA receptor-mediated transmission but does not induce long-term potentiation at hippocampal synapses. Neuropharmacol 1994;33:1357-1385.

Figure Captions

Figure 1. Superior colliculus labeled by NADPHd histochemistry in a P35 juvenile rat. (A) Rostral SC showing band of NADPH labeling in the SGL but very little fiber or cell labeling in the IGL; (B) Middle SC showing increased NADPH fiber and cell labeling in the IGL (arrows). Note scattered neurons in the DGL. (C) Caudal SC showing the two tiers of fiber labeling in the IGL as well as fiber patches (arrows). Labeling in the SGL and DGL is similar to that in B. sgl = superficial gray layer; ol = optic layer; igl = intermediate gray layer; dgl = deep gray layer; pag = periaqueductal gray. Scale bar = 200 μm.

Figure 2. Fibers labeled by choline acetyltransferase (ChAT) antibody in the superior colliculus (SC) of a P35 juvenile rat. (A) middle SC section; (B) more caudal SC section. Note the band of immunoreactivity within the SGL as well as the two tiers of fiber labeling within the IGL. Fiber patches are indicated by arrows.

sgl = superficial gray layer; ol = optic layer; igl = intermediate gray layer; dgl = deep gray layer; pag = periaqueductal gray. Scale bar = 200 μm.

Figure 3. NADPH labeled neurons in the neonatal rat superior colliculus. (A) At P5, small NADPH positive neurons are seen within the PAG and DL. Only 4-5 lightly labeled cells are visible in the IGL (arrows). (B) By P8, neurons within the PAG and DL are well-labeled by NADPH. A number of neurons are also seen within the IL, mostly within the lateral half of that layer. Asterisk marks regions illustrated in C and D. (C) Higher magnification view of IL cells illustrated in B. Note the dense labeling in the dendrites of some neurons. (D) High magnification view showing the morphology of the neurons in C. Note dendritic labeling in these cells. sl = superficial layers; il = intermediate layers; dl = deep layers; pag = periaqueductal gray. Scale bar, A-B = 200 μm; C = 50 μm; D = 20 μm.

Figure 4. NADPH labeled neurons in the neonatal rat superior colliculus. (A) At P14, NADPH labeled neurons are seen throughout the DGL, IGL, and SGL. Some neuropil labeling is also seen

within the IGL and SGL. Asterisk marks region illustrated in C. (B) By P21, many NADPH labeled neurons are seen within the IGL and SGL. In addition, fiber labeling within the IGL is obvious and forms a two tier pattern similar to that seen using antibodies to ChAT (see Figure 2). Asterisk marks region illustrated in D. (C) Higher magnification of labeled IGL cells illustrated in A. Note that some thin axon-like fibers and boutons are labeled by this age. (D) Higher magnification of labeled neurons illustrated in B. Note the dense thin fiber and bouton labeling at this age. sgl = superficial gray layer; ol = optic layer; igl = intermediate gray layer; dgl = deep gray layer; pag = periaqueductal gray. Scale bar, A,B = 200 μm; C,D = 20 μm.

Figure 5. NTS computer plots of the distribution of NADPH labeled neurons in the superior colliculus of neonatal rats (P5 to P21). A few neurons are present in the IGL by P5. The earliest neurons within the SGL are seen at P9. High densities of NADPH labeled neurons are seen by P14.

Figure 6. Scattergram showing the total number of NADPH labeled neurons found within the intermediate gray layer (IGL) of the normal rat superior colliculus at different ages. Neuron number increases between P8 to P35, then declines in the adult.

Figure 7. Anti-choline acetyltransferase (ChAT) labeling in fibers within the igl of the rat superior colliculus at different ages (P14, P18, P21). (A-C) Control sections from animals injected with saline; (D-F) Sections from experimental animals injected with a NOS inhibitor (Nω-nitro-L-arginine). There were no obvious qualitative differences in the distribution or density of labeled fibers between the two groups.

Figure 8. NADPH labeling in the neonatal rat superior colliculus at different ages following daily injections of the NOS inhibitor Nω-Nitro-L-arginine. (A) By P14, cellular labeling in the IGL is intense while fiber labeling is present but light. (B) By P18, more fiber labeling is visible in both the IGL and SGL. (C) By P21, NADPH labeled fibers form two tiers within the IGL, just as they do in the normal rat. Scale bar = 200 μm.

Acknowledgments

We thank Grace Butler for invaluable assistance in the immunocytochemistry experiments and in preparation of the figures. Drs. John Haycock and Robert Roskoski assisted with the biochemical assays of NOS. Dr. Steven McLoon graciously provided advice regarding the use of the inhibitor NoArg. A student intern, Tazikie Thompson, who was supported by the Howard Hughes Foundation, plotted the distribution of NADPH labeled cells in some age groups. This research was supported by USPHS NIH grant EY-02973 from the National Eye Institute and U.S. Army Research And Development Grant DAMD 17-93-V-3013-P40001. Christopher Scheiner is a Board of Regents Fellow supported by LEQSF Grant (95-00)-GF-12.

304.3

ON/OFF SUBLAMINATION IN THE FERRET LGN IS INDEPENDENT OF SYSTEMIC CHANGES IN BLOOD PRESSURE AND REQUIRES NEURONAL NOS. K. S. Cramer* and M. Sur, Department of Brain & Cognitive Sciences, M.I.T., Cambridge, MA 02139.

Blockade of nitric oxide synthase (NOS) with N-Nitro-L-Arginine (L-NoArg) during the third and fourth postnatal weeks in the ferret disrupts the formation of ON/OFF sublaminae (Cramer and Sur, 1994). Because NO is a potent vasodilator, we examined the role of systemic changes in blood pressure on sublamination during systemic treatment with L-NoArg. Mean arterial blood pressure (MAP) was measured during the fourth postnatal week in four animals treated with 40 mg/kg/day i.p. L-NoArg from postnatal day 14 (P14) and in four normal, age-matched controls. MAP (± s.e.m.) increased from 57.6 ± 4.6 mmHg to 83.1 ± 4.8 mmHg following L-NoArg treatment. When animals received the antihypertensive calcium channel blocker verapamil, 5 mg/kg/day i.p., together with L-NoArg, blood pressure was normal (60.0 ± 1.6; n = 4). In these animals, sublamination was assessed in sections of LGN contralateral to an intraocular injection of WGA-HRP; disruption of sublamination was similar to that seen in animals treated with L-NoArg alone, suggesting that NOS blockade-induced changes in retinogeniculate projections occur independently of changes in MAP.

Sublamination in the LGN relies at least in part on the neuronal form of NOS. Neuronal NOS immunohistochemistry was similar to NADPH-diaphorase histochemistry in its transient expression during retinogeniculate segregation. In addition, ON/OFF sublamination was disrupted by blockade of the neuronal form of NOS from P14 to P26 with 7-nitroindazole, which appears not to produce hypertension. While systemic changes in blood pressure are not involved in the segregation of sublaminae, further experiments are necessary to examine the role of local changes in cerebral blood flow produced by NO release. *Supported by EY07023*

304.4

ROLE OF SPONTANEOUS RETINAL ACTIVITY IN REORGANIZATION OF RETINOGENICULATE CONNECTIONS DURING DEVELOPMENT. P.M. Cook*, G. Prusky and A.S. Ramoa Dept. of Anatomy, Virginia Commonwealth Un., Richmond, VA 23298 and Dept. of Psychology, Un. of Lethbridge, Lethbridge AB T1K3M4.

The adult form and function of the lateral geniculate nucleus (LGN) arise after extensive modifications in circuit organization that include segregation of axonal arbors from the two eyes into eye-specific layers. Previous studies have shown that intracranial infusion of tetrodotoxin (TTX) in fetal cats prevents segregation (Shatz and Stryker, 1988), suggesting that spontaneous action potential activity contributes to remodeling of the retinogeniculate pathway. We have examined the activity-dependent mechanisms of eye-specific segregation using a technique which allows direct inferences about the role of spontaneous retinal activity. Our method uses continuous intraocular application of TTX to block spontaneous discharge of retinal ganglion cells in newborn ferrets, which display retinogeniculate remodeling during the first 2 weeks of postnatal life. After a 2 week infusion, intraocular injection of horseradish peroxidase (HRP) revealed the projection pattern contralateral and ipsilateral to the HRP injected eye. Eye-specific segregation of retinogeniculate projections was observed at postnatal day 14 in controls as well as in ferrets that received monocular (n=3) or binocular (n=1) injection of TTX. However, segregation was aberrant in the monocularly injected animals. First, projections from the untreated eye occupied an approximately 50% larger volume of both LGNs than those from the TTX-treated eye. The total size of the LGN, however, remained unaltered and this suggests that the normal eye invaded territory normally occupied by the TTX treated eye. Moreover, a low density of afferents from the contralateral eye were observed to terminate in layer A1, which normally receives only ipsilateral eye input. These results suggest that binocular competition modulates rearrangements in retinogeniculate projections. Additionally, they are consistent with the hypothesis that spontaneous retinal activity may fine-tune segregation of retinal afferents into eye-specific layers. (Supported by NSF IBN-9421983)

304.5

POSTNATAL DEVELOPMENT OF SYNAPTIC PLASTICITY IN THE RAT SUPERIOR COLLICULUS: LONG-TERM DEPRESSION IN THE SUPERFICIAL LAYERS. R. J. Cork*, F-S. Lo and R. R. Mize. Anatomy Department, and Neuroscience Center of Excellence, LSU Medical Center, New Orleans, LA 70112.

We have been studying the development of the synaptic circuitry in the rat superior colliculus (SC) between ages P1 and P10. Using an in-vitro brainstem preparation, we have measured extracellular field potentials, and made whole-cell recordings of postsynaptic potentials, from the superficial layers of SC. We have also used immunocytochemistry and NADPH-histochemistry to map the development of various molecules thought to be involved in modulating synaptic transmission (i.e. NMDAR1, and NOS). Field potentials or post-synaptic potentials were measured following stimulation of optic tract (OT) fibers. Whole cell recordings showed EPSPs with two components. The later component was blocked by APV, suggesting that it was mediated by the NMDA receptor. NMDAR1 antibody also intensely labeled the neuropil of the superficial layers at P1. From P3 some neurons also showed an IPSP following the EPSP. The IPSP could be blocked by bicuculline, an antagonist of $GABA_A$ receptors. Between ages P1 and P8, tetanic stimulation (50 Hz, 20 s, submaximal intensity) induced a long-term (>90 min.) depression (LTD) of the field potential and the EPSP. Neither APV (10 μM or 50 μM) nor bicuculline (10 μM) could prevent LTD, suggesting that it is independent of either NMDA or $GABA_A$ receptor activation. Nitrendipine (5 μM), an L-type Ca^{2+}-channel blocker that blocks induction of LTD in the hippocampus, also failed to prevent LTD induction in the SC. The magnitude of the LTD decreased steadily from P1 to P8 and at P9/P10 tetanic OT stimulation induced a mixture of depression and long-term potentiation (LTP). Consistent with the idea that NOS promotes LTP, significant NOS expression was first observed in cells of the superficial layers at P9.

Supported by DOD cooperative agreement DAMD 17-93-V-3013, NIH grant EY02973, and the LSUMC Neuroscience Center.

304.6

INHIBITION OF NITRIC OXIDE SYNTHASE FAILS TO DISRUPT THE DEVELOPMENT OF CHOLINERGIC FIBER PATCHES IN THE RAT SUPERIOR COLLICULUS. C.A. Scheiner*, R.J. Cork and R.R. Mize. Dept. of Anatomy and the Neuroscience Center, Louisiana State University Medical Center, New Orleans, LA 70112

Nitric oxide (NO) has been proposed to be a retrograde messenger involved in synaptic refinement during development. The patch-cluster system in the intermediate gray layer (IGL) of the superior colliculus (SC) is an excellent model for studying the role of NO because both the clustered neurons and one of the fiber systems (ACh) that form the patches contain NOS during development. We have used No-nitro-L-arginine, an inhibitor of nitric oxide synthase (NOS), to determine if inhibition of NOS disrupts the formation of the ACh patches. Sprague-Dawley rats received 1-100 μM of NoArg from birth until sacrifice at P10, P14, P18, P21-22, or P28. Control animals were litter mates of the experimental animals plus other younger and older animals. ACh fibers were identified using choline acetyltransferase (ChAT) immunocytochemistry and NOS containing cells were labelled with nicotinamide adenine dinucleotide phosphate diaphorase (NADPH-d) histochemistry. NADPH-d was expressed in cells within the periaquaductal gray (PAG) and the deep gray layer (DGL) of the SC by P4, the earliest age examined. By P9, many cells in the IGL expressed NADPH-d, while few in the superficial layers were labeled. Some of these neurons in the IGL formed obvious clusters, while others were loosely scattered throughout the layer. NADPH-d labeling in IGL cells declined by P14-P18 and virtually absent in the adult. ChAT labeled fibers first appeared in the IGL at P10 and were readily visualized by P14. At this age, the ChAT fibers were fairly uniformly distributed through the IGL, but by P18 they had a patch like distribution with as many as five patches spaced at 250-300 μM intervals. Inhibition of NOS from birth produced no qualitative differences in the distribution or density of ChAT labeled fibers at any of the ages examined. We therefore conclude that NO does not contribute to the refinement of cholinergic fiber patches in the rat SC, probably because the fiber system is not glutamatergic. Supported by NIH NEI-02973, DOD cooperative agreement DAMD 17-93-V-3013,a Louisiana State Board of Regents Graduate Student scholarship, and the LSUMC Neuroscience Center.

304.7

ROLE OF RETINAL ACTIVITY IN MATURATION OF ELECTROPHYSIOLOGICAL MEMBRANE PROPERTIES AND SYNAPTIC RESPONSES OF FERRET LGN A.S. Ramoa* and G. Prusky Dept. of Anatomy, Virginia Commonwealth University, Richmond, VA 23298 and Dept. of Psychology, University of Lethbridge, AB T1K3M4.

The adult form and function of the lateral geniculate nucleus (LGN) arise after extensive modifications in circuit organization that, in the ferret, occur during the first postnatal month. We have shown that electrophysiological membrane properties and synaptic responses in LGN neurons of the ferret change markedly during this critical period of development (J. Neurosci. 14:2089, 1994; J. Neurosci. 14:2098, 1994; J. Neurosci. 15:5739, 1995). These changes, which appear to be coordinated to facilitate circuit remodeling of LGN neurons, include: late maturation of low-threshold Ca++ spikes and inhibitory potentials as well as developmental switches in the expression of NMDA receptor isotypes. We examined whether these changes are regulated by retinal activity. Our method uses continuous intraocular application of tetrodotoxin starting as early as the day of birth to block spontaneous discharge of retinal ganglion cells. Whole-cell recordings in the LGN slice preparation revealed that maturation of low-threshold calcium spikes and hyperpolarization-activated currents was unaltered by a 3 to 4-week binocular infusion of tetrodotoxin. In contrast, synaptic properties were markedly affected. Treated animals at P40 were found to display long duration NMDA-EPSCs that resembled those present in normal newborn animals rather than the shorter-duration EPSCs seen in normal animals at similar age ($P<0.01$). Additionally, application of ifenprodil, which binds with higher affinity to heteromeric receptors containing the NR-2B subunit, blocked more potently NMDA-EPSCs in newborn and TTX-treated animals animals at P40 than in normal P40 animals ($p<0.01$), suggesting that a developmental switch in the subunit composition of the NMDA receptor is prevented by intraocular TTX. In conclusion, retinal activity may regulate developmental changes in synaptic properties of LGN neurons (NSF IBN-9421983).

304.8

CHOLINERGIC PROCESSES IN XENOPUS TECTUM. M.J. Titmus*, L. Pleban, R. Lima & S.B. Udin, Dept. of Physiology & Biophysics, SUNY, Buffalo, NY 14214.

The ipsilateral visual input to Xenopus tectum comes into register with the contralateral map during development. The major transmitter for the contralateral (retinotectal) input is glutamate, and the major transmitter for ipsilateral input, relayed via the nucleus isthmi, is probably acetylcholine. The role of NMDA receptors in the activity-dependent process of organization of the ipsilateral map is demonstrated by the ability of NMDA receptor blockers to prevent matching of the ipsilateral map to the contralateral map during the critical period, but little is known about the role of acetylcholine.

Immunohistochemistry indicates that nicotinic receptors are located in the layers of the tectum that receive binocular inputs; unilateral eye enucleation indicates that most of those receptors are located on retinotectal axons. Receptor binding using tritiated cytisine also indicates the presence of nicotinic receptors in the tectum. Muscarinic receptors are located on cells and dendrites located appropriately to receive isthmotectal input.

Calcium imaging using Fura-2 in tectal slices demonstrates no measurable response to nicotinic agonists alone, but shows significant synergism when nicotine or cytisine are applied with NMDA. In contrast, muscarinic agonists decrease calcium influxes elicited with NMDA. These results suggest that activity of isthmotectal axons can significantly modulate the effects of glutamate released from retinotectal axons.

Supported by USPHS Grant EY-10690 to M.J.T and S.B.U.

MODULATION OF INTRACELLULAR CALCIUM DYNAMICS IN RAT HIPPOCAMPAL NEURONS BY PLATELET-ACTIVATING FACTOR. Mark A. DeCoster and Nicolas G. Bazan. Louisiana State University Medical Center, Neuroscience Center, New Orleans, LA 70112.

Platelet-activating factor (PAF) is a potent lipid mediator of several cellular responses. PAF is able to transiently increase intracellular calcium ($[Ca^{2+}]_i$) in several neuronal cell systems, mostly in cell lines and pituitary cells. PAF addition mobilizes $[Ca^{2+}]_i$ in hippocampal neurons; however, this response was found in only 7.7% of the cells analyzed (Bito et al., *Neuron*, 9:285, 1992). In the present study confocal microscopy was used to monitor the possible modulatory effect of PAF on calcium dynamics in rat primary hippocampal neurons. In short-term experiments, $[Ca^{2+}]_i$ was simultaneously monitored in multiple neurons; basal calcium oscillatory activity was observed in most cells. When 4 μM methylcarbamyl PAF (mcPAF) was added to these cultures, the average $[Ca^{2+}]_i$ was increased slightly in cells and the range of calcium oscillations was increased approximately 3-fold. These changes were not observed when only bovine serum albumin (the vehicle for PAF) was added. However, in agreement with the results of Bito et al. (1992), we found that not all cells responded to PAF addition: in our studies, about 25% of the cells responded. Glutamate (80 μM) was added at the end of each scan as a positive control for neuronal viability. To investigate the possibility of longer term effects of PAF, we pretreated hippocampal cultures overnight with PAF, mcPAF, lysoPAF, or BSA and monitored $[Ca^{2+}]_i$ changes induced by glutamate on the subsequent day. In general, we found that PAF (200-400 nM) and mcPAF (2-4 μM) pretreatment reduced the $[Ca^{2+}]_i$ changes induced by low concentrations of glutamate (100-500 nM) when compared with cells pretreated with lysoPAF (2-4 μM) or the vehicle. In multiple experiments, when pretreatment with PAF was used, the $[Ca^{2+}]_i$ changes caused by glutamate were reduced from sustained to transient increases. In two cases, the $[Ca^{2+}]_i$ increases in response to 500 nM glutamate were completely reversed by PAF pretreatment. These inhibitory effects by PAF were overcome by higher glutamate (5 μM) concentrations. In conclusion, PAF induces calcium oscillations in hippocampal neurons. In addition, based upon the previous findings showing that PAF-induces glutamate release (Clark et al., Neuron 9:1211-6, 1992; Kato et al., Nature 267:175-9, 1994), our present results suggest that sustained PAF-induced glutamate release may produce glutamate receptor desensitization. (Supported by DAMD-17-93-V-3013 and NS 23002)

NOTES:

NEUROTOXICITY AND MODULATION OF CALCIUM DYNAMICS IN RAT CORTICAL NEURONS BY PHOSPHOLIPASES. Miriam Kolko, Mark A. DeCoster and Nicolas G. Bazan. Neuroscience Center, LSU Medical Center, New Orleans, LA 70112-2234.

Phospholipases A_2 (PLA_2s) are important modulators of neuronal function. Ischemia and seizures promote an enhanced activation of PLA_2 in brain that, in turn, leads to the accumulation of free arachidonic acid (Biochim. Biophys. Acta 218:1-10, 1970) and platelet-activating factor (Biochim. Biophys. Acta 963:375-383, 1988). Nonpancreatic secretory PLA_2s ($sPLA_2$s) participate in the inflammatory injury response. A receptor for $sPLA_2$s has been cloned from muscle (Lambeau, et al., *JBC*. 269:1575, 1994). Two $sPLA_2$s from snake venom (OS_1 and OS_2), bind tightly to this receptor. OS_2 and $sPLA_2$ from bee venom bind avidly to brain membranes, while OS_1 does not. The present study evaluated the neurotoxic potential of these $sPLA_2$s in rat cortical neurons *in vitro* using lactate dehydrogenase (LDH) release as the toxicity assay and the excitotoxic amino acid glutamate (80μM) as a control. Bee venom and OS_2 (0.01-10 μg/mL) showed dose dependent toxicity while OS_1 did not cause cell death. The toxicity experiments were combined with studies investigating the effect of the $sPLA_2$s on intracellular free calcium concentration ($[Ca^{2+}]_i$). The fluorescent calcium indicator fluo-3 was used with a confocal microscope to measure real-time calcium dynamics in these neurons. We observed basal oscillations in $[Ca^{2+}]_i$ in the imaged cultures with a 2.3 mM extracellular calcium concentration. Bee venom and OS_2 dose-dependently (0.5-10 μg/mL) altered ($[Ca^{2+}]_i$) dynamics, while OS_1 had no effect. Both bee venom and OS_2 (0.5 - 10 μg/mL) obliterated calcium oscillations, and also decreased $[Ca^{2+}]_i$ to below baseline levels. Subsequent addition of glutamate to the cultures showed an immediate rise in the $[Ca^{2+}]_i$. We did not see any calcium modulations in the cultures exposed to $sPLA_2$ concentrations below 0.5 μg/mL, even though the $sPLA_2$s were toxic to about 0.025 μg/mL. Using a cytological stain we found that bee venom and OS_2 destroy neuronal cell bodies and processes at concentrations as low as 0.025 μg/mL and are generally cytotoxic to neurons and glia at the high concentrations. In contrast, 80 μM glutamate damages only neurons. Since the neurotoxicity of bee venom and OS_2 do not appear to correlate with calcium modulations at lower concentrations, a calcium-independent toxicity may be occurring at these low PLA_2 concentrations. Furthermore, submaximally toxic concentrations of bee venom combined with 80 μM glutamate demonstrated higher toxicity levels than the two compounds added separately. Thus, LDH release from these studies resulted in more than additive activity, indicating that glutamate and bee venom are having a synergistic effect. Since OS_1 is not affecting neuronal damage or the calcium dynamics in our experiments, these data support the observed binding properties of $sPLA_2$s in muscle and brain tissue, and provide evidence for modulatory roles of PLA_2s in neuronal signal transduction. (Supported by DAMD-17-93-V-3013 and NS 23002).

NOTES:

248.3

EXPRESSION OF GLUTAMATE RECEPTORS OF RAT CEREBELLAR GRANULE CELLS DEPENDS UPON THE VOLUME OF CULTURE MEDIUM.

C.Zona,L.Dus,N.Canu*,M.T.Ciotti and P.Calissano Dept. of Experimental Medicine, II University of Roma, and Institute of Neurobiology C.N.R. Roma, Italy

In a preliminary series of studies we have found that the response of cerebellar granule cells cultured in vitro for 8 days to a cytotoxic glutamate pulse (100uM, 20 min. incubation) varies according to the volume of medium in which neurons are grown. When cells are cultured in low volume (LV) ($1.2x10^6$ cells/1.2 ml/17 mm dishes) the glutamate pulse causes 80-90% cell death. When sister cultures are prepared in a high volume (HV) of 4.0 ml the cell death following glutamate treatement is reduced to 20-30%. Addition of a conditioned medium (CM) derived from LV cultures to HV cultures markedly increases their response to the toxic gluatamate treatement. In order to investigate this volume dependency and the action of CM on glutamate sensitivity, we have measured sodium currents, the currents evoked by AMPA/kainate and NMDA as well as the mRNA (1A, 1B, 2A,2B,2C) and the protein subunits forming the AMPA/Kainate (GluR2/3,GluR6/7) and NMDA (NMDAR1,2A/B) receptors. We found that the glutamate resistant phenotype ensuing in HV culture conditions is accompanied by, and probably causally connected with, a lowered functional and physical expression of both voltage operated sodium channels as well as kainate and NMDA receptors.

We hypothesize that such volume dependency to the cytotoxic action of glutamate is connected with the extent of production and release in culture of a substance operationally defined as glutamate sensitizing activity or GSA.

248.4

ANTISENSE OLIGONUCLEOTIDES TO CALPAIN I mRNA PROTECT CULTURED HIPPOCAMPAL SLICES FROM NMDA-INDUCED PATHOPHYSIOLOGY. E. Bednarski[1], P. Vanderklish[1], C. Gall[2], T. Saido[3], B.A. Bahr[1], G. Shaw[1*], & G. Lynch[1]. [1]Ctr. for Neurobiol. of Learning & Memory, and [2]Dept. of Anat. & Neurobiol., Univ. of Calif., Irvine, CA 92717; [3]Dept. of Mol. Biol., Tokyo Metro. Inst. Med. Science, 3-18-22 Honkomagome, Bunkyo, Tokyo, 113.

Two measures of NMDA-induced excitotoxic damage were reduced in cultured hippocampal slices that were previously exposed to antisense oligonucleotides (25μg/ml for 5 days) directed against the mRNA for calpain I. First, antisense intervention attenuated the generation of spectrin breakdown products (BDP's) following a 10-20 min NMDA (200 μM) infusion by approximately 42% ($p<.04$, t-test, 2 tails) on immunoblots developed with a BDP-specific antibody. These reductions in BDP formation were associated with a comparable degree of protease suppression, as measured by decreases in immunoblots (~42%) and *in vitro* activity estimates (~60%, $p<.01$, t-test, 2 tails), strengthening the assumption that increases in the concentration of spectrin fragments indeed reflect recent episodes of calpain I activity. Second, translational suppression of calpain I protected CA1 neurons from enduring NMDA-induced (200 μM for 15 min) synaptic dysfunction. Although slices transfected with antisense probes mimicked sibling cultures treated with an equivalent concentration of sense oligonucleotides in their initial response to NMDA (complete loss of synaptic potentials), they recovered more quickly and to a greater extent (to 74% of baseline EPSP amplitude after 55 min, $p<.03$, t-test, 2 tails) than did sense controls (to 21% of baseline at same time point). These results suggest that proteolysis by calpain I plays a significant role in excitotoxicity and that translational suppression of the protease protects cultured slices from the extreme spectrin proteolysis and pathophysiology normally elicited by intense NMDA receptor activation (supported by NIA AG00538 and NIMH MH14599).

248.5

OVEREXPRESSION OF RECOMBINANT HUMAN CALPASTATIN IN *E. COLI* AND ITS NEUROPROTECTIVE EFFECTS AGAINST EXCITOTOXICITY

Okhee Hong*, Robert Chapman, Chulhee Kang[1] and Ralph Nixon. McLean Hospital, Harvard Med. Sch., Belmont, MA 02178 and [1]Dept. Biochem. and Biophys., Washington State Univ., Pullman, WA 99164.

Calpastatin is an endogenous inhibitor acting specifically on the calcium-activated neutral proteinases (calpains), which have been implicated in neurodegenerative processes including Alzheimer's disease. Two species of calpastatin with molecular weights of 110 (tissue-type) and 70 kDa (erythrocyte-type) have been described in mammals (Inomata et al., '93). The larger species of calpastatin consists of five domains L, 1, 2, 3 and 4 among which domains 1, 2, 3, and 4 are repetitive and share homology with each other. Calpain inhibitory activities have been observed for each of the repetitive domains. The function of the domain L is not known. To further our understanding of the structure-function relationship of calpastatin molecules and to explore neuroprotective effect of calpastatin, we overexpressed each domain or combination of domains of calpastatin in *E. coli* . Single and multiple domains of calpastatin were cloned by reverse transcriptase polymerase chain reaction (RT-PCR) using human neuroblastoma mRNA as templates or by PCR using human liver or brain cDNA as templates. Each of the domain(s) L, 1, 1-2, 1-3, and 4 was cloned in T7 polymerase driven *E. coli* expression vectors. The level of recombinant DNA expression was 10% or greater of the total protein for each construct. Recombinant calpastatins D1, D1-2, D1-3 and 4 showed high specific activity toward calpain and demonstrated neuroprotection at an equal or higher level achieved by an NMDA receptor antagonist MK801 against glutamate excitotoxicity in mouse primary cortical neurons in culture. This neuroprotection was abolished by preabsorbing recombinant calpastatin with calpastatin antibodies. The result strongly indicates that the recombinant calpastatin may be a potential therapeutic agent of neurodegenerative diseases. The mechanism of the neuroprotection by calpastatin is being investigated.

248.6

ROLE OF CALPAIN IN THE DEVELOPMENT AND RECOVERY OF EXCITOTOXIC DENDRITIC INJURY IN VITRO. B.T. Faddis* and M.P. Goldberg. Center for the Study of Nervous System Injury and Dept. of Neurology, Washington University School of Medicine, St. Louis, MO 63110.

One of the earliest morphological changes following NMDA receptor activation in cultured cortical neurons is appearance of focal swellings along dendrites. The formation of these dendritic varicosities is largely calcium dependent and may be reversible. Also, the microtubule-stabilizing compound, taxol, attenuates NMDA-induced dendritic varicosity formation in mouse cortical cell cultures (Soc. Neurosci. Abstr. 20:1529), suggesting that the microtubule cytoskeleton plays a role in the maintenance of dendritic structure. Because several cytoskeletal proteins are targets of the calcium-activated enzyme, calpain, we investigated the role of calpain in dendritic varicosity formation.

Application of 30 μM NMDA for 10 minutes caused widespread dendritic varicosity formation visualized by MAP2 immunofluorescence. Pre-treatment of neuronal cultures with 1-100 μM MDL28,170 (generously provided by Marion Merrell Dow Inc.) or Calpain Inhibitor I for 2 hours did not alter the formation of dendritic varicosities induced by NMDA. These calpain inhibitors did substantially attenuate the NMDA-induced loss of MAP2 and increase of spectrin BDP immunoreactivity, suggesting sufficient cell permeability of these compounds (see abstract by Meschia et al., this meeting).

The NMDA exposure used in these studies was sublethal, as assessed by LDH release measured 24 hours post-exposure, and dendrites returned to normal morphology within 2 hours following NMDA removal. However, the presence of calpain inhibitors pre- and post-treatment blocked this recovery for at least 8 hours. These results suggest that calpain activation does not play a role in varicosity formation, but may be necessary for recovery of dendritic structure following injury.

(Supported by NIH NS32140 and NS01543, to MPG)

248.7

NMDA INDUCES CALPAIN-MEDIATED PROTEOLYSIS OF MICROTUBULE-ASSOCIATED PROTEIN 2 AND SPECTRIN IN CULTURED NEURONS. J.F. Meschia*, B.T. Faddis, M.P. Goldberg. Cntr. for the Study of Nervous System Injury, Dept. of Neurol., Washington Univ. School of Med., St. Louis, MO 63110.

Microtubule-associated protein 2 (MAP2) is a somatodendritic cytoskeletal element which is rapidly lost following cerebral ischemia or traumatic brain injury in vivo. The calcium-dependent neutral protease, calpain, may contribute to loss of cytoskeletal proteins and to neuronal injury in this setting. To assess the mechanisms and possible significance of calpain activation, we examined potential targets of calpain proteolysis in cortical cultures exposed to NMDA, using immunofluorescence and Western blotting.

Primary dissociated neurons from mouse neocortex were exposed to 30 μM NMDA for periods of 10 to 120 min. NMDA exposures of 20 min resulted in widespread neuronal death one day later. Immediately following NMDA exposure cultures were fixed and processed for indirect immunofluorescence, or were harvested and total MAP2 was measured using 7.5% SDS-PAGE followed by Western blotting and enzymatic chemiluminescence. A decrease in MAP2 immunoreactivity was first detectable with 60 min of continuous NMDA exposure, and MAP2 was virtually absent with 120 min exposure. There was little appreciable loss of MAP2 during 120 min NMDA exposure when calcium was omitted from the exposure medium. NMDA exposure (60-120 min) also resulted in appearance of calpain-specific spectrin breakdown products (Ab provided by R. Siman, Cephalon, Inc.). Addition of the calpain inhibitor, MDL28,170 (1-100 μM), substantially attenuated the loss of MAP2 immunoreactivity but did not reduce neuronal cell death. These observations suggest that sustained NMDA receptor stimulation in cortical neurons activates calpain, resulting in delayed proteolysis of MAP2 and spectrin. However, calpain activation may not be required to initiate irreversible neuronal death. (Supported by NIH NS32140 and NS01543, to MPG).

248.8

EFFECT OF SECRETORY PHOSPHOLIPASES A_2 AND GLUTAMATE ON VIABILITY OF RAT CORTICAL NEURONS AND CALCIUM DYNAMICS. M. Kolko, M. A. DeCoster*, G. Lambeau, M. Lazdunski and Nicolas G. Bazan. Neuroscience Center, LSU Medical Center, New Orleans, LA 70112-2234.

Nonpancreatic secretory phospholipases A_2 (sPLA$_2$s) may be involved in modulation of neuronal function. A receptor binding sPLA$_2$s has been cloned from muscle (Lambeau, et. al. JBC, 1994). Two sPLA$_2$s from snake venom (OS_1 and OS_2) bind to this receptor. OS_2 and sPLA$_2$ from bee venom (BV) bind avidly to brain membranes, while OS_1 does not. We evaluated the neurotoxicity of OS_1, OS_2 and BV combined with glutamate (GLU). Lactate dehydrogenase (LDH) release was used as the toxicity assay. BV and OS_2 dose dependently (0.01-10 μg/mL) caused neurotoxicity and OS_1 did not. GLU (80 μM) was as toxic as approximately 0.5 μg/mL BV. Submaximally toxic concentrations of BV combined with GLU demonstrated higher toxicity levels than the two compounds added separately. BV (0.05 μg/mL) and GLU together showed three times more toxicity than the sum of the separate toxicity levels, indicating that GLU and BV are having a synergistic effect. The toxicity experiments were combined with studies investigating the effect of the sPLA$_2$s on intracellular free calcium concentration ($[Ca^{2+}]_i$). The fluorescent calcium indicator fluo-3 was used with a confocal microscope to measure real-time calcium dynamics in these neurons. We observed basal oscillations in $[Ca^{2+}]_i$ in the cultures. BV and OS_2 dose-dependently (0.5-10 μg/mL) altered ($[Ca^{2+}]_i$) dynamics, while OS_1 had no effect. Both BV and OS_2 (0.5 - 10 μg/mL) obliterated calcium oscillations, and also decreased $[Ca^{2+}]_i$ to below baseline levels. We did not see any calcium modulations in the cultures exposed to sPLA$_2$ concentrations below 0.5 μg/mL, even though the sPLA$_2$s were toxic to about 0.025 μg/mL. These results indicate that calcium-independent toxicity may be occurring at low sPLA$_2$ concentrations. Our results support the observed binding properties of sPLA$_2$s in muscle and brain tissue, and provide evidence for modulatory roles of sPLA$_2$s in neuronal signal transduction. (Supported by DAMD-17-93-V-3013).

444.1

INTERCELLULAR CALCIUM WAVES PROPAGATED VIA GAP JUNCTIONS IN NEURONS

A.C. Charles* and R.F. Tyndale Dept. Of Neurology, UCLA, Los Angeles, CA 90024 and Addiction Research Foundation and Dept. Of Pharmacology, Univ. Of Toronto, Canada M5S 2S1

Spontaneous waves of increased intracellular calcium concentration were rapidly propagated over groups of primary mouse cortical neurons and immortalized hypothalamic (GT1-1) neurons in culture. Ca^{2+} waves were propagated at a rate of 100-200 μm/sec over 10-200 cells. Ca^{2+} waves were abolished by the removal of extracellular calcium and by TTX. Similar intercellular Ca^{2+} waves were induced by mechanical stimulation of a single cell. GT1-1 neurons showed flourescence recovery after photobleaching of a single cell, and intercellular Ca^{2+} waves were abolished by the gap junction blocker octanol. By contrast, a different clone of the GT1 neurons (GT1-7) showed frequent spontaneous Ca^{2+} oscillations but no intercellular Ca^{2+} waves, no intercellular communication of the response to mechanical stimulation, and no fluorescence recovery after photobleaching. Comparison of expression of connexin mRNA in the GT1-1 and GT1-7 lines using RT-PCR revealed a 5-fold greater level of connexin26 mRNA in the GT1-1 line, but no difference in the levels of connexin32 or connexin43 mRNA. These results show that neurons are capable of extensive Ca^{2+} signaling via gap junctions, and suggest that connexin26 is the gap junction protein which enables intercellular Ca^{2+} signaling in GT1 neurons. Intercellular Ca^{2+} waves in cultured neurons may represent a model for gap-junctional signaling between neurons in the developing nervous system, and between subsets of neurons in the adult brain.

444.2

THYROID HORMONE CONTROL OF CALCIUM WAVES IN *XENOPUS LAEVIS* OOCYTES.

L. M. John, J. D. Lechleiter, and P. Camacho*. Dep't of Neuroscience, Univ. of Virginia, Charlottesville, VA 22903.

Inositol 1,4,5 trisphosphate (IP_3)-induced intracellular Ca^{2+} release mediates the action of many neurotransmitter signalling pathways. Spiral Ca^{2+} wave propagation and annihilation of IP_3-induced Ca^{2+} release reveals an underlying excitable process which can be accounted for by the Ca^{2+} dependent properties of the IP_3-bound IP_3 receptor (IP_3R). We previously demonstrated the importance of cytosolic Ca^{2+} buffering on this dynamic process by overexpression of sarco-endoplasmic reticulum Ca^{2+}-ATPases (SERCAs) in *Xenopus* oocytes (Science 260, 226-229). Thyroid hormones and growth hormones have been shown to increase the expression of Ca^{2+}-ATPases in smooth muscles and cardiac myocytes. Additionally, thyroid hormones have been implicated in the regulation of Ca^{2+} uptake and/or release in mitochondria. Given the importance of Ca^{2+} sequestration in the dynamics of Ca^{2+} wave activity, we examined the effects of thyroid hormones on IP_3-induced Ca^{2+} signalling in *Xenopus* oocytes. To accomplish this, oocytes were injected with mRNA encoding the *Xenopus* thyroid receptor (TRβA1) and assayed for IP_3-induced Ca^{2+} wave activity 1-3 days later using confocal imaging. Exposure of oocytes expressing TRβA1s to L-3,3',5-triiodothyronine (T_3, 50-100 μM for 20-60 min before recording) resulted in an increase in the number of oocytes exhibiting IP_3-induced regenerative Ca^{2+} wave activity (58%; n=65) compared with control, non-mRNA injected oocytes (21%; n=24). In addition, TRβA1 expressing oocytes showed an increase in Ca^{2+} wave amplitude from 0.77±0.49 ($\Delta F/F$) to 0.95±0.41and an increase in interwave periods from 24.4±11.3 to 64.9±42s in the presence of T_3. We conclude that acute exposure to thyroid hormone dynamically modulates IP_3-mediating Ca^{2+} signalling. These data will be discussed in relation to the action of thyroid hormone on mitochondrial Ca^{2+} buffering. The work was supported by NIH GM48451 and AHA878.

444.3

ASSOCIATION OF TYPE I AND TYPE III INOSITOL 1,4,5 TRISPHOSPHATE RECEPTORS.

F.C. Nucifora Jr., A.H. Sharp, S.L. Milgram[1], R.E. Mains*, C.A. Ross. Laboratory of Molecular Neurobiology, Johns Hopkins University, School of Medicine, 720 Rutland Ave., Ross 615, Baltimore, MD 21205. 1. Department of Physiology University of North Carolina.

The Inositol 1,4,5-trisphosphate receptor (IP_3R) is an intracellular calcium channel involved in coupling cell membrane receptors to calcium signal transduction pathways within the cell. The IP_3R is believed to form a tetrameric structure to produce the calcium channel in endoplasmic reticulum membranes. Several isoforms (I, II, III) of IP_3Rs have been identified which are coded by separate genes, and are expressed in many tissues with differing patterns of cellular expression. We have generated specific affinity purified polyclonal anti-peptide antibodies to each of the three isoforms. Western Blot analysis of RINm5F and ATt20 cells shows high levels of endogenously expressed type I and type III IP_3R, but undetectable levels of type II. Co-immunoprecipitation experiments were performed by immunoprecipitating from these cells with the type I specific antibody and Western Blotting with the type III specific antibody, or by immunoprecipitating with the type III specific antibody and Western Blotting with the type I specific antibody. Both experiments yielded a band at 260 kDa, the appropriate size of both the type I and type III IP_3R. Immunocytochemistry performed on these cell lines with either antibody demonstrated similar ER staining patterns. The type III IP_3R was absent from the secretory granules of ATt20 cells. These data indicate that type I and type III IP_3Rs can associate into a molecular complex.

444.4

CONFOCAL MEASUREMENTS OF BASELINE NUCLEAR AND CYTOPLASMIC FLUORESCENCE: COMPARISON OF CA^{2+} INDICATOR AND NON-CA^{2+} INDICATOR DYES.

M.N. Rand*, S. Aguilan, & J.D. Kocsis. Dept. of Neurology and Sect. Neurobiology, Yale Medical School, New Haven, CT 06510; and VAMC, West Haven, CT 06516.

At baseline resting potentials, neurons which have been loaded with Ca^{2+} indicator dyes using a micropipette have higher levels of fluorescence in the nucleus than in the cytoplasm, and it has been suggested that this effect is due to the presence of more dye in the nucleus. To evaluate this idea confocal microscopy was used to compare nuclear to cytoplasmic fluorescence ratios (N/C ratios) of cultured adult rat dorsal root ganglion neurons filled by micropipette with either Ca^{2+} indicator or non-Ca^{2+} indicator dyes. Both 10 kD dextran-conjugated and free forms of the Ca^{2+} indicator and non-Ca^{2+} indicator dyes were used. In all cases, N/C ratios of Ca^{2+} indicator dyes were significantly higher than those of the non-Ca^{2+} indicator dyes (dextran-conjugated: 1.89 vs 1.11; free dye: 3.30 vs 1.58). N/C ratios of the non-Ca^{2+} indicator dyes remained constant whereas N/C ratios of Ca^{2+} indicator dyes varied significantly over time. Some of the neurons also developed blebs on their plasma membrane which filled with water, aqueous solutes and dye; for non-Ca^{2+} indicator dyes bleb fluorescence was always higher than nuclear fluorescence, and for Ca^{2+} indicator dyes nuclear fluorescence was always higher than bleb fluorescence. These results suggest that micropipette dye-loaded neurons have higher levels of nuclear Ca^{2+} at baseline resting potentials, and have important implications for the evaluation of depolarization-induced intracellular Ca^{2+} signals. Supported in part by the NIH and Department of Veterans Affairs.

444.5

CLONING AND SEQUENCING OF AN IP_3-RECEPTOR cDNA FROM LOBSTER OLFACTORY ORGAN.

S.D. Munger *[1,2], B.W. Ache[1,2,3] and R.M. Greenberg[1]. Whitney Laboratory[1] and Depts. of Neuroscience[2] and Zoology[3], Univ. of Florida, St. Augustine, FL 32086.

Several lines of evidence suggest that inositol 1,4,5-trisphosphate (IP_3)-receptors (IP_3Rs) occur in the plasma membrane of neuronal and nonneuronal cells, but little is known about the structural similarities of these plasma membrane IP_3Rs to the better known intracellular IP_3Rs. IP_3 directly gates two types of ion channels in the plasma membrane of lobster olfactory receptor neurons (ORNs); these channels are functionally similar to IP_3Rs localized to endoplasmic reticulum (ER) and nuclear membranes in vertebrates (Fadool & Ache, *Neuron*, 9: 907; Hatt & Ache, *PNAS*, 91: 6264). A polyclonal antibody directed against the ER IP_3R of rat cerebellum recognizes membrane proteins of appropriate size in lobster ORNs; this antibody also perturbs function of the lobster IP_3Rs in excised patch recordings (Fadool & Ache, *ibid.*). We have exploited the suggested structural similarities between plasma membrane and ER IP_3Rs by amplifying a partial cDNA, homologous to known IP_3Rs, from reverse transcribed lobster olfactory organ RNA using degenerate primers and PCR. We extended the clone to the 3'-noncoding region using 3'-RACE (Rapid Amplification of cDNA Ends). We have constructed an IP_3R mini-cDNA library, and have isolated overlapping clones by plaque hybridization and PCR. The open reading frame of the cDNA isolated to date, which codes for 1400 amino acids and comprises *ca.* 50% of the anticipated coding region, exhibits 40-45% identity to known IP_3Rs. While Northern analysis demonstrates a low level of expression of a >10 kb message in the brain, but none in the nose, the more sensitive ribonuclease protection assay shows the message to be expressed in the nose and, at higher levels, in the brain. We are currently working to extend the cDNA to the 5'-end and to localize the receptor by *in situ* hybridization and immunohistochemistry. {This work supported by ONR grant N00014-90-J-1566}

444.6

PLATELET-ACTIVATING FACTOR INDUCED INTRACELLULAR CALCIUM OSCILLATIONS IN RAT HIPPOCAMPAL NEURONS.

M. A. DeCoster, H. E. P. Bazan*, and N. G. Bazan. LSU Medical Center, Neuroscience Center, New Orleans, LA 70112-2234

As has been previously shown, we have found using confocal microscopy and fluorescent calcium indicators, that intracellular calcium concentration ($[Ca^{2+}]_i$) oscillates spontaneously in rat hippocampal neurons *in vitro*. While addition of glutamate (GLU) to these hippocampal cultures causes distinct $[Ca^{2+}]_i$ changes ranging from transient, single spikes (100-500 nM GLU) to sustained increases (20-80 μM GLU), GLU does not appear to induce $[Ca^{2+}]_i$ oscillations. We have investigated the ability of the potent lipid mediator platelet activating factor (PAF) to affect $[Ca^{2+}]_i$ dynamics in hippocampal neurons. When 4 μM methylcarbamyl PAF (mcPAF) was added to the hippocampal neurons, the average $[Ca^{2+}]_i$ was increased slightly in cells. Furthermore, the variance of fluorescence values after mcPAF additions was 8-fold higher than before additions, indicating an increase in oscillatory $[Ca^{2+}]_i$ dynamics induced by PAF. Neurons not spontaneously oscillating were observed to be induced to oscillate by PAF addition, and neurons spontaneously oscillating increased in oscillatory behavior upon PAF addition. In agreement with Bito *et al.* (Neuron, 9:285, 1992) we found that not all neurons responded to acute PAF application. In contrast, long-term effects of PAF treatment on hippocampal cultures appeared to affect the majority of cells. Overnight treatment with PAF (200-400 nM) and mcPAF (2-4 μM) reduced the neuronal $[Ca^{2+}]_i$ changes induced by GLU the next day when compared with cells pretreated with lysoPAF (2-4 μM) or the vehicle alone. In two cases, the $[Ca^{2+}]_i$ increases in response to 500 nM GLU were completely inhibited by PAF pretreatment. Since PAF has been shown to enhance hippocampal excitatory synaptic transmission (Clark et al., Neuron 9:1211, 1992) we postulate that induction of $[Ca^{2+}]_i$ oscillations by PAF may be an early signal of GLU release, resulting in GLU receptor desensitization (Supported by DAMD-17-93-V-3013).

1476

HUMAN TYPE II PHOSPHOLIPASE A_2 INDUCED Mac-1 EXPRESSION ON HUMAN NEUTROPHILS

J. Takasaki, Y. Kawauchi, T. Yasunaga and Y. Masuho, Yamanouchi Pharmaceutical Co. Ltd., Tsukuba-City, Ibaraki-Pref., 305, Japan.

To investigate the effect of type II phospholipase A_2 (PLA_2-II) on neutrophil function, we assessed the Mac-1 expression on human neutrophils by flow cytometry after incubation of the cells with human PLA_2-II. PLA_2-II at a concentration of 10 μg/ml increased the Mac-1 expression by 150% compared with unstimulated cells at 30 min. Under thses conditions, PLA_2-II increased the exocytosis from secretory vesicles but not from either azurophilic, specific or gelatinase granules. The results suggest that PLA_2-II induces translocation of Mac-1 from the secretory vesicles to the plasma membrane. The Mac-1 induction mediated by PLA_2-II was inhibited by an anti-PLA_2-II antibody, which was able to inhibit the catalytic activity. However, the Mac-1 induction by PLA_2-II was not inhibited by either a 5-lipoxygenase, cyclooxygenase inhibitor or a PAF antagonist. Thus, we examined the effects of fatty acids and lysophospholipids on Mac-1 expression. Only arachidonic acid induced Mac-1 expression. These results imply that PLA_2-II induces Mac-1 expression on neutrophils via production of arachidonic acid.

1477

Regulation of Cytoplasmic Phospholipase A2(cPLA2) During Macrophage Differentiation and Lipid Loading. Z.-F. Huang, J.B. Massey, and D.P. Via. Baylor College of Medicine.

Prostanoid formation by macrophage (MAC) and MAC-derived foam cells may have important autocrine and paracrine influences on cells of the atherosclerotic lesion. We examined the expression of cPLA2, a rate limiting enzyme in prostanoid synthesis, during MAC differentiation. Freshly isolated human monocytes had lower levels of cPLA2 mRNA and mass than differentiated MAC. mRNA levels doubled during 10 days in vitro differentiation and declined to 50% above baseline by day 15. cPLA2 mass paralleled changes in mRNA levels while enzymatic activity was regulated in a more complex manner. Removal of serum resulted in a rapid (2-4 hr) five fold rise in cPLA2 mRNA, protein, and enzymatic activity. MAC- conditioned medium blocked this increase suggesting the presence of a secreted autocrine regulator. THP-1 monocytic cells normally had higher basal levels of cPLA2 mRNA, protein, and enzymatic activity than fresh human monocytes. Terminal differentiation into MAC by 80nM phorbol ester resulted in loss of cPLA2. Phorbol ester also downregulated expression of cPLA2 in primary MAC. Lipid loading of primary human MAC with acetylated LDL to produce foam cells, had little influence cPLA2 levels. The data suggest that lipid loading does not directly affect cPLA2 regulation but the differentiation stage of MAC may signficantly affect cPLA2 mediated prostanoid synthesis in the atherosclerotic lesion.

1478

MODULATION OF CALCIUM, NEUROTOXICITY AND ARACHIDONIC ACID RELEASE BY PHOSPHOLIPASE A TYPE II AND GLUTAMATE IN VITRO. M. Kolko, E.B. Rodriguez de Turco, M.A. DeCoster, and N.G. Bazan, LSU Eye Center, LSUMC, New Orleans, LA.

Secretory phospholipase A Type II ($sPLA_2$) may modulate neuronal function, under both physiological and pathological conditions. This 14 kDa enzyme, present in synaptic vesicles, is released by depolarization or neurotransmitter stimulation. Moreover, ischemia induces $sPLA_2$ gene expression in rat brain. We evaluated the effect of $sPLA_2$ from bee venom (BV) alone and with glutamate (GLU) on neurotoxicity through lactate dehydrogenase (LDH) release, intracellular free calcium concentration ($[Ca^{2+}]_i$), and [^3H] arachidonic acid (AA) release on primary cultures of cortical neurons. At 0.01 μml, BV was not toxic, did not affect basal oscillations in ($[Ca^{2+}]_i$), but did induce [3H]AA release from phospholipids (PL). BV dose dependently (0.025-10 μg/ml) caused neurotoxicity, altered $[Ca^{2+}]_i$ dynamics, and stimulated [3H]AA release. GLU (80 μ M) toxicity was similar to 0.5 μ g/ml BV (100% above control). Concentrations of BV (0.01 to 0.05 μ g/ml), which resulted in a 40-80% increase in LDH release when combined with GLU (80 μ M), elicited synergy in neurotoxocity (2.5-fold higher LDH release than their individual LDH values) and [3H]AA (1.5-fold). MK-801 blocked the synergy but not the BV effects. In contrast to the sustained $[Ca^{2+}]_i$ response induced by GLU, BV dose-dependently (0.5-10 μ g/mL) induced a trancient increase in $[Ca^{2+}]_i$ followed by decreased basal oscillations and a significant fall in $[Ca^{2+}]_i$. These results indicate that calcium-independent toxicity may occur at low $sPLA_2$ concentrations and provide evidence for modulatory roles of $sPLA_2$s in neuronal signal transduction. Supported by DAMD-17-93-V-3013.

1479

Ceramide Inhibits PKC Activation of G-Protein-Dependent Phospholipase D *In Vitro*. Mark E. Venable and Lina M. Obeid, Duke University Medical Center, Durham, N.C. 27710

We investigated ceramide inhibition of the activation of PLD in HL-60 cells and cell lysates. In intact HL-60 cells, phorbolmyristateacetate (PMA) activated PLD as measured by [^{3}H]palmitate-labeled phosphatidylcholine conversion to phosphatidylethanol (PEt) in the presence of 2% ethanol. C_6-Ceramide inhibited this PLD activation in intact HL-60 cells after 4 hr treatment and was maximally active at 10 μM. The activity was specific in that structural analogs were inactive. Although ceramide inhibited PMA-induced activation of PLD it did not inhibit translocation of PKC to the membrane. In a cell-free assay using exogenous dipalmitoylphosphatidyl[^{3}H]choline in a phosphatidylethanol-amine and phosphatidylinositol-4,5-bisphosphate liposome we confirmed that PLD is activated by a soluble G-protein. Ceramide had no effect on this activity under a variety of conditions. However, activation of PLD by GTPγS could be synergistically enhanced by the addition of PKC activators. This upstream effect was inhibited rapidly and specifically by ceramide (30 μM). Taken together, these data show that ceramide interferes specifically with PKC-mediated activation of PLD.

1480

INTERFACIAL ACTIVATION OF PHOSPHATIDYLINOSITOL-SPECIFIC PLC TOWARDS INOSITOL CYCLIC 1,2-MONOPHOSPHATE. M.F. Roberts, C. Zhou, and Y. Wu, Boston College, Chestnut Hill, MA 02167.

Phosphatidylinositol-specific phospholipase C (PI-PLC) from *Bacillus thuringiensis* catalyzes PI hydrolysis in discrete steps: (i) an intramolecular phosphotransferase reaction to form inositol cyclic 1,2-monophosphate (cIP); followed by (ii) a cyclic phosphodiesterase activity converting water-soluble cIP to inositol-1-phosphate. We have studied the phosphodiesterase activity of PI-PLC towards cIP with particular reference to the possibility of interfacial activation towards a substrate that does not partition in an interface. In comparison to the first step, PI-PLC had only modest activity towards cIP (K_m= 90 mM; V_{max}= 136 μmol min^{-1} mg^{-1}). The activity showed a cooperative dependence on cIP concentration (Hill coefficient of 2). Almost all detergents examined increased enzyme specific activity 2-fold (only at concentrations ≥ CMC) with little alteration of K_m. However, PC micelles or vesicles had a much more profound effect: K_m for cIP decreased to 29 mM with diC_7PC micelles added, V_{max} increased almost 7-fold, and the cooperativity in cIP binding was abolished. The phosphocholine headgroup was critical to this larger kinetic effect since other short-chain phospholipid micelles caused only the generic 2-fold increase observed with bile salts, Triton X-100, and other detergents. Monomeric PC led to a small activation that increased linearly with increasing monomer. ^{1}H NMR studies of partially deuterated PCs indicated that under these conditions the enzyme nucleated the binding of several PC molecules. This represents a novel and specific type of interfacial activation of a phospholipase toward a water soluble substrate. [Supported by GM 26762]

1481

EVIDENCE FOR THE EXISTENCE OF G-PROTEIN-DEPENDENT AND G-PROTEIN-INDEPENDENT ACTIVATION OF PHOSPHOLIPASE D IN LYMPHOCYTES. Y-Z. Cao, P. V. Reddy, L. M. Sordillo and C. C. Reddy, Dept. of Veterinary Science, Penn State Univ., University Park, PA 16802.

Previously we reported that tumor-promoting phorbol esters stimulate phospholipase D (PLD) independent of protein kinase C activation in bovine lymph node lymphocytes. (Cao et al., Biochem. Biophys. Res. Commun. 171, 955-962, 1990; IBID 217, 908-915, 1995). In the present study, we examined the effects of prostaglandins (PGs), E_2, $F_{2\alpha}$, D_2, and H_2 on PLD activity as measured by [1-^{14}C] arachidonic acid incorporation into phosphatidylethanol (PEt) in bovine lymphocytes. All PGs stimulated the formation of PEt in a dose-dependent manner in the concentration range between 0.1 - 10μM. Prostaglandin E_2 had the maximum stimulatory effect in the order of PGE_2 > $PGF_{2\alpha}$ > PGH_2 > PGD_2. The PG-stimulated formation of PEt was enhanced by staurosporine, a PKC inhibitor. When both were included, the effect of PGE_2 and 12-0-tetradecanoylphorbol-13-acetate (TPA) on the PLD activation was additive. Furthermore, NaF, a G-protein activator, stimulated the PEt formation and this stimulation was enhanced by staurosporine. Interestingly, the stimulatory effects of PGs and NaF were not additive; however, the formation of PEt by NaF and TPA was additive. These results suggest that, similar to TPA activation of PLD, PGs increase PLD activity independent of PKC and the stimulation by PGs and TPA in lymphocytes may involve both G-protein-dependent and G-protein-independent signaling pathways. (Supported through PHS grant numbers HL31245 and AI-06347.)

1645

ALTERING NEUROTRANSMITTER LEVELS *IN VITRO* FOLLOWING GLUTAMATE DECARBOXYLASE GENE TRANSFER. J.D. Fritz, N. Hale, A. Utz, J. Northington, L. Wu, A. C. Powers, T. Verdoorn, and D. Robertson. Vanderbilt Univ., Nashville, TN 37232.

Adenoviral vectors encoding either isoform of human glutamate decarboxylase (GAD_{65} or GAD_{67}) under the control of the CMV promoter were constructed. Expression of GAD_{65} or GAD_{67} was verified by Western blot analysis of rat pituitary cells 48 hours after adenoviral-mediated GAD (AdGAD) gene transfer. Transgene expression was observed in ~100% of rat cerebellar granule neurons 3 days after adenoviral-mediated β-galactosidase gene transfer. Extracellular [GABA] increased >25 fold (79 μM verses 3 μM) in neurons 9 days after $AdGAD_{65}$ gene transfer. Intracellular [GABA] also increased in these neurons (20 μM verses 0.0 μM) and remained as such from 3-9 days after vector addition. Intracellular glutamate concentration decreased almost 50% in neurons 3 days after $AdGAD_{65}$ gene transfer, but returned to baseline (50-60 μM) by 9 days after vector addition. Similar [GABA] and [glutamate] were observed in neurons following $AdGAD_{67}$ gene transfer and in non-neuronal cell lines. [GABA] and [glutamate] were determined by HPLC using a Pico-Tag column (Waters) for free amino acid analysis. These data suggest that glutamatergic neurons can produce and release GABA following AdGAD gene transfer *in vitro*. Conversion of glutamatergic neurons to those expressing both glutamate and GABA could yield therapies in a variety of neurodegenerative disorders.

1646

MODULATION OF CHRONIC NEUROTOXICITY BY COMBINED KAINATE AND GLUTAMATE TREATMENT OF HIPPOCAMPAL NEURONS. H. Cinar, M.A. DeCoster, and N.G. Bazan. LSU Medical Center, Neuroscience Center, New Orleans, LA 70112-2234.

Acute treatment with excitatory amino acids, (EAAs) such as kainate (KA) and glutamate (G) cause neurotoxicity characterized by rapid increases in second messengers such as intracellular calcium; however, cell death in this model is delayed until approximately 16-24 hours. While these mechanisms of EAA neurotoxicity are understood for acute treatment, less is known of the effects of chronic treatment with these compounds. We therefore incubated primary rat hippocampal neurons overnight with KA and G (30 uM to 3 mM). Neuronal injury was determined by assaying lactate dehydrogenase (LDH) release. Dose-response curves showed different toxicity patterns for KA and G treatments. At lower concentrations KA was less toxic than G, but at concentrations higher than 300 uM, KA toxicity was 5 to 7 times of the control levels. G attained a toxicity level at most 2 to 3 times that of the baseline. Surprisingly, the toxicity of equimolar KA+G (300 =B5M + 300 =B5M) treatment was similar in magnitude to that induced by glutamate alone. Thus, the expected additive effects of toxic equimolar KA + G treatment was not obtained. One possible explanation for these results is the reported neuroprotective effect of activation of the metabotropic receptor by G; this action could mask the expected additive toxicity of KA+G treatments. A second possibility would involve the differential uptake of EAAs by astrocytes, which account for 10-15% of the cells in our culture. The role of both potential mechanisms will be investigated. (Supported by DAMD-17-93-V-3013).

1647

INHIBITION OF MUSCARINIC RECEPTOR BINDING BY PERVANADATE, ORTHOVANADATE, METAVANADATE AND AN ENDOGENOUS INHIBITOR FROM ALZHEIMER'S BRAIN. H. Venters Jr., M. Najarian, T. Ala and W.H. Frey II. Neurology, Ramsey Clinic, Health Partners, St. Paul, MN 55101.

Frey et al. have previously reported (Brain Res. 655: 153-160, 1994) that an endogenous inhibitor (<3,500 daltons) of ^{3}H-QNB antagonist binding to the muscarinic receptor (mAChR) is elevated in brain tissue from patients with Alzheimer's disease (AD). Further research has suggested that this inhibition is irreversible and is mediated by the thiyl radical of glutathione which forms in the presence of the inhibitor. We now report the results of research on the effect of metavanadate (known to generate thiyl radicals from glutathione), orthovanadate, and pervanadate on ^{3}H-QNB binding to the mAChR. All three vanadium compounds inhibited binding in the presence of glutathione, with the order of decreasing potency and the concentration required for 50% inhibition (I_{50}) being: pervanadate (95 μM) > orthovanadate (132 μM) > metavanadate (452 μM). Omission of glutathione decreased the inhibition of the vanadium compounds from 2 to 6 fold. In contrast to our results with the endogenous AD inhibitor, preincubating the vanadium compounds with the mAChR in the presence of glutathione at 37°C for 1 hour markedly decreased the I_{50} values as follows: pervanadate (13 μM) > orthovanadate (46 μM) > metavanadate (118 μM). Similarities of the vanadium compounds with the endogenous AD inhibitor were also noted, with the inhibition of each being blocked by Trolox, EDTA and Mn^{2+}. Further studies are needed to identify the endogenous AD inhibitor. (Supported by Ramsey Foundation grant #N585).

1648

MECHANISM OF MASTOPARAN ACTION IN THE STIMULATION OF ACETYLCHOLINE RELEASE AND ITS INHIBITION BY BOTULINUM TOXIN A IN PC12 CELLS. P. Ray, M. Flink and W. Middleton. Walter Reed Army Institute of Research, Washington D. C. 20307.

We demonstrated that in PC12 cells, the mechanism of stimulated acetylcholine (ACh) release inhibition by botulinum toxin A (BoTx) was via interference of phospholipase A_2 (PLA_2) stimulated arachidonic acid (AA) release from cell membranes (Ray, *et al.*, J. Biol. Chem., 268:11057-11064, 1993). In this study, we further investigated the roles of PLA_2 and AA in ACh release and BoTx effect. Mastoparan (Mas), a PLA_2 activator, attenuated the BoTx effects. Mas increased intracellular free calcium concentration ($[Ca^{2+}]_i$) as well [^{3}H]AA and [^{3}H]ACh release in a concentration-dependent manner. The effects of Mas were enhanced synergistically by extracellular K^+. A specific Ca^{2+}-dependent cytosolic PLA_2 inhibitor, 7,7-Dimethyleicosadienoic acid (DEDA) abolished [^{3}H]AA and [^{3}H]ACh release due to Mas plus K^+, but the Ca^{2+}-independent specific PLA_2 inhibitor, (E)-6-(bromomethylene) tetrahydro-3-(1-napthalenyl)-2H-pyran-2-one (HELSS) had no effect. The effects of Mas plus K^+ were blocked by either EGTA or the N-type Ca^{2+} channel blocker ω-conotoxin, but not the L-type Ca^{2+} channel blocker nifedipine, indicating that these Mas effects were dependent on Ca^{2+} influx via the neuronal type voltage-sensitive Ca^{2+} channels. BoTx inhibition of [^{3}H]AA and [^{3}H]ACh release was fully prevented by Mas plus 80 mM K^+. These results indicate that Mas prevents the BoTx effects via Ca^{2+} influx, PLA_2 activation, and AA release; and provide additional support for our proposed role of AA in stimulated ACh release and its inhibition by BoTx.

1649

INCREASED NEUROTOXICITY FOLLOWING SIMULTANEOUS EXPOSURE TO PYRIDOSTIGMINE BROMIDE (PB), DEET, AND CHLORPYRIFOS. M.B. Abou-Donia, K.R. Wilmarth, Ali A. Abdel-Rahman, Karl F. Jensen, Frederick W. Oehme, and Thomas L. Kurt. Dept. of Pharmacol., Duke Univ. Med. Center, Durham, NC, 27710; USEPA, RTP, NC, 27711; Kansas State Univ., Manhattan, KS, 66506; Univ. of Texas, Southwestern Med. School, Dallas, TX, 75205.

The service personnel during the Persian Gulf War were exposed to pesticides such as the insect repellent, DEET (*N,N*-diethyl-*m*-toluamide) and the insecticide, chlorpyrifos (*O,O*-diethyl *O*-3,5,6-trichloropyridinyl phosphorothioate) and to PB (3-dimethylaminocarbonyloxy-*N*-methylpyridinium bromide) that was given as a prophylactic agent against possible nerve gas attacks. We determined the neurologic deficits produced by individual or coexposure of hens 5 days/week for 2 months to 5 mg PB /kg/day in water, po; 500 mg DEET /kg/day, neat, sc; and 10 mg chlorpyrifos kg/day in corn oil, sc. Binary treatments produced greater neurotoxicity than that caused by individual exposures. Neurotoxicity was further enhanced following coexposure to these chemicals. PB decreased plasma butyrylcholinesterase (BuChE) activity to 17% of control compared to 51% and 83% from chlorpyrifos and DEET, respectively. BuChE was inhibited further in combined treatment groups compared to individual dosed groups. In contrast, only chlorpyrifos alone or in combination with other compounds produced a significant inhibition of brain acetylcholinesterase activity. Brain neurotoxicity target esterase was significantly inhibited only in hens given chlorpyrifos with PB or DEET or with both chemicals. We hypothesized that test compounds compete for xenobiotic metabolizing enzymes in the liver and blood, and that carbamylation of peripheral aliesterases by PB increases the concentration of the lipophilic DEET and chlorpyrifos in circulation and their availability to the central nervous system. This increase in the effective concentrations of these chemicals in the nervous system could then reach levels equivalent to near-lethal doses of individual compounds associated with neurologic deficits. (Funding provided by the Perot Foundation.)

1650

THE THERAPEUTIC WINDOW OF 4-AMINOPYRIDINE, A COMPOUND EFFECTIVE AGAINST THE LETHAL EFFECTS OF SAXITOXIN. S.A. Keller, B.J. Benton, D. Spriggs, B.R. Capacio and F.-C.T. Chang (SPON: R. Ray). U.S. Army Med. Res. Inst. of Chem. Def., APG, MD 21010.

We have shown that saxitoxin (STX) induced lethality can be reversed by 4-aminopyridine (4-AP) if given at the time of respiratory arrest. The purpose of this study was to examine 4-AP's therapeutic window and to determine if its efficacy can be further enhanced when co-administered with STX. Three (3) groups of unanesthetized guinea pigs were used in this study. These animals were chronically instrumented for concurrent recordings of diaphragm EMG, skeletal muscle EMG, Lead II ECG and EEG. All animals were given a lethal dose of STX (5 μg/kg; im) which resulted in a progressive cardiorespiratory depression, and ultimately, respiratory arrest. Group 1 animals served as toxin controls. Group 2 animals received artificial ventilation at the point of respiratory arrest, followed by 4-AP (2 mg/kg, im). Group 3 animals were treated with 4-AP (2 mg/kg, im) immediately after STX and were ventilated at the time of apnea. Results from groups 2 and 3 animals showed that STX-induced cardiorespiratory failure could be restored to a level comparable to that of control. The diaphragm activities showed a slightly faster return in group 3 animals (1.13±0.21 min) as compared to group 2 animals (2.88±0.78 min). There was no difference, however, in the time it took for group 2 (42.1±8.5 min) and group 3 (39±7.1 min) animals to resume spontaneous breathing. In conclusion, we have shown that i) STX-induced lethality can be reversed by an experimental therapeutic modality which consists of artificial ventilation and 4-AP; and, ii) the therapeutic window of 4-AP is quite broad (from the time of intoxication to apnea); that is, administration of 4-AP at an earlier time point does not enhance the therapeutic effectiveness of 4-AP (as measured by the time taken for the return of spontaneous breathing).

2151

PAF INDUCES CYCLOOXYGENASE (COX-2) GENE EXPRESSION IN THE CORNEAL EPITHELIUM PARTIALLY BY A RECEPTOR-MEDIATED CALCIUM INFLUX. Y. Tao, H.E.P. Bazan, M.A. DeCoster, N.G.Bazan LSU Eye Center and Neuroscience Center, New Orleans, LA 70112

This study investigated the role and source of Ca^{2+} in the signaling of platelet-activating factor (PAF)-induced COX-2 gene expression in the corneal epithelium. Rabbit corneas were incubated in organ-culture in Hank's Ca^{2+}-free or minimum Eagle's medium, and the COX-2 mRNA expression in the epithelium was studied. Primary cultures of corneal epithelium were loaded with the fluorescent dye fluo-3, and changes of intracellular Ca^{2+} were analyzed by confocal microscopy. We found that PAF stimulated the expression of COX-2 mRNA that peaks at 4 hrs in the corneal epithelium incubated in MEM. The expression was inhibited by the PAF antagonist BN50730. When incubated in Ca^{2+}-free medium, there was a 40% inhibition of the induction. The Ca^{2+} ionophore A23187 caused a small but significant increase of COX-2 in the epithelium, which was abolished in Ca^{2+}-free medium. When added together, A23187 potentiated the effect of PAF. Confocal microscopic imaging showed that when incubated in Ca^{2+}-containing medium, PAF transiently increased intracellular Ca^{2+} which peaks between 30 and 60 seconds after adding PAF. Such effect of PAF was not seen when the cells were incubated with BN50730, when the cells were treated with vehicle, or when the cells were incubated in Ca^{2+}-free medium. In conclusion, Ca^{2+} is partially required in the induction of the COX-2 gene in the corneal epithelium. The source of such Ca^{2+} is likely to be extracellular, and its entry may be mediated via a PAF receptor. (NIH EY04928)

2152

POOL DEPLETION INDUCES A NOVEL CALCIUM INFLUX PATHWAY ACTIVATED BY CAFFEINE. C.A. Ufret-Vincenty, A. Alfonso, and D.L. Gill. Department of Biological Chemistry, University of Maryland School of Medicine, Baltimore, MD 21201.

Ca^{2+} influx through store-operated channels (SOCs) activated rapidly after Ca^{2+} pool depletion represents an important component of Ca^{2+} signals generated in cells. A new and distinct Ca^{2+} influx component activated by caffeine is induced in cells after Ca^{2+} pools are emptied using the intracellular Ca^{2+} pump inhibitors, thapsigargin (TG) or 2,5-di-*tert*- butylhydroquinone (DBHQ). Both blockers cause depletion of intracellular Ca^{2+} pools and cell growth arrest; upon refilling of pools, normal cell-cycle progression is resumed (Short, A.D., et al. PNAS 90, 4986-4990, 1993). Here, the Ca^{2+}-sensitive dye, fura-2, was used to study Ca^{2+} homeostasis in DDT_1MF-2 smooth muscle cells growth-arrested by TG- or DBHQ-treatment. In DDT_1MF-2 cells the SOC-mediated Ca^{2+} influx component after emptying Ca^{2+} pools is short- lived and appears to be rapidly deactivated. After treatment of DDT_1MF-2 cells with either 3 μM TG or 10 μM DBHQ, 10 mM caffeine induces a large transient influx of Ca^{2+} distinct from SOC- mediated Ca^{2+} entry. Caffeine-sensitive Ca^{2+} influx following DBHQ-treatment is activated more rapidly than that following TG-treatment. When caffeine is added to untreated DDT_1MF-2 cells no effect on cytosolic Ca^{2+} concentration is observed. The disappearance of caffeine-induced Ca^{2+} influx is also different for TG- and DBHQ-treated cells. In DBHQ-treated cells, bradykinin- sensitive Ca^{2+} pools quickly refill and cells become insensitive to caffeine immediately after DBHQ removal. In the case of TG-treated cells, reversal of TG-induced growth arrest with either high (20%) serum or 1-10 μM arachidonic acid, in addition to removal of TG, is required to allow agonist-sensitive Ca^{2+} pools to refill concomitantly with the disappearance of caffeine-induced Ca^{2+} influx. In summary, the results show that a Ca^{2+} influx pathway activated by caffeine is observed under conditions of growth arrest induced by either TG or DBHQ and appears to be directly correlated with depletion of intracellular Ca^{2+} pools. (NIH grants NS19304 and GM15407; NSF grant MCB 9307746).

2153

PLATELET-ACTIVATING FACTOR MODULATES INTRACELLULAR CALCIUM DYNAMICS IN RAT HIPPOCAMPAL NEURONS. M. A. DeCoster and N. G. Bazan, LSU Medical Center, Neuroscience Center, New Orleans, LA 70112-2234

We have found using confocal microscopy and fluorescent calcium indicators, that intracellular calcium concentration ($[Ca^{2+}]_i$) oscillates spontaneously in rat hippocampal neurons *in vitro*. While addition of glutamate (GLU) to these hippocampal cultures consistently elicits distinct $[Ca^{2+}]_i$ changes ranging from transient, single spikes (100-500 nM GLU) to sustained increases (20-80 μM GLU), GLU does not appear to induce $[Ca^{2+}]_i$ oscillations. Here we have investigated the ability of the potent lipid mediator platelet activating factor (PAF) to affect $[Ca^{2+}]_i$ dynamics in hippocampal neurons. When 4 μM methylcarbamyl PAF (mcPAF) was added acutely to hippocampal neurons, the average $[Ca^{2+}]_i$ was increased slightly. The variance of fluorescence values after mcPAF additions was 8-fold higher than before additions, indicating an increase in oscillatory $[Ca^{2+}]_i$ dynamics induced by PAF. Neurons not spontaneously oscillating were observed to be induced to oscillate by PAF addition, and neurons spontaneously oscillating increased in oscillatory behavior upon PAF addition. In agreement with Bito *et al.* (Neuron, 9:285, 1992) we found that not all neurons responded to acute PAF application. Long-term treatment with PAF appeared to affect the majority of hippocampal cells. Overnight treatment with PAF (200-400 nM) and mcPAF (2-4 μM) reduced the neuronal $[Ca^{2+}]_i$ changes induced by GLU the next day when compared with cells pretreated with lysoPAF (2-4 μM) or vehicle alone. In two cases, the $[Ca^{2+}]_i$ increases in response to 500 nM GLU were completely inhibited by PAF pretreatment. Since PAF has been shown to enhance hippocampal excitatory synaptic transmission (Clark et al., Neuron 9:1211, 1992) we postulate that induction of $[Ca^{2+}]_i$ oscillations by PAF may be an early signal of GLU release, resulting in GLU receptor desensitization (Supported by DAMD-17-93-V-3013).

2154

CALCIUM-STIMULATED PHOSPHORYLATION OF MAP-2 IN PANCREATIC β-CELLS IS MEDIATED BY CaM KINASE II. K.A. Krueger, H. Bhatt, M. Landt and R.A. Easom, UNTHSC at Fort Worth, Fort Worth, TX 76107 and Washington University School of Medicine, St. Louis, MO 63110.

An elevation of intracellular Ca^{2+} is a critical signal in the initiation of insulin secretion from the pancreatic β-cell but the mechanism involved is not understood. Previously, we have demonstrated that the multifunctional Ca^{2+}/calmodulin-dependent protein kinase II (CaM kinase II) is activated by glucose implicating this enzyme in the secretory process, but its cellular targets are unidentified. One of the best substrates of CaM kinase II *in vitro* that could function in secretory events, is the microtubule-associated protein, MAP-2. The current study represents an evaluation, *in situ*, of MAP-2 as a substrate of CaM kinase II using a permeabilized β-cell model. By immunoblot analysis, the presence of MAP-2 in the βTC3 cell was established. In α-toxin-permeabilized βTC3 cells, Ca^{2+} induced the concentration-dependent activation of CaM kinase II. In parallel and by immunoprecipitation, Ca^{2+} also induced the phosphorylation of MAP-2 that closely correlated with CaM Kinase II activation. Ca^{2+}-induced phosphorylation of MAP-2 was not inhibited by an inhibitor of protein kinase A (H89) at concentrations that prevented phosphorylation induced by forskolin. These data provide evidence that MAP-2 is phosphorylated by CaM kinase II in the pancreatic β-cell *in situ*, and that this event may provide an important link in the mediation of Ca^{2+}-dependent insulin secretion. (Supported by NIH grant DK-47925).

2155

RE-EVALUATION OF THE ROLE OF CaM KINASE II IN INSULIN SECRETION FROM PANCREATIC β-CELLS. H. Bhatt, J. Tarpley and R.A. Easom, UNTHSC at Fort Worth, Fort Worth TX 76107.

Current evidence addressing the role of CaM kinase II in insulin secretion is conflicting. We have previously demonstrated that glucose activates the multifunctional Ca^{2+}/calmodulin-dependent protein kinase II (CaM Kinase II) in a concentration-dependent manner that correlates with insulin secretion. Others have demonstrated that the CaM kinase II inhibitor, KN-62 (1 μM), failed to inhibit Ca^{2+}-induced insulin secretion from streptolysin O-permeabilized HIT cells, leading to the implication that this enzyme has no role in the secretory process. In this study, however, KN-62 at concentrations up to 100 μM did not inhibit CaM Kinase II activity in cellular extracts of βTC3 cells in the presence of exogenous calmodulin, and only modestly in the absence of the cofactor. In α-toxin-permeabilized βTC3 cells, Ca^{2+} induced the rapid activation of CaM kinase II in a concentration-dependent manner that was maintained for at least 30 min. This activation was not prevented by KN-62 (0-100 μM) negating the suggestion that CaM kinase II is not involved in Ca^{2+}-induced insulin secretion. The kinase inhibitor, K252a and a selective peptide inhibitor, [Ala^{286}] CaMK 281-302 strongly inhibited CaM kinase II activity in βTC3 cells and conditions have been established to permit the evaluation of the effects of these compounds on Ca^{2+}-induced insulin secretion. A more stringent correlation of the extent of inhibition of CaM Kinase II and insulin secretion by these compounds will permit a better assessment of the role of this enzyme in insulin secretion. (Supported by NIH 47925).

2156

OTHER EFFECTS OF ACETAZOLAMIDE IN RAT LIVER MITOCHONDRIA

A. Saavedra-Molina and M. Clemente-Guerrero.
Instituto de Investigaciones Químico-Biológicas. Universidad Michoacana. Morelia, Mich. 58030. MEXICO.

Preliminary studies using the carbonic anhydrase inhibitor acetazolamide showed a reduction in citrulline synthesis by intact guinea pig liver mitochondria (Arch. Biochem. Biophys. 1986. 251, 198-204) and it was concluded that this sulfonamide produces also an inhibition of urea synthesis in isolated guinea pig hepatocytes.

In this report we demonstrated that in rat liver mitochondria in the presence of different concentrations of acetazolamide, citrulline synthesis was decreased in a dose-response fashion obtaining the maximum inhibition (35%) with 300 μM; however, other effects were found. By using fluo-3 as a mitochondrial fluorescent calcium indicator, matrix free calcium ($[Ca^{2+}]_m$) was measured in a KCl-based buffer (pH 7.4) in the presence of EGTA. The effect of acetazolamide was a decrease (45%) of $[Ca^{2+}]_m$. When the same reaction was performed in the presence of 3 μM $CaCl_2$, mitochondrial matrix free calcium increased 3-4 fold (from 1.2 μM-3.6 μM) with 50-200 μM acetazolamide. The results obtained described another effect of the sulfonamide acetazolamide on mitochondrial matrix free calcium, which indicate that calcium ions could exert a physiological effect on citrulline synthesis.

(Supported in part by Conacyt 95-02-082 and CIC-UMSNH 1996).

THE JOURNAL OF BIOLOGICAL CHEMISTRY
Vol. 271, No. 51, Issue of December 20, pp. 32722–32728, 1996
Printed in U.S.A.

Synergy by Secretory Phospholipase A_2 and Glutamate on Inducing Cell Death and Sustained Arachidonic Acid Metabolic Changes in Primary Cortical Neuronal Cultures*

(Received for publication, July 23, 1996, and in revised form, September 17, 1996)

Miriam Kolko‡, Mark A. DeCoster, Elena B. Rodriguez de Turco, and Nicolas G. Bazan§

From the LSU Neuroscience Center and Department of Ophthalmology, Louisiana State University Medical Center, School of Medicine, New Orleans, Louisiana 70112

Secretory and cytosolic phospholipases A_2 (sPLA$_2$ and cPLA$_2$) may contribute to the release of arachidonic acid and other bioactive lipids, which are modulators of synaptic function. In primary cortical neuron cultures, neurotoxic cell death and [^{3}H]arachidonate metabolism was studied after adding glutamate and sPLA$_2$ from bee venom. sPLA$_2$, at concentrations eliciting low neurotoxicity (≤100 ng/ml), induced a decrease of [^{3}H]arachidonate-phospholipids and preferential reesterification of the fatty acid into triacylglycerols. Free [^{3}H]arachidonic acid accumulated at higher enzyme concentrations, below those exerting highest toxicity. Synergy in neurotoxicity and [^{3}H]arachidonate release was observed when low, nontoxic (10 ng/ml, 0.71 nM), or mildly toxic (25 ng/ml, 1.78 nM) concentrations of sPLA$_2$ were added together with glutamate (80 μM). A similar synergy was observed with the sPLA$_2$ OS2, from Taipan snake venom. The NMDA receptor antagonist MK-801 blocked glutamate effects and partially inhibited sPLA$_2$ OS2 but not sPLA$_2$ from bee venom-induced arachidonic acid release. Thus, the synergy with glutamate and very low concentrations of exogenously added sPLA$_2$ suggests a potential role for this enzyme in the modulation of glutamatergic synaptic function and of excitotoxicity.

Membrane unsaturated fatty acid turnover and the synthesis of bioactive lipids are modulated by phospholipases A_2 (PLA$_2$),[1] ubiquitous mammalian enzymes that catalyze the hydrolysis of *sn*-2-acyl ester bonds of phospholipids (PLs) (1). Arachidonic acid (AA), eicosanoids, and platelet-activating factor (PAF) are bioactive lipids generated through PLA$_2$ activation (2). Although some PLA$_2$ are calcium-independent (3, 4), most found in the brain are characterized by calcium dependence (4, 5). PLA$_2$s are overstimulated in the brain during seizures and ischemia (6–8) as a consequence of increased calcium influx and/or intracellular calcium mobilization, which, in turn, results in the accumulation of bioactive lipids that participate in cell damage (8, 9).

There are secretory and cytosolic PLA$_2$s (sPLA$_2$ and cPLA$_2$s, respectively). sPLA$_2$ (14 kDa) are active at submillimolar concentrations of calcium and do not display selectivity for unsaturated fatty acids at the *sn*-2-position of PLs (4, 5). sPLA$_2$s are found in pancreatic secretions (type I), platelets, neurons, mast cells, snake venoms, inflammatory exudates (type II), and bee venom (type III) (4, 5, 10). In contrast, cPLA$_2$ (type IV) has a higher molecular mass (85 kDa), is active at submicromolar Ca^{2+} concentrations, and shows selectivity for *sn*-2-arachidonoyl-PLs (5, 11). cPLA$_2$ is activated by translocation to intracellular and nuclear membranes when there is an agonist-induced increase in intracellular calcium concentration ($[Ca^{2+}]_i$) in the brain (12, 13) as well as in other tissues (4, 14).

Among the neural forms of PLA$_2$ are (*a*) a calcium-sensitive and arachidonoyl-specific 85-kDa cPLA$_2$ (12, 15, 16), highly expressed in astrocytes (17), other cytosolic calcium-dependent forms (12, 16), and calcium-independent forms (3, 18, 19); and (*b*) membrane-bound forms (15), including a very high molecular mass (180-kDa) form from human temporal cortex (20). Secretory PLA$_2$ are also present in the brain. The expression of sPLA$_2$ type II is stimulated in the rat brain by ischemia/reperfusion (21) and in cultured astrocytes by inflammatory mediators (22). Moreover, sPLA$_2$ type II is stored in synaptic vesicles and released by depolarization or neurotransmitter stimulation, and its secretion is coupled with the activation of catecholamine release (23). Furthermore, sPLA$_2$ causes activation of Glu release in the rat cerebral cortex (24).

sPLA$_2$ bind to cell surface receptors, the N type and the M type (25–28) identified using sPLA$_2$ purified from snake and bee venoms as ligands. Neurotoxic sPLA$_2$ from Taipan snake venom, OS2, and from bee venom bind to the N-type receptor with high affinity (25, 26). Other sPLA$_2$s such as OS1, also purified from Taipan snake venom, display higher enzymatic activity than the sPLA$_2$s OS2 and bee venom (2.7- and 7-fold higher, respectively) (25). Although OS1 binds with high affinity to M-type receptors (26–28), it does not bind to N-type receptors (25) and is therefore non-neurotoxic.

Activation of cPLA$_2$ mediates the formation of modulators of synaptic transmission such as free AA (8), eicosanoids (29, 30), and PAF (31). Ischemia and seizures promote a rapid increase in brain free AA (6, 7, 32, 33), oxygenated metabolites of AA, and free radicals, all of which are potent neuronal injury mediators (for review, see Ref. 8). A sustained activation of cPLA$_2$ has been reported after ischemia/reperfusion (13, 15). Glu, which causes excitotoxic neuronal damage, increases calcium influx through NMDA receptors in postsynaptic neurons, leading to PLA$_2$-mediated AA release (34–37), which is blocked by the NMDA antagonist MK-801 (38). Recently, the activation of two calcium-dependent cPLA$_2$s (100 and 14 kDa) by Glu was reported (16).

* This work was supported by National Institutes of Health Grant NS23002 and DAMD 17-93-V-3013. Part of this work has appeared in abstract form (45). The costs of publication of this article were defrayed in part by the payment of page charges. This article must therefore be hereby marked "*advertisement*" in accordance with 18 U.S.C. Section 1734 solely to indicate this fact.

‡ Fulbright fellow. Present address: University of Copenhagen Medical School, Copenhagen, Denmark.

§ To whom correspondence should be addressed: LSU Neuroscience Center, 2020 Gravier St., Suite B, New Orleans, LA 70112. Tel.: 504-568-6700 (ext. 321); Fax: 504-568-5801; E-mail: nbazan@lsumc.edu.

[1] The abbreviations used are: PLA$_2$, phospholipase A$_2$(s); sPLA$_2$, secretory phospholipase A$_2$(s); cPLA$_2$, cytosolic phospholipase A$_2$; PAF, platelet-activating factor; AA, arachidonic acid; PL, phospholipid; CHE, cholesterol ester; TAG, triacylglycerol; FFA, free fatty acids; DAG, diacylglycerol; LDH, lactate dehydrogenase.

Other PLA_2s are modulators of membrane PL metabolism and/or generate membrane fusogenic molecules, *i.e.* free fatty acids and lyso-PLs. However, non-AA-specific-$sPLA_2$s contribute, together with the $cPLA_2$, to modulate AA metabolism under physiological conditions and in primed conditions (5, 39–42). $sPLA_2$ venoms have long been known to be neurotoxic (10, 43). For example, $sPLA_2$ from Naja mocambique, as well as the PLA_2 activator melittin, have previously been shown to promote neural injury, *in vitro* and *in vivo* (44). The present study has tested the hypothesis that $sPLA_2$ potentiates neurotoxicity by Glu by briefly exposing rat cortical neuronal cultures to this neurotransmitter in the presence of and in the absence of $sPLA_2$. This hypothesis is supported in part by the observation that $sPLA_2$ is released at synapses from vesicles that also store Glu (23). $sPLA_2$ from bee venom and Taipan snake venom OS2, ligands of the N-type $sPLA_2$ receptor, and OS1 from Taipan snake venom, a ligand of the M-type $sPLA_2$ receptor, have been used (25–28). Moreover, sustained changes in neuronal [^{3}H]AA metabolism under these conditions have been observed. Our study has addressed the following: (*a*) the effect of Glu-activated $cPLA_2$ and exogenously added $sPLA_2$ on [^{3}H]AA release from neuronal PLs; (*b*) the action of MK-801 on agonist-induced AA changes and neurotoxicity; (*c*) the neurotoxic potential of exogenously added $sPLA_2$ (OS2 and bee venom $sPLA_2$); and (*d*) the neurotoxic effect of the excitatory neurotransmitter Glu and $sPLA_2$ when added to the cells simultaneously.

EXPERIMENTAL PROCEDURES

Materials—[5,6,8,9,11,12,14,15-^{3}H]Arachidonic acid ([^{3}H]AA; 185 Ci/mmol) was purchased from DuPont NEN. Silicagel GHL TLC plates were from Analtech, Inc. (Newark, DE). Bovine serum albumin fatty acid-free and lipid standards were from Sigma. Organic solvents (high pressure liquid chromatography grade) were from EM Science. $sPLA_2$ from bee venom and OS1 and OS2 from Taipan snake venom were purified as described previously (25).

Primary Neuronal Cultures—Cortical neuronal cultures were established from 15-day-old rat embryos as described previously (46, 47). Cells were plated in poly-L-lysine-coated dishes at a density of 4×10^5 cells/well in 48-well plates for toxicity experiments and 7.5×10^5 cells/well in 24-well plates for lipid analysis. The cells were cultured in neuronal culture medium (NCM) containing 10% fetal calf serum and 10% horse serum in a 5% CO_2 incubator at 37 °C. Astrocyte proliferation was prevented by adding cytosine arabinoside (10^{-5} M) at day 4 after plating, left on for 3 days, and then replaced with minimum essential medium containing 10% horse serum. Cells were used for experiments at 14–21 days *in vitro*. The percentage of neuronal *versus* glial cells remained at approximately 80 *versus* 20%, respectively, as previously reported (48).

Neuronal Toxicity Assay—Lactate dehydrogenase (LDH) release was used to quantitatively assess cell injury. Cells were treated as described previously (47), and LDH release was measured 20 h after exposure to $sPLA_2$ and/or Glu. Briefly, cells were exposed for 45 min at room temperature to highly purified $sPLA_2$ from bee venom and snake venom (OS1 or OS2) and/or Glu (80 μM) in Locke's solution without magnesium. Locke's solution was exchanged with minimum essential medium without phenol red, and the cultures were returned to the CO_2 incubator for 20 h at 37 °C. Using similar cortical neuron culture, this procedure results in minimal LDH release before 12 h and maximal release by 20 h (49). The LDH release was assayed using the Sigma kit with the aid of a DU series 640 Beckman spectrophotometer equipped with a graphic video display.

[^{3}H]Arachidonic Acid Metabolism and Lipid Analysis—Cells were labeled overnight with [^{3}H]AA (0.5 μCi/well, specific activity 184.6 Ci/mmol) in minimum essential medium supplemented with 0.2% fatty acid-free bovine serum albumin. 18–20 h later, the medium of cell cultures was replaced with minimum essential medium. The cells were exposed to Glu and/or $sPLA_2$ as described previously and returned to the CO_2 incubator for 2 and 20 h at 37 °C. The supernatants were removed, and 750 μl of methanol was added to each well. The cells were scraped and transferred into a glass tube, and chloroform was added in the following proportion: chloroform-methanol, 2:1 (v/v). Lipids were extracted by sonication for 30 min, and the lipid extracts were washed following the procedure of Folch *et al.* (50). Aliquots in duplicate were taken to determine total [^{3}H]AA incorporation by liquid scintillation counting.

Neutral lipids and total PLs were isolated by monodimensional TLC on precoated 0.25-mm-thick silica gel GHL plates using hexane:diethyl ether:acetic acid, 40:60:1.3 (v/v/v), as a developing solvent. For the results presented in Table I, the composition of the chromatographic solvent was changed to 60:10:1.3 (v/v/v) in order to isolate cholesterol ester (CHE) from triacylglycerols (TAG) that run together in the first system. The results indicated that changes observed in previous experiments in the CHE plus TAG fraction were due mainly to TAG. Lipid standards were added to the samples as a carrier and were spotted in a parallel line on the TLC plate to individualize each lipid band. TLC plates were developed with iodine, lipid bands were scraped, and the radioactivity was determined in a Beckman scintillation counter.

Statistical Analysis—The significance of the data was evaluated with Student's *t* test for unpaired data. Statistical values were considered significantly different when $p < 0.05$.

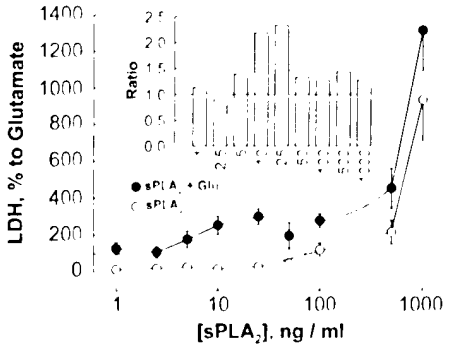

FIG. 1. **Secretory phospholipase A_2 from bee venom and Glu elicit synergy of neurotoxicity.** Rat cortical neurons were treated for 45 min at room temperature in Locke's solution with Glu (80 μM) and with increasing concentrations of $sPLA_2$ from 1 ng/ml (71 pM) to 10^3 ng/ml (71 nM) in the presence or absence of Glu (80 μM). The media were assayed for LDH release 20 h later. LDH released by Glu in each plating was considered as 100%, and all other values were normalized to a percentage of the Glu LDH value. Mean values ± S.D. from at least *n* = 10 individual determinations are shown. Values of LDH for 25 ng/ml $sPLA_2$ (130%) or higher were significantly above Glu alone ($p < 0.05$). The *dotted line* indicates a Glu value (100%) attained at 100 ng/ml $sPLA_2$ concentration. *Inset*, plotted values are the ratio between percentage of LDH release induced by $sPLA_2$ added together with Glu divided by the sum of the percentage LDH values obtained with $sPLA_2$ and Glu (100%) assessed individually in the same plating. A ratio of 1 (*dotted line*) indicates that the effects are additive.

RESULTS

Potent Neurotoxicity Elicited by $sPLA_2$—Neurotoxicity of $sPLA_2$ from bee venom, added alone or with Glu (80 μM) to primary neuronal cortical cultures, was studied by measuring LDH release (Fig. 1). A neurotoxic concentration of Glu (47) resulted in 92 ± 7% increase in LDH release compared with control cells ($n = 54$ from 10 different platings). No significant toxicity was observed with bee venom $sPLA_2$ concentrations up to 10 ng/ml (Fig. 1*A*). At higher concentrations up to 10^3 ng/ml, the neurotoxicity displayed by $sPLA_2$ was biphasic. First, there was a dose-dependent increase in LDH release (up to 500 ng/ml, $EC_{50} = 7.1$ nM), followed by a sharp 4.3-fold increase in LDH at 10^3 ng/ml ($EC_{50} = 57$ nM). The $sPLA_2$ neurotoxicity at 100 ng/ml (7.1 nM) was similar to that of 80 μM Glu (Fig. 1). An additive neurotoxic effect was observed when cells were exposed simultaneously to 80 μM Glu and low (1–5 ng/ml) or high ($50–10^3$ ng/ml) $sPLA_2$ concentrations (Fig. 1, *inset*). The combination of $sPLA_2$ in a concentration range of 10–25 ng/ml with Glu led to a significant synergy on LDH release, resulting in values 2.3–2.4-fold higher than those of the additive effects of $sPLA_2$ and Glu.

The $sPLA_2$ OS2 purified from snake venom was found to be more potent as a neurotoxin than the $sPLA_2$ from bee venom. For example, at 25 ng/ml OS2 was approximately 2.7-fold more

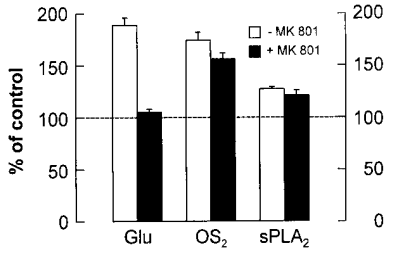

FIG. 2. **MK-801 elicits neuroprotection against Glu but not against $sPLA_2$ from bee venom or OS2.** Rat cortical neurons were treated as described in the legend to Fig. 1 and assayed for LDH release. Values are normalized to percentage of control wells, treated with Locke's solution only; some wells were treated with MK-801 (300 nM) for 10 min prior to the addition of toxins or Glu and remained in the wells during treatment. Mean values are shown ± S.E. from a representative set of culture plates derived from the same plating, treated and assayed on the same day. The *dotted line* (100%) indicates control, (nontoxic) levels for LDH. MK-801 blocks Glu ($p < 0.001$) by 100% but does not affect OS2 ($p < 0.11$) and bee venom $sPLA_2$ ($p < 0.33$) neurotoxicity.

toxic than bee venom $sPLA_2$ at the same concentration (Fig. 2). Furthermore, under conditions where the noncompetitive NMDA antagonist MK-801 blocked 100% of 80 μM Glu toxicity, MK-801 partially blocked OS2, but not bee venom $sPLA_2$-induced toxicity. OS1 did not evoke neuronal death even at 10 μg/ml (LDH percentage above control = 18 ± 9%).

$sPLA_2$ Promotes Arachidonic Acid Release from Phospholipids—[^{3}H]AA-prelabeled neuronal cells were exposed to different concentrations of bee venom $sPLA_2$ for 45 min and further incubated for 20 h (Fig. 3). No differences were observed in total [^{3}H]AA labeling recovered per dish at very low, nontoxic $sPLA_2$ concentration (1 ng/ml). At higher concentrations (25–50 ng/ml), the recovery was decreased by 10% and by 20–30% at more toxic concentrations (500–10^3 ng/ml), reflecting cell loss and matching the neurotoxicity assays (Fig. 1). After 20 h the [^{3}H]AA distribution displayed a concentration-dependent loss of [^{3}H]AA-PLs paralleled by an increase in free [^{3}H]AA, [^{3}H]AA-TAG and [^{3}H]AA-DAG. A significant loss in PL labeling was observed even at the lowest $sPLA_2$ concentration (−7%, $p < 0.05$), reaching values 50% lower at the highest toxic concentrations (500–10^3 ng/ml). Up to 100 ng/ml $sPLA_2$, the loss of [^{3}H]AA from phospholipids (−29%) was paralleled by its active reesterification into TAG, which showed a 25% increase above the control value. Within this range of $sPLA_2$ concentration, free [^{3}H]AA showed a small yet significant gradual increase, reaching values 2- and 4.5-fold higher than controls at 1 ng/ml and 100 ng/ml, respectively. The [^{3}H]AA-TAG labeling plateaued at 500 ng/ml $sPLA_2$. This was paralleled by a large increase in free [^{3}H]AA accumulation, which reached a value 20-fold higher than control. [^{3}H]DAG labeling was very low, displaying the same pattern of changes as free [^{3}H]AA and reaching a 2-fold increase in percentage of labeling at high $sPLA_2$ concentration (500 ng/ml).

Triacylglycerols Are a Finite Reservoir for the Uptake of [^{3}H]AA Released by $sPLA_2$ and Glu—To ascertain if [^{3}H]AA released by bee venom $sPLA_2$ was acylated into TAG and whether or not this correlated with neurotoxicity, the following experiment was performed. The [^{3}H]AA metabolism as affected by a nontoxic concentration of $sPLA_2$ (1 ng/ml) and by a toxic concentration of Glu (80 μM), added individually or combined, was studied at 2 and 20 h after treatment with the agonists (Fig. 4). $sPLA_2$ induced a similar decrease in [^{3}H]AA-PL labeling both at 2 and 20 h. Differences were observed, however, in the distribution of labeling between free [^{3}H]AA and [^{3}H]AA-TAG. Free [^{3}H]AA accumulation was greater at 2 h, decreasing by 20 h concomitantly with an increase in [^{3}H]AA-TAG.

Glu alone triggered a similar loss in [^{3}H]AA-PL compared

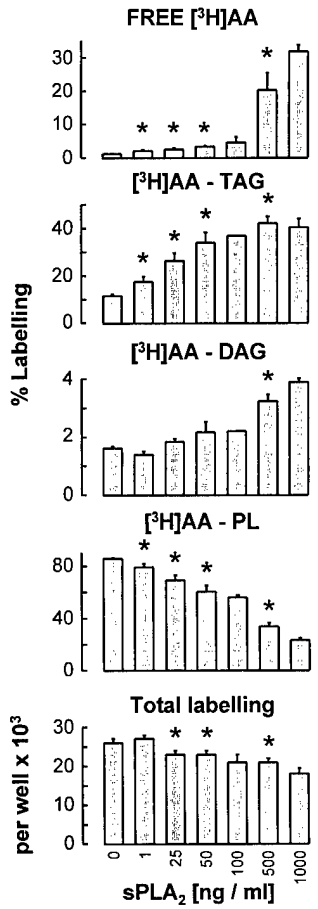

FIG. 3. **Hydrolysis of [^{3}H]arachidonoyl-phospholipids from cortical neurons by $sPLA_2$ from bee venom.** Cortical neuronal cells cultures, labeled overnight with 0.5 μCi/well [^{3}H]AA, were treated for 45 min with increasing concentrations of $sPLA_2$. The percentage of labeling of neuronal free [^{3}H]AA, [^{3}H]AA-TAG, [^{3}H]AA-DAG, and [^{3}H]AA-PLs and total labeling recovered per dish were assessed 20 h later. Mean values ± S.E. from values obtained with 10 different platings are shown. Mean values ± dispersion from the mean are shown for $sPLA_2$ concentrations of 100 ng/ml and 10^3 ng/ml ($n = 2$). An *asterisk* denotes statistically significantly different from control ($p < 0.05$).

with $sPLA_2$ by 2 h; however, by 20 h, loss of [^{3}H]AA from PL was 2.8-fold greater than at 2 h. After treatment with Glu alone, free [^{3}H]AA and [^{3}H]AA-TAG varied as a function of time (similar to when $sPLA_2$ was added alone), with higher accumulation of free [^{3}H]AA by 2 h and a preferential reesterification of [^{3}H]AA into TAG by 20 h.

$sPLA_2$ and Glu added together greatly magnified the pattern of [^{3}H]AA changes as a function of time. A synergy on free [^{3}H]AA accumulation was observed due to an apparently less efficient esterification into TAG. By 20 h the level of free [^{3}H]AA reached 1.8–2-fold higher values than when both agonists were individually added. The loss of [^{3}H]AA from PLs was additive, as was the accumulation of [^{3}H]AA-DAG induced at 2 and 20 h.

MK-801 Does Not Block Arachidonic Acid Release Induced by $sPLA_2$ from Bee Venom but Partially Blocks the Effect of OS2 from Snake Venom—The involvement of NMDA receptors on AA release from PLs induced by $sPLA_2$ and Glu was investigated by preincubating cells with 300 nM MK-801 for 10 min prior to adding the agonists, followed by lipid analysis 20 h later. Both at low, nontoxic (1 ng/ml) (data not shown) and at higher (25 ng/ml) bee venom $sPLA_2$ concentrations (Table I), MK-801 did not block the release of [^{3}H]AA from PLs. The phospholipid labeling was decreased by 17% ($p < 0.002$), from 87% in controls to 70% in $sPLA_2$-treated cells. Most of the

[^{3}H]AA released from PL (+11%) was found reesterified into TAG (5 *versus* 16% for control and $sPLA_2$-treated, respectively) and to a lesser extent in CHE (+4%, $p < 0.03$), while free [^{3}H]AA labeling was doubled (from 1 to 2%, $p < 0.03$). MK-801 pretreatment did not alter the profile of lipid labeling, *i.e.* the decrease in PLs and the parallel increase in TAG and free AA labeling.

Glu (80 μM), although more toxic than 25 ng/ml bee venom $sPLA_2$ ($sPLA_2$ toxicity 29% compared with Glu; Fig. 1), induced only a 6% ($p < 0.002$) decrease in PL labeling concomitantly with increased labeling of TAG (+2%, $p < 0.004$), CHE (+2%, $p < 0.02$), and FFA (+0.4%, $p < 0.03$). MK-801 pretreatment blocked by 100% Glu-induced PL degradation and other lipid changes. Higher degradation of PLs was observed when bee venom $sPLA_2$ and Glu were added together to the cells (−30%). Labeling of TAG increased by 24%, and labeling of free [^{3}H]AA increased by 3% ($p < 0.03$). MK-801 pretreatment blocked partially the changes induced by bee venom $sPLA_2$ and Glu, leading to the same profile of lipid labeling induced by $sPLA_2$ alone.

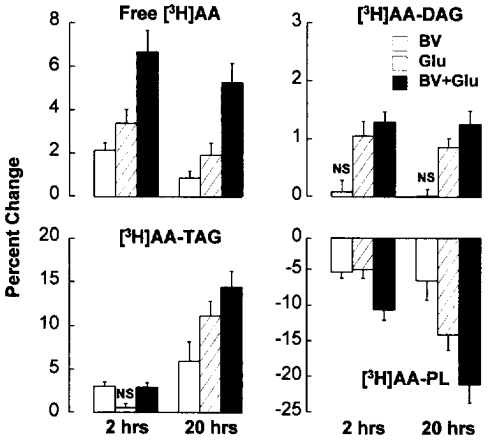

FIG. 4. **$sPLA_2$ and Glu trigger both acute and sustained effects on arachidonic acid metabolism in cortical neurons.** Cortical neuronal cultures prelabeled overnight with [^{3}H]AA (0.5 μCi/well) were treated individually for 45 min with a nontoxic concentration of bee venom $sPLA_2$ (1 ng/ml), Glu (80 μM), or both agonists together. Cells were harvested 2 and 20 h later and the percentage distribution of lipid labeling was determined. *Percent change* represents the percentage of labeling in stimulated cells minus the percentage of labeling of individual lipids in controls. Mean values ± S.E. from at least $n = 5$ determinations for 2 h and $n = 11$ for 20 h are shown. All *percent change* values are significantly different from controls ($p < 0.05$) except for those shown as *NS* (not significantly different).

The $sPLA_2$ from snake venom, OS2, added to the cells at the same concentration as $sPLA_2$ from bee venom (25 ng/ml), induced a much greater degradation of [^{3}H]AA-PLs. MK-801, in contrast to the results with bee venom, partially blocked [^{3}H]AA-PL hydrolysis induced by OS2 when added alone or together with Glu (Table I). Moreover, the total labeling recovered per well treated with OS2 and OS2 plus Glu was decreased by 35%, indicating a massive loss of cells. The DPM/well obtained when the cells were pretreated with MK-801 was similar to controls. Minimal changes in [^{3}H]AA-lipid labeling were observed when the cells were treated with the $sPLA_2$ (25 ng/ml) from snake venom OS1 (data not shown), which does not bind to neuronal membranes and which was found to be non-neurotoxic (see above).

$sPLA_2$ Display a Synergy with Glu in [^{3}H]AA Release from Phospholipids—$sPLA_2$ (25 ng/ml) from snake and bee venoms added with Glu displayed synergy leading to a higher [^{3}H]AA-PL degradation than the sum of the effect of the individual agonists (Table I, Fig. 5). Although the toxicity and PL hydrolysis induced by OS2 was much greater than that of bee venom $sPLA_2$ (Table I), the synergy with Glu was similar, reaching values for PL hydrolysis 1.4-fold higher for both $sPLA_2$ (Fig. 5*C*). A synergy was also observed in the accumulation of [^{3}H]AA-TAG that increased by 2-fold for bee venom $sPLA_2$ and 1.4-fold for OS2 (Fig. 5*B*). The synergy in free [^{3}H]AA accumulation was much greater with OS2 (3.5-fold) than with $sPLA_2$ from bee venom (2-fold) (Fig. 5*A*), and the synergy of $sPLA_2$ plus Glu was blocked by MK-801 (Table I).

Accumulation of Free [^{3}H]AA in Cortical Neurons Precedes the Toxicity Induced by High Concentrations of Bee Venom $sPLA_2$—Treatment of neuronal cultures with increasing concentrations of $sPLA_2$ resulted in increased neurotoxicity (Fig. 1) and higher degradation of AA-PLs (Fig. 4). Changes in lipid labeling plotted as a function of $sPLA_2$ toxicity are shown in Fig. 6. The accumulation of free [^{3}H]AA was minimal and proportional to increased LDH up to 100%, when $sPLA_2$ toxicity was equal to that of 80 μM Glu (≤100 ng/ml $sPLA_2$). Within this range of neurotoxicity, most of the [^{3}H]AA released from PLs (−30%) was reesterified into TAG. While PLs displayed a gradual loss of [^{3}H]AA up to LDH values of 200% (−50% decrease in PL labeling), accumulation of free [^{3}H]AA peaked between LDH values of 100 and 200%. This increase in free [^{3}H]AA preceded a 4.3-fold increase in LDH release observed for $sPLA_2$ concentrations between 500 ng/ml (217%) and 10^3 ng/ml (937% LDH).

TABLE I

Percentage of labeling of [^{3}H]AA-lipids from neuronal cells in culture 20 h after treatment with $sPLA_2$ and glutamate

Cells were labeled overnight with [^{3}H]AA and then exposed for 45 min to $sPLA_2$ from bee venom (25 ng/ml), OS2 from Taipan snake venom (25 ng/ml), glutamate (80 μM) and/or MK-801 (300 nM). Vales represent percentage distribution of labeling among neutral lipids and phospholipids recovered from cells. Mean values ± S.E. are shown for the number of individual determinations (n) indicated. For samples with $n = 2$, mean values ± S.D. are shown. Asterisks denote values statistically significantly different from control (Student's t test, $p < 0.05$).

Condition		Labeling					Total
		CHE	TAG	FFA	DAG	PL	
		%	%	%	%	%	*dpm/well*
Control	$n = 8$	5.8 ± 0.8	4.9 ± 0.5	1.0 ± 0.1	1.7 ± 0.1	86.6 ± 1.3	261,084 ± 10,723
Glu	$n = 4$	8.2 ± 0.6*	7.3 ± 0.5*	1.3 ± 0.1*	2.3 ± 0.2*	80.8 ± 1.0*	242,010 ± 15,687
Glu + MK-801	$n = 4$	6.7 ± 0.6	4.7 ± 0.1	1.0 ± 0.0	1.5 ± 0.2	86.1 ± 0.6	261,186 ± 24,050
$sPLA_2$	$n = 4$	9.9 ± 1.2*	15.7 ± 1.3*	2.3 ± 0.1*	2.1 ± 0.3	70.1 ± 2.3*	226,002 ± 11,425*
$sPLA_2$ + MK-801	$n = 4$	7.5 ± 1.5	14.6 ± 2.2*	2.3 ± 0.3*	1.8 ± 0.2	73.8 ± 3.2*	251,838 ± 14,374
$sPLA_2$ + GLU	$n = 4$	7.4 ± 1.1	28.8 ± 4.0*	4.0 ± 0.8*	2.9 ± 0.1*	56.9 ± 4.9*	225,108 ± 15,953
$sPLA_2$ + GLU + MK-801	$n = 4$	7.3 ± 0.7	13.5 ± 1.4*	2.2 ± 0.8*	2.5 ± 0.4	74.4 ± 1.2*	229,122 ± 11,353
OS2	$n = 3$	11.3 ± 1.9*	22.2 ± 3.7*	4.7 ± 0.9*	2.1 ± 0.1*	59.6 ± 6.3*	168,961 ± 50,967*
OS2 + MK-801	$n = 2$	6.2 ± 2.0	16.6 ± 4.1	2.3 ± 0.9	2.3 ± 0.1	72.6 ± 6.9	224,448 ± 42,155
OS2 + GLU	$n = 3$	6.0 ± 0.3	32.8 ± 2.6*	15.4 ± 3.3*	3.8 ± 0.2*	41.8 ± 5.8*	173,664 ± 1144*
OS2 + GLU + MK-801	$n = 2$	5.0 ± 0.5	14.8 ± 3.0	2.5 ± 0.6	2.1 ± 0.0	75.5 ± 4.1	233,448 ± 13,950

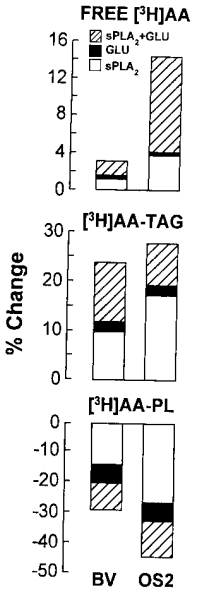

FIG. 5. **Synergistic effect of bee venom $sPLA_2$ plus glutamate on [^{3}H]AA release from phospholipids.** Percentage changes for $sPLA_2$ from bee venom (*BV*) and OS2 from Taipan snake venom (25 ng/ml) and glutamate (80 μM) were calculated from values shown in Table I as described in the legend to Fig. 4. The *open areas* on the *bar graphs* show the changes induced by $sPLA_2$ alone, and the *shaded areas* show changes induced by Glu alone. The additive effects of $sPLA_2$ plus Glu are indicated by the height of *open plus shaded area*; the synergistic effect of $sPLA_2$ and Glu added together is denoted by the *hatched area*, which is *above* and *beyond* the additive areas.

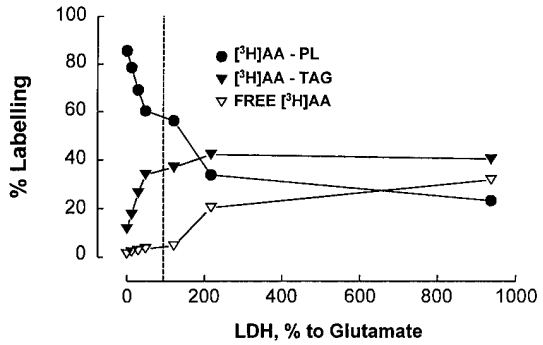

FIG. 6. **$sPLA_2$-induced neurotoxicity correlates with changes in arachidonic acid metabolism.** Plotted values were taken from those shown in Fig. 1 (percentage of LDH release) and Fig. 3 (percentage of lipid labeling) for increasing bee venom $sPLA_2$ concentrations. Cells were treated and data were analyzed as described under "Experimental Procedures." The *vertical dotted line* indicates the percentage of labeling that occurred for $sPLA_2$ concentration (100 ng/ml) with equivalent toxic effect as 80 μM Glu.

DISCUSSION

This study shows that treatment of primary cortical neurons in culture with $sPLA_2$ induces (*a*) a concentration-dependent increase in neurotoxicity; (*b*) sustained activation of [^{3}H]AA mobilization reflected in a gradual loss of [^{3}H]AA from PLs and in an accumulation of free[^{3}H]AA followed by its reesterification into TAG; and (*c*) synergy with Glu (80 μM) for both neurotoxicity and [^{3}H]AA-PL hydrolysis.

Neurotoxicity and sustained changes in AA metabolism, triggered by 45-min exposure of primary cortical neurons to Glu were blocked by the NMDA receptor antagonist MK-801 (Fig. 2, Table I) in agreement with previous studies (34–37, 51–53). Moreover, the release of [^{3}H]AA from PLs was observed 2 h after the treatment of neuronal cultures with Glu, and even greater release was observed 20 h later (Fig. 4). Long lasting changes in AA metabolism may be the result of calcium and protein kinase C-mediated, sustained activation of neuronal $cPLA_2$ by Glu (16). Moreover, increased $cPLA_2$ activity correlates with Glu neurotoxicity and precedes irreversible neuronal injury (16). It is also possible that, as in mast cells (54), Glu may regulate $cPLA_2$ activity at early time points by protein kinase C-mitogen activated protein kinase phosphorylation and later by enhanced expression of the enzyme. Modulation of gene expression and increased protein synthesis are involved in long term cellular responses as in neuronal plasticity or delayed neuronal death. In fact, $cPLA_2$ activation by NMDA-glutamatergic synaptic activity may lead to the formation of PAF, a potent bioactive lipid, which, in turn, mediates the induction of early response genes and subsequent gene cascades (2, 55–57). PAF could also potentiate excitotoxicity by enhancing Glu release (58, 59).

Although the toxicity of Glu (80 μM) was similar to that induced by bee venom $sPLA_2$ (100 ng/ml; Fig. 1), the hydrolysis of [^{3}H]AA-PLs 20 h after Glu treatment (−15%; Fig. 4) was half of that generated by 100 ng/ml bee venom $sPLA_2$ (−29%; Fig. 3). These results and the fact that MK-801 blocked Glu neurotoxicity support the notion that mechanisms other than $cPLA_2$ activation mediated by Glu-activated NMDA-gated calcium channels contribute to its neurotoxic action (8). Glu may also activate metabotropic receptors that, in turn, activate phospholipase C with the release of AA-DAG, a potent activator of protein kinase C (60). Sequential degradation of AA-DAG by diacylglycerol lipases and monoacylglycerol lipases contribute also to increased free [^{3}H]AA (61).

Bee venom $sPLA_2$-dependent sustained changes in [^{3}H]AA-lipid metabolism (2 and 20 h after adding the enzyme) reveal an active release of [^{3}H]AA from PLs, transient accumulation of free [^{3}H]AA, and reesterification into TAG. A similar effect was observed with Glu, with increased labeling of free [^{3}H]AA by 2 h decreasing by 20 h concomitantly with increased [^{3}H]AA-TAG labeling. Interestingly, free [^{3}H]AA was shunted into TAG even when cells were exposed to very low, nontoxic concentrations of $sPLA_2$ (1–10 ng/ml). Thus, the pathway activated by $sPLA_2$ may be physiologically relevant, withholding AA from its conversion to eicosanoids and from exerting effects of its own. AA is a modulator of synaptic function and potentiates Glu-NMDA neurotransmission, leading to excitotoxic damage (8). Free AA can be further metabolized to eicosanoids, potent modulators of synaptic function (29, 30), which, when overproduced, become injury mediators (8). TAG may also be a transient reservoir of AA when there is activation of degradative pathways, protecting the cells from the loss of this essential fatty acid. In fact, part of the [^{3}H]AA released during repeated seizures from neuronal membrane PLs in rat brain is shunted into TAG (7). This pathway was also activated in retina by experimental detachment (62), where another polyunsaturated fatty acid, docosahexaenoate (22:6n-3), is actively esterified into TAG. A reversible accumulation of AA-TAG occurs in non-neural cells cultured in the presence of high concentrations of FFA (63, 64). In the present study, even 20 h after transient cell stimulation with nontoxic concentrations of $sPLA_2$, [^{3}H]AA released from PLs remained as [^{3}H]AA-TAG. This indicates long lasting metabolic changes, since between 2 and 20 h post-treatment, PLs did not recover basal labeling, and free [^{3}H]AA was shunted into TAG.

The TAG reservoir appears to have a limited capacity to store AA. The maximum was reached at bee venom $sPLA_2$ concentrations between 50 and 100 ng/ml. AA-PL hydrolysis in neuronal cortical cells was much more sensitive to $sPLA_2$ than toxicity, within a range of LDH release similar to that exerted by Glu (Fig. 6). Thus, for $sPLA_2$ concentrations ≤100 ng/ml (toxicity ≤100% to Glu), the bulk of [^{3}H]AA mobilized from PLs

was recovered in TAG. Only when TAG reached a 30% increase in labeling above basal level did further degradation of [^{3}H]AA-PLs induced by higher, more toxic $sPLA_2$ concentrations result in preferential accumulation of free [^{3}H]AA. Taken together these results suggest that as long as the cells are able to shunt AA to TAG, they are protected from accumulation of free AA, and the neurotoxicity of $sPLA_2$ is minimized. Moreover, similar mechanisms allow significant mobilization of [^{3}H]AA from PLs without neurotoxic consequences (*i.e.* at 1 ng/ml $sPLA_2$). This supports the potential physiological relevance of $sPLA_2$ actions in promoting the formation of second messenger modulators of synaptic activity.

Neurotoxicity generated by $sPLA_2$ was biphasic with a linear increase up to 500 ng/ml and a sharp increase thereafter (Fig. 1). The estimated EC_{50} for the two components (7.1 nM and 56.8 nM, respectively) is consistent with the two high affinity binding sites for OS2 in synaptic membranes (25). Moreover, $sPLA_2$ from bee venom competes with OS2 for both binding sites (25). At present there is no information regarding the location of these receptors in the same or different cells or at the pre- and/or post-synaptic level.

Bee venom $sPLA_2$ at nontoxic (10 ng/ml) and mildly toxic (25 ng/ml) concentrations, when added together with Glu, displayed synergy in neurotoxicity (Fig. 1). Moreover, a 2.3-fold higher toxicity induced by $sPLA_2$ (25 ng/ml) plus Glu was also paralleled by synergy on PL degradation and 2-fold higher accumulation of free [^{3}H]AA. OS2, which is more toxic than $sPLA_2$ from bee venom (Ref. 25 and present results), displayed a more prominent synergy (3.5-fold) on free [^{3}H]AA accumulation. The results reported here open up several questions for future exploration; *e.g.* is Glu-induced $cPLA_2$ activation potentiating $sPLA_2$-mediated degradation of [^{3}H]AA-PLs and cellular toxicity, or *vice versa*? Recent studies carried out in $P388D_1$ macrophages revealed that PAF-induced AA mobilization involves two different PLA_2s (39) and that activation of $cPLA_2$ favors subsequent $sPLA_2$-induced AA release (40). Also, nerve growth factor, a regulator of mast cell function, has been reported to potentiate $sPLA_2$-induced histamine release (65). These observations suggest that $sPLA_2$ actively hydrolyzes lipids in disorganized membrane areas (66). Further studies combining lower, nontoxic concentrations of Glu and mammalian $sPLA_2$ type II, present together with Glu in synaptic vesicles (23), may further elucidate the involvement of both agonists in AA mobilization during glutamatergic synaptic activity.

Up to 25 ng/ml $sPLA_2$ from bee venom induced long lasting changes in AA-PL hydrolysis but did not involve the NMDA-glutamate pathway, since changes in AA metabolism and neurotoxicity were not blocked when $sPLA_2$ stimulation occurred in the presence of MK-801 (Fig. 2, Table I). Moreover, MK-801 partially blocked OS2 effect on AA-PL hydrolysis (Table I). This effect could be related to the origin/structure of the type II $sPLA_2$ from snake venoms and type III $sPLA_2$ from bee venom. Since the toxicity of OS2 at 25 ng/ml is 2.7-fold higher than that of $sPLA_2$ from bee venom at the same concentration (Fig. 2), the possibility of Glu-NMDA involvement at higher bee venom $sPLA_2$ concentrations on [^{3}H]AA-PL hydrolysis cannot be ruled out. Nevertheless, the present results suggest that, at least for OS2, stimulation of Glu release at presynaptic endings followed by its interaction with NMDA receptors may be involved in the acute effects of OS2 resulting in a sustained [^{3}H]AA-PL hydrolysis. Also, it is of interest that the profile of [^{3}H]AA lipid labeling for OS2 stimulation in the presence of MK-801 was identical to that generated by bee venom $sPLA_2$ alone and not blocked by MK-801, indicating a similar receptor-mediated component common for both $sPLA_2$. As previously discussed, this could also be the result of $sPLA_2$ interaction with receptors displaying different affinity for the enzymes.

In summary, this study shows that exogenously added $sPLA_2$ and Glu induce sustained changes in neuronal AA-PL metabolism and that $sPLA_2$ plus Glu exerts synergistic mobilization of AA and subsequent neurotoxicity. The present results, taken together with the recent observation that $sPLA_2$ type II in synaptic vesicles is released together with neurotransmitters (23), open up the possibility that glutamatergic neurotransmission involves the corelease of glutamate and $sPLA_2$. Our observations also imply that excitotoxicity may involve not only glutamate, as currently assumed, but may also involve $sPLA_2$ at the synaptic cleft. Further studies will assess if Glu could potentiate endogenous mammalian $sPLA_2$ actions that could, in turn, stimulate further Glu release. In this connection it is relevant that the synthesis of PAF, a retrograde messenger of long term potentiation (58), may be enhanced by $sPLA_2$ at the synapse. "Cross-talk" between $cPLA_2$ and $sPLA_2$ has recently been suggested in signal transduction events in macrophages (40), and a complex interplay between Glu-activated $cPLA_2$ and $sPLA_2$ could be envisioned at the synapse. Several of these ideas are currently under investigation in our laboratory.

Acknowledgments—We thank Drs. Gérard Lambeau and Michel Lazdunski for the gift of the phospholipases OS1 and OS2 and bee venom. The expert technical assistance of Fannie Richardson is acknowledged.

REFERENCES

1. Van den Bosch, H. (1980) *Biochim. Biophys. Acta* **604,** 191–246
2. Bazan, N. G. (1994) in *Pharmacology of Cerebral Ischemia* (Krieglstein, J., and Oberpichler-Swenk, H., eds) pp. 3–15, Wissenschaftlich Verlagsgeselschaft mbH, Stuttgart
3. Pierik, A. J., Nijssen, J. G., Aarsman, A. J., and Van den Bosch, H. (1988) *Biochim. Biophys. Acta* **962,** 345–353
4. Dennis, E. A. (1994) *J. Biol. Chem.* **269,** 13057–13060
5. Kudo, I., Murakami, M., Hara, S., and Inoue, K. (1993) *Biochim. Biophys. Acta* **117,** 217–231
6. Bazan, N. G. (1970) *Biochim. Biophys. Acta* **218,** 1–10
7. Birkle, D. L., and Bazan, N. G. (1987) *J. Neurochem.* **48,** 1768–1778
8. Bazan, N. G., Rodriguez de Turco, E. B., and Allan, G. (1995) *J. Neurotrauma* **12,** 791–814
9. Nicotera, P., Bellomo, G., and Orrenius, S. (1992) *Toxicology* **32,** 449–470
10. Davidson, F. F., and Dennis, E. A. (1990) *J. Mol. Evol.* **31,** 228–238
11. Fujimori, Y., Murakami, M., Kim, D. K., Hara, S., Takayama, K., Kudo, I., and Inoue, K. (1992) *J. Biochem. (Tokyo)* **111,** 54–60
12. Yoshijara, Y., and Watanabe, Y. (1990) *Biochem. Biophys. Res. Commun.* **170,** 484–490
13. Bonventre, J. V., and Koroshetz, W. J. (1993) *J. Lipid Mediators* **6,** 457–471
14. Clark, J. D., Schievella, A. R., Nalefski, E. A., and Lin, L.-L. (1995) *J. Lipid Mediat. Cell. Signal.* **12,** 83–117
15. Rordorf, G., Uemura, Y., and Bonventre, J. V. (1991) *J. Neurosci.* **11,** 1829–1836
16. Kim, D. K., Rordorf, G., Nemenoff, R. A., Koroshetz, W. J., and Bonventre, J. V. (1995) *Biochem. J.* **310,** 83–90
17. Stephenson, D. T., Manetta, J. V., White, D. L., Chiou, X. G., Gitter, B., May, P. C., Sharp, J. D., Kramer, R. M., and Clemens, J. A. (1994) *Brain Res.* **637,** 97–105
18. Hirashima, Y., Farooqui, A. A., Mills, J. S., and Horrocks, L. A. (1992) *J. Neurochem.* **59,** 708–714
19. Yang, H.-C., Farooqui, A., and Horrocks, L. A. (1994) *Biochem. J.* **299,** 91–95
20. Ross, B. M., Kim, D. K., Bonventre, J. V., and Kish, S. J. (1995) *J. Neurochem.* **64,** 2213–2221
21. Lauritzen, I., Heurteaux, C., and Lazdunski, M. (1994) *Brain Res.* **651,** 353–356
22. Oka, S., and Arita, H. (1991) *J. Biol. Chem.* **266,** 9956–9960
23. Matsuzawa, A., Makoto, M., Atsumi, G., Imal, K., Prados, P., Inoue, K., and Kudo, I. (1996) *Biochem. J.* **318,** 701–709
24. O'Regan, M. H., Smith-Barbour, M., Perkins, L. M., and Phillips, J. W. (1995) *Neurosci. Lett.* **185,** 191–194
25. Lambeau, G., Barhanin, J., Schweitz, H., Qar, J., and Lazdunski, M. (1989) *J. Biol. Chem.* **264,** 11503–11510
26. Lambeau, G., Schmid-Alliana, A., Lazdunski, M., and Barhanin, J. (1990) *J. Biol. Chem.* **265,** 9526–9532
27. Lambeau, G., Ancian P., Barhanin, J., and Lazdunski, M. (1994) *J. Biol. Chem.* **269,** 1575–1578
28. Lambeau, G., Ancian, P., Nicolas, J.-P., Beiboer, S. H. W., Moinier, D., Verheij, H., and Lazdunski, M. (1995) *J. Biol. Chem.* **270,** 5534–5540
29. Piomelli, D. (1994) *Crit. Rev. Neurobiol.* **8,** 65–83
30. Shimizu, T., and Wolfe, L. S. (1990) *J. Neurochem.* **55,** 1–15
31. Bazan, N. G. (1992) in *Neurochemical Correlates of Cerebral Ischemia* (Bazan, N. G., Braquet, P., and Ginsberg, N. D., eds) pp. 321–333, Plenum Publishing Corp., New York
32. Siesjö, B. K., Ingvar, M., and Westerberg, Z. (1982) *J. Neurochem.* **39,** 796–802
33. Katsura, K., Rodriguez de Turco, E. B., Folbergrova, J., Bazan, N. G., and Siejö, B. K. (1993) *J. Neurochem.* **61,** 1677–1684

34. Dumuis, A., Sebben, M., Haynes, J.-P., and Bockaert, J. (1988) *Nature* **336,** 68–70
35. Lazarewicz, J. W., Wroblewski, J. T., Palmer, M. E., and Costa, E. (1988) *Neuropharmacology* **27,** 765–769
36. Lazarewicz, J. W., Salinska, E., and Wroblewski, J. T. (1992) *Adv. Exp. Med. Biol.* **319,** 73–89
37. Pellerin, L., and Wolfe, L. S. (1991) *Neurochem. Res.* **16,** 983–989
38. Umemura, A., Mabe, H., Nagai, H., and Sugino, F. (1992) *J. Neurosurg.* **76,** 648–651
39. Balsinde, J., Barbour, S. E., Bianco, I. D., and Dennis, E. (1994) *Proc. Natl. Acad. Sci. U. S. A.* **91,** 11060–11064
40. Balsinde, J., and Dennis, E. A. (1996) *J. Biol. Chem.* **271,** 6758–6765
41. Fonteh, A. N., Bass, D. A., Marshall, L. A., Seeds, M., Samet, J. M., and Chilton, F. H. (1994) *J. Immunol.* **152,** 5438–5446
42. Reddy, S. T., and Herschman, H. R. (1996) *J. Biol. Chem.* **271,** 186–191
43. Kini, R. M., and Evans, H. J. (1989) *Toxicon* **27,** 613–635
44. Clapp, L. E., Klette, K. L., DeCoster, M. A., Bernton, E., Petras, J. M., Dave, J. R., Laskosky, M. S., Smallridge, R. C., and Tortella, F. C. (1995) *Brain Res.* **693,** 101–111
45. Kolko, M., Rodriguez de Turco, E. B., DeCoster, M. A., and Bazan, N. G. (1996) *FASEB Abstr.*, A1255
46. DeCoster, M. A., Koening, M. L., Hunter, J. C., and Tortella, F. C. (1992) *Neuroreport* **3,** 773–776
47. Klette, K. L., DeCoster, M. A., Moreton, J. E., and Tortella, F. C. (1995) *Brain Res.* **704,** 31–41
48. DeCoster, M. A., and Yourick, D. L. (1994) *Int. J. Dev. Neurosci.* **12,** 227–233
49. Frandsen, A., and Shousboe, A. (1990) *Int. J. Dev. Neurosci.* **8,** 209–216
50. Folch, J., Lees, M., and Sloane Stanley, G. H. (1957) *J. Biol. Chem.* **226,** 497–509
51. Rothman, S. M., and Olney, J. W. (1987) *Trends Neurosci.* **10,** 299–302
52. Choi, D. W. (1988) *Neuron* **1,** 623–634
53. Meldrum, B. S., and Garthwaite, J. (1990) *Trends Pharmacol. Sci.* **11,** 379–383
54. Nakatani, Y., Murakami, M., Kudo, I., and Inoue, K. (1994) *J. Immunol.* **153,** 796–803
55. Doucet, J. P., Squinto, S. P., and Bazan, N. G. (1990) *Mol. Neurobiol.* **6,** 27–55
56. Bazan, N. G., Squinto, S. P., Braquet, P., Panetta, T., and Marcheselli, V. L. (1991) *Lipids* **26,** 1236–1242
57. Bazan, N. G. (1995) *Nature* **374,** 501–502
58. Clark, G. D., Happel, L. T., Zorumski, C. F., and Bazan, N. G. (1992) *Neuron* **9,** 1211–1216
59. Kato, K., Clark, G. D., Bazan, N. G., and Zorumski, C. F. (1994) *Nature* **367,** 179–182
60. Nishizuka, Y. (1992) *Science* **258,** 607–614
61. Aveldaño, M. I., and Bazan, N. G. (1975) *Brain Res.* **100,** 99–110
62. Santos, F. F., Rodriguez de Turco, E. B., Gordon, W. C., Peyman, G. A., and Bazan, N. G. (1996) *Int. Ophthalmol.* **29,** 149–159
63. Denning, G. M., Figard, P. H., Kaduce, T. L., and Spector, A. A. (1983) *J. Lipid Res.* **24,** 933–1001
64. Spector, A. A., and Yorek, M. A. (1985) *J. Lipid Res.* **26,** 1015–1035
65. Murakami, M., Hara, N., Kudo, I., and Inoue, K. (1993) *J. Immunol.* **151,** 5675–5684
66. Upreti, G. C., and Jain, M. K. (1980) *J. Membr. Biol.* **55,** 113–121